



<https://theses.gla.ac.uk/>

Theses Digitisation:

<https://www.gla.ac.uk/myglasgow/research/enlighten/theses/digitisation/>

This is a digitised version of the original print thesis.

Copyright and moral rights for this work are retained by the author

A copy can be downloaded for personal non-commercial research or study,  
without prior permission or charge

This work cannot be reproduced or quoted extensively from without first  
obtaining permission in writing from the author

The content must not be changed in any way or sold commercially in any  
format or medium without the formal permission of the author

When referring to this work, full bibliographic details including the author,  
title, awarding institution and date of the thesis must be given

Enlighten: Theses

<https://theses.gla.ac.uk/>  
[research-enlighten@glasgow.ac.uk](mailto:research-enlighten@glasgow.ac.uk)

SOME STUDIES OF FAST NEUTRON REACTIONS

IN MEDIUM WEIGHT ELEMENTS.

by

P. J. STONES

DEPARTMENT OF NATURAL PHILOSOPHY

UNIVERSITY OF GLASGOW

PRESENTED AS A THESIS FOR THE DEGREE OF Ph.D.

IN THE UNIVERSITY OF GLASGOW

## PREFACE

The work described in this thesis was carried out during the period June 1961 to July 1964 in the Department of Natural Philosophy, The University of Glasgow.

The thesis presents the results of two studies of neutron induced reactions. The measurement of the excitation function, energy distribution, and ratio of forward to backward yield of protons emitted from the medium weight elements Ni<sup>58</sup>, Fe<sup>54</sup>, Cu<sup>63</sup>, bombarded with fast neutrons from the reaction  $H^2(d,n)He^3$  is described. Also, an investigation of the angular distribution of alpha particles emitted from medium weight elements bombarded with neutrons from the reaction  $H^3(d,n)He^4$  is presented.

Following an introductory chapter reviewing the interpretation of nuclear reactions of the type produced by fast neutrons, the techniques used by other workers in this field and a discussion of experiments in the neutron energy range 1 Mev. to 10 Mev. are introduced in Chapter 11.

Chapter 111 describes the apparatus designed by the author following discussions with Dr. W. Jack, to measure the excitation function, absolute cross-section, and the ratio of forward to backward yield of protons from (n,p) reactions, the energy of the incident neutrons being varied from 2.4 Mev. to 3.4 Mev. The experimental method and results are also presented in this chapter. The results obtained from these measurements

suggested the presence of some previously unknown levels in the residual nuclei  $\text{Co}^{58}$  and  $\text{Mn}^{54}$ . Measurements of the energy spectra of emitted protons under conditions of improved resolution which were carried out to investigate the presence of such levels are presented in Chapter IV. The decisions involved in the experimental procedure were the responsibility of the author, although he was assisted in the working of the H.T. Sets by Dr. J. G. Lynch, Mr. G. McBeth and Mr. N. McDicken. The analysis and interpretation of the results, carried out solely by the author, are presented, and their position in the general scheme of (n,p) reactions produced by  $\sim 3$  Mev. neutrons discussed in Chapter V.

In Chapter VI the apparatus used in a study of the angular distributions of alpha particles emitted from medium weight elements bombarded with  $\sim 15$  Mev. neutrons and the results this study are presented. This series of experiments was the responsibility of Mr. G. McBeth, although the author assisted in the experimental procedure and in the discussion of the results. In view of the author's limited participation in this series of experiments, the account of the experimental procedure, interpretation, and discussion is presented in less detail than that of the (n,p) experiments.

I would like to thank Professor P.I. Dee for his sustained

interest and encouragement throughout the course of this work.  
Thanks are also due to the technical and workshop staff. I  
also wish to acknowledge the receipt of a Research Studentship  
from the Department of Scientific and Industrial Research.

*December, 1965.*

---

# Some Studies of Fast Neutron Reactions in Medium Weight Elements

## CONTENTS

### Chapter 1. Interpretation of Nuclear Reactions Produced by Intermediate Energy Nucleons.

- 1.1. Introduction.
- 1.2. Formation of the Compound Nucleus.
- 1.3. Decay of the Compound Nucleus.
- 1.4. Partial Statistical Theory.
- 1.5. Complete Statistical Theory.
- 1.6. Nuclear Level Density.
- 1.7. Angular Distributions and the Statistical Theory.
- 1.8. Direct Interactions and Angular Distributions.
- 1.9. Fluctuations of Cross-Sections and Angular Distributions.

### Chapter 11. Previous Experimental Work on (n,p) Reactions in Medium Weight Elements in the Neutron Energy Range 1 Mev. to 10 Mev.

- 11.1. Introduction.
- 11.2a. Neutron Flux.
- 11.2b. Background Problems.
- 11.2c. Detection Efficiency.
- 11.3. Activation Technique.
- 11.4. Nuclear Emulsion Technique.
- 11.5. Counter Techniques.
- 11.6. Conclusion.

Chapter 111.     Determination of the Absolute Cross-Section, Energy Spectra, and Forward and Backward Yield of Protons from (n,p) Reactions in Ni<sup>58</sup>, Fe<sup>54</sup>, Cu<sup>63</sup>.

- 111.1.     Introduction.
- 111.2.     General Considerations.
- 111.3.     Development of a Charged-Particle Detection System.
- 111.4.     Design of Apparatus for Measurement of Excitation Functions and Forward to Backward Yields.
- 111.5.     Development of the Neutron Source.
- 111.6.     Neutron Flux Monitoring.
- 111.7.     Arrangement of Apparatus.
- 111.8.     Calibration.
- 111.9.     Accumulation of Data.
- 111.10.    Experimental Targets.
- 111.11.    Spectra of Emitted Protons.
- 111.12.    Experimental Results.

Chapter 1V.     Determination of Energy Spectra, and Absolute Cross-Sections for (n,p) Reactions in Ni<sup>58</sup> and Fe<sup>54</sup> at E<sub>n</sub> = 3.45 Mev., with Improved Resolution.

- 1V.1.     Introduction.
- 1V.2.     Design of Telescope.
- 1V.3.     Neutron Source and Monitoring.
- 1V.4.     Arrangement of Apparatus.
- 1V.5.     Associated Electronics.
- 1V.6.     Calibration.
- 1V.7.     Experimental Procedure.
- 1V.8.     Experimental Spectra.

Chapter V.      Discussion and Conclusions.

- V.1.      Neutron Beam Width.
- V.2.      Comparison of Present Results with other  
          (n,p) Results.
- V.3.      Theoretical Variation of Cross-Section with  
          Neutron Energy.
- V.4.      Ratio of Forward to Backward Proton Yield.
- V.5.      Systematics of (n,p) Reactions.
- V.6.      Energy Spectra obtained with "good" Energy  
          Resolution.
- V.7.      Conclusion.

Chapter VI.    The Angular Distribution of Alpha Particles  
                  Emitted from Medium Weight Targets bombarded  
                  with 14.8 Mev. Neutrons.

- VI.1.     Introduction.
- VI.2.     Previous Studies of (n, $\alpha$ ) Reactions.
- VI.3.     Experimental Technique.
- VI.4.     Experimental Apparatus.
- VI.5.     Experimental Method.
- VI.6.     Target Materials.
- VI.7.     Experimental Results.
- VI.8.     Discussion and Interpretation of Results.
- VI.9.     Conclusion.

Appendix A.   The Effect of Neutron Energy Spread on Measured  
                  Excitation Curves.

CHAPTER I.Interpretation of nuclear Reactions Produced  
by Intermediate Energy Nucleons.I.1. Introduction.

In the early 1930's the theoretical framework used in the description of nuclear interactions was that of the independent particle model. An incident nucleon, on entering the nucleus, was assumed to move in a potential well formed by all the nucleon-nucleon interactions in the nucleus. The probability for scattering was large, while the probability for absorption was small; also, it was predicted that there would be large width single particle levels associated with standing waves set up in the potential well. However, experimental evidence, especially on slow neutron resonances, (Moon and Tillman, 1935; Szilard, 1935; Bjerger and Westcott, 1935; Amaldi and Fermi, 1936;) showed the occurrence of sharp resonance peaks in excitation functions and the predominance of absorption over scattering.

In order to explain these observations, Niels Bohr, 1936, emphasized the necessity of going to the other extreme of the independent particle model by considering the nucleons as strongly interacting particles. In this compound nucleus picture, an incident nucleon is quickly absorbed and shares its kinetic energy with the particles of the nucleus. The compound state thus formed is independent of the method of formation. The compound state is long lived, decay occurring when sufficient energy is placed on one particle to allow it to escape. The narrow resonances

observed in slow neutron experiments are explained by the long lifetime of the compound state.

In 1936 also, Breit and Wigner, derived an expression which gave a good fit to the observed cross-sections. Bethe, 1937, gave a quantitative discussion of nuclear reactions in terms of the compound nucleus mechanism. The detailed consequences of Bohr's theory were considered by Weisskopf, 1937, Bethe and Placzek, 1937, and Weisskopf and Ewing, 1940. Several papers (Kapur and Peirls, 1938; Wigner and Eisenbud, 1947) were published which were of a more rigorous nature, and did not depend on any model. However in the explanation of experimental results, it is more advantageous to use simplified theories based on models; models such as the 'statistical model', 'direct interaction theory' and the 'optical model' will be discussed later in this chapter.

In 1952, Barschall found that a systematic analysis of total neutron cross sections between 0.1 and 3 Mev. showed large width resonances, of an order of an Mev., with sharp compound nuclear resonances superimposed. This 'gross structure' as it was known, was quickly shown to be explained by the optical model, which was reminiscent of the early independent particle models. The optical model, unlike the compound nucleus model, is essentially a weak absorption model. The motion of an incident nucleon is described by replacing the target nucleus by a complex potential ( $V+iW$ ). Feschbach, Porter and Weisskopf, 1953, '54, were able to relate the imaginary part of the potential well to compound

nucleus formation, i.e. absorption, while the real part of the potential explained the scattering processes. This model gives wider scope to the explanation of nuclear mechanisms than Bohrs' compound nucleus model; indeed, the compound nucleus model is contained in a special case in the optical model when the imaginary part of the potential is very high. The optical model is amenable to the treatment of other processes such as direct 'knock-out' processes, the excitation of collective, rotational and vibrational states; such non compound nucleus processes are often known as 'direct nuclear reaction' mechanisms.

A compromise between the two extremes, the use of single particle states only, or of compound nuclear states only, was introduced by Lane, Thomas and Wigner, 1955. Their description also uses the idea of a potential well, but instead of treating the non-elastic processes by the introduction of an imaginary potential, Lane et al. used a real potential. Nuclear reactions were explained by considering the replacement of the average potential of all the nucleons by the sum of the individual potentials of the nucleons in the target nucleus.

The experimental work presented in this thesis, viz.:- the study of protons emitted from medium weight elements bombarded with neutrons of the order of 3 MeV, and also, the investigation of the angular distribution of alpha particles emitted from targets upon bombardment from 15 Mev neutrons, will be described mainly in terms of compound nucleus theory, although the extent of other reaction mechanism theories, and also the validity of the compound nucleus

theory in such a description must be considered.

### I.2. Formation of the compound nucleus.

Consider the reaction  $A(a,b)B$ . According to the postulates of the compound nucleus mechanism of nuclear reactions, the formation and decay of a compound nucleus may be considered to be independent except in so far as conservation laws are obeyed.

(The conditions for this assumption to be applicable will be discussed later in this chapter). Thus the cross section for the

above nuclear reaction may be written as  $\sigma(a,b) = \sigma_c(a) g_c(b)$  where  $\sigma_c(a)$  refers to the probability of formation of the compound nucleus and  $g_c(b)$  refers to the probability of the decay of the

compound nucleus by emission of particle 'b'. The cross section for the formation of the compound nucleus by a particle of angular momentum  $l\hbar$  is normally expressed in terms of the penetrability

$T_l$  :-  $\sigma_c = \pi \lambda^2 \sum (2l+1) T_l$ , where  $2\pi\lambda$  is the wavelength of the incident particle. The penetrabilities  $T_l$ , and hence  $\sigma_c$ ,

have been calculated using the 'continuum' model, developed by Feshbach and Weisskopf, 1947, '49. This is a strong coupling model based upon a simple model of nuclear structure, the only information

required about the internal conditions being its radius and the wave number of the particle 'a' within the nucleus. The

penetrabilities may also be calculated by using a weak coupling

model. Feshbach, Porter and Weisskopf, 1954, have derived an

expression for  $\sigma_c$  for neutrons using a square well complex potential.

### I.3. Decay of the compound nucleus.

The formation of a state or level in a compound system gives

rise to the level of width  $\Gamma$  where  $\Gamma$  is related to the lifetime,  $\tau$ , of the state by means of Heisenberg's Uncertainty Principle, viz:-  $\tau = \hbar / \Gamma$ . The probability of decay of the state per unit time is  $\Gamma / \hbar$ . If the various competing modes of decay have probabilities of decay  $\Gamma_i / \hbar$  i.e. partial width  $\Gamma_i$ , then  $\Gamma = \sum_i \Gamma_i$ . With increasing excitation of the compound nucleus, the level density  $\omega(E)$  of the compound nucleus and of the residual nuclei increase. ( $\omega(E) \propto \exp[2(\alpha E)^{1/2}]$  Bethe, 1936, '37.). Thus the number of modes of decay, and hence  $\Gamma_i$ , increase. If a sufficient number of modes of decay are present, the decay of the compound system may be treated by means <sup>of</sup> statistical methods. The decay of the compound system may be considered in two cases for the description of the work presented in this thesis. When there is a large number of levels excited in the compound nucleus but only a few levels excited in the residual nucleus, the partial statistical theory (I.4.) may be applied (e.g. in the description of (n,p) cross sections at 3 Mev). The complete statistical theory of the compound nucleus mechanism may be applied when a large number of levels in the residual nucleus are excited (as in the case of (n, $\alpha$ ) reactions at 15 Mev).

#### I.4. Partial Statistical Theory.

As stated previously, one of the basic assumptions of the compound nucleus theory is that there is independence of formation and decay of the compound nucleus. For this to be so, it is generally agreed that there should be a sufficient number of states excited in the compound nucleus for a statistical average to be

formed. Friedman and Weisskopf, 1955, have pointed out that, although the independence hypothesis is certainly true when only one state in the compound nucleus is formed, it may not necessarily be so when many levels are formed having a mixture of a number of unspecified phases. The phases should initially depend upon the method of forming the compound nucleus, and there is no guarantee that the probability of decay by a given mode does not depend upon the phases. However, it is hoped that if very many states are excited the distribution of the compound nucleus states at the time of decay will be independent of the mode of formation. It is to be noted, that the requirement of many states to be excited requires that the energy spread of the incident beam of nucleons should be much wider than the level spacing at the energy of excitation in the compound nucleus.

The mathematical treatment of the formation and decay of the compound nucleus has been treated by several authors, notably by Wolfenstein, 1951, and by Hauser and Feshbach, 1952, in a quantal treatment and classically by Ericson, 1960. Hauser and Feshbach show that the cross section for the process of an incidental neutron of spin  $i$  and angular momentum  $l$  incident upon a target nucleus of spin  $I$  forming a compound nucleus of spin  $J$  which then decays by the emission of a particle of spin  $i'$  to individual states in the residual nucleus may be represented by

$$\sigma(\alpha/\alpha') = \pi \lambda^2 \sum_{J, j, l, j', l'} \frac{(2J+1)}{(2i+1)(2I+1)} \cdot \frac{T_{\alpha' j' l'}^J T_{\alpha j l}^J}{\sum_{\alpha'' j'' l''} T_{\alpha'' j'' l''}^J}$$

where  $j = \text{channel spin} = I + i = J - l$

$\alpha \equiv$  channel designation (energy, type, etc.)

$T \equiv$  penetrability

and dashes refer to emergent particles.

The summations are restricted to the conservation laws of energy, momentum and parity. The term  $\pi \lambda^2 T_{\alpha j \ell}^J$  represents the cross section for formation of the compound nucleus while the term

$T_{\alpha' j' \ell'}^J / \sum_{\alpha'' j'' \ell''} T_{\alpha'' j'' \ell''}^J$  represents the decay of the compound nucleus. A basic assumption in the derivation of the formula is that the energy resolution of the incident beam is broad enough so that many levels of the compound nucleus are excited. The corresponding wave functions are assumed to have random phase so that when phase averages are performed all interference terms will vanish. The above formula may be simplified if there are no spin-orbit interactions; the penetrabilities then depend only upon  $\ell$ , and not upon  $j$  and  $J$ . If the incident and emergent particles have spin  $\frac{1}{2}$ , then the cross section may be written

$$\sigma(\alpha/\alpha') = \frac{\pi \lambda^2}{2(2I+1)} \sum_{\ell} T_{\alpha \ell} \frac{\sum_j \epsilon_{j, \ell}^J (2J+1) \sum_{j'} \epsilon_{j', \ell'}^J T_{\alpha' \ell'}}{\sum_{j''} \epsilon_{j'', \ell''}^J T_{\alpha'' \ell''}}$$

where  $\epsilon_{j, \ell}^J = 2$  if  $J$  is such that  $|J - \ell| \leq j_{1,2} \leq J + \ell$   
 $= 1$  if only one value of  $j$  satisfies the above inequality.

$= 0$  for all other values of  $J$ .

$$(j_{1,2} = I \pm \frac{1}{2}).$$

An assumption in the derivation of the above formulae is that the products and the ratios of average widths can be replaced by an averaging over the products and ratios. When there are only a few

decay channels, (e.g. elastic scattering and radiative capture at low energies,) this may lead to fluctuations. Fluctuations may manifest themselves if the number of levels excited at one time in the compound nucleus is not enough to satisfy the conditions of a statistically independent distribution e.g. if the energy band width is too small, fluctuations of level density and widths will show themselves in an excitation function.

### I.5. Complete Statistical Theory.

If the energy of the incident particle is above  $\sim 8$  Mev and the target nucleus is of at least medium weight, then the decay of the compound nucleus may leave the residual nucleus in a region of high density of levels. The cross section for this process may be obtained by summing the formulae of the preceding section over the states of interest.

Consider the cross section for an incident particle in channel  $\alpha$ , with energy  $E$ , leading to an emergent particle in channel  $\alpha'$  with energy between  $E'$  and  $E' + dE'$ . The residual nucleus will have an excitation energy  $\epsilon' = E - E' - Q$ , where  $Q$  is the reaction energy involved in the process. The density of levels in the residual nucleus at an excitation energy  $\epsilon'$ , with spin  $I'$ , may be designated by  $\omega_{\alpha'}(I', \epsilon')$ . The cross section involves a summation over all residual nuclei spins  $I'$  at the excitation energy of  $\epsilon'$ , consistent with the conservation laws. i.e.

$$\sigma_{\alpha\alpha'}(E, E') dE' = \pi \lambda^2 \sum_{J, j, l} \frac{(2J+1)}{(2i+1)(2I+1)} \cdot \frac{T_{\alpha j l}^J(E) \sum_{J', I'} T_{\alpha' j' l'}^J(E') \omega_{\alpha'}(I', \epsilon') d\epsilon'}{\sum_{\alpha'' j'' l'' I''} \int_0^{\epsilon - Q} d\epsilon'' T_{\alpha'' j'' l''}^J(\epsilon'') \omega_{\alpha''}(I'', \epsilon'') d\epsilon''}$$

Hauser and Feshbach show that by making the assumptions that

(a) the level density may be expressed as  $\omega(I', \epsilon') = (2I'+1)\omega(\epsilon')$  (this assumption will be discussed later), and (b) that the penetrabilities are independent of spin, depending only on orbital angular momentum  $l$ , then the expression for the cross section reduces to the form

$$\sigma(E, E') dE' = \sigma_{c,\alpha}(E) \cdot \frac{(2i'+1) E' \sigma_{c,\alpha'}(E') \omega_{\alpha'}(E') dE'}{\sum_{\alpha''} (2i''+1) \int_0^{E-Q} E'' \sigma_{c,\alpha''}(E'') \omega_{\alpha''}(E'') dE''}$$

where  $\sigma_{c,\alpha}(E) = \pi \lambda^2 \sum (2l+1) T_l$ , the cross section for formation of the compound nucleus. This expression was originally derived by Weisskopf, 1940, by making use of much simpler assumptions involving reciprocity relations.

#### 1.6. Nuclear Level Density.

Since the predictions of the statistical theory are dependent upon the variation of the level density with excitation energy of the residual nucleus, we will give a brief review of the present views on this subject.

The outstanding feature of nuclear level densities is their rapid increase with excitation energy. The level density is strongly influenced by shell effects; the density of levels for magic or nearly magic nuclei is one to three orders of magnitude smaller than level densities in non-magic nuclei at the same excitation energy, and there is also a striking dependence upon the odd-even character of the nucleus (c.f. the experimental results of Bulloch and Moore, 1960, and Allan, 1961). In order to explain the behaviour of nuclear level densities several authors have considered the problem in detail. Bethe, 1936, '37, approached the problem

by using the methods of statistical thermodynamics. He considered the nucleus to be composed of a Fermi gas of  $A$  particles. He found that the level density at energy  $E$  could be expressed by  $\omega(E) = C \exp \left[ 2 (aE)^{\frac{1}{2}} \right]$ , where  $a$  is parameter, and  $C$  is approximately constant with energy. Newton, 1956 and Cameron, 1958, have considered the shell effects in a Fermi gas model. The odd-even effect has been treated by assuming a shift in the position of the effective ground state of a nucleus caused by a nucleon pairing (c.f. Lang and Le Couteur, 1954). The distribution of angular momentum has been considered by Bethe, 1937, and Bloch, 1954, using a thermodynamical method, and by Ericson, 1960, who used the notion of random coupling of angular momenta vectors. It is found that the density of states of spin  $J$  at an effective excitation energy  $U$  is given by

$$\omega(U, J) = \frac{(2J+1)}{2(2\pi)^{1/2} \sigma^3} \omega(U) \exp \left[ \frac{-J(J+1)}{2\sigma^2} \right]$$

where  $\sigma^2$  is the mean square deviation of the random projection of angular momenta vectors, associated with the excited particles and holes, on an arbitrary axis. The effect of  $\sigma^2$  is to decrease the number of higher spins at a given excitation energy, and hence the name 'spin cut-off' parameter. Ericson, 1960, has shown that  $\sigma^2 = \mathcal{J}T / \hbar^2$  where  $T$  is a nuclear temperature. This may be taken as a definition of the moment of inertia,  $\mathcal{J}$ , of a nucleus. Bloch, 1954, has shown that most models used in the computation of nuclear level densities lead to a spin dependence of the form

$$\omega \propto \exp \left[ -\frac{I^2}{2\sigma^2} \right] - \exp \left[ -\frac{(I+1)^2}{2\sigma^2} \right]$$

which may be rearranged to the form

$$\omega \propto 2 \exp\left[-\frac{1}{2\sigma^2}\right] \cdot \text{Sinh}\left[\frac{I+1/2}{2\sigma^2}\right] \cdot \exp\left[-\frac{(I+1/2)^2}{2\sigma^2}\right]$$

For  $2\sigma^2 \gg I + \frac{1}{2}$  this may be approximated to

$$\omega \propto \frac{(2I+1)}{2\sigma^2} \exp\left[-\frac{(I+1/2)^2}{2\sigma^2}\right]$$

It is only with the stronger requirement  $2\sigma^2 \gg (I+\frac{1}{2})^2$  does  $\omega$  reduce to the form  $(2I+1)$ . Since empirical values of  $2\sigma^2$  are of the order of 10 (Douglas and MacDonald, 1959), the assumption  $\omega \propto (2I+1)$  breaks down for  $I$  values as low as 2 or 3. Since a knowledge of the exact spin dependence of nuclear level densities is necessary for the application of compound nuclear theory in the investigations of nuclear reactions, much work has been carried out recently in the determination of the spin cut-off parameter. Part of this work will be discussed in the section on angular distributions of nuclear reactions.

### I.7. Angular Distributions and Statistical Theory.

As before, we may consider the two cases of a few levels and a continuum of levels in the residual nucleus. In order to simplify the treatment of angular distributions, Wolfenstein, 1951, and Hauser and Feshbach, 1952, found that it was again necessary to postulate a spin dependence of the level density of the form  $\omega(I) \propto (2I+1)$ . It has been shown by Wolfenstein, Hauser and Feshbach, and Lane and Thomas, 1958, that the assumption  $\omega(I) \propto (2I+1)$  leads to an angular isotropic distribution. Ericson, 1960., has treated the case of the angular distribution

of reaction products from the decay of a compound nucleus in a state of high excitation to single levels in the residual nucleus in a classical manner :- Consider the case of a neutron or proton incident upon a target nucleus of spin  $\underline{I}$ . If the incident orbital angular momentum is denoted by  $\underline{l}$ , then the angular momentum of the intermediate compound state (assumed to be in high excitation state) is  $\underline{J} = \underline{l} + \underline{I}$  (ignoring the spin of the incident particle). The orbital angular momentum of the emitted particle is denoted by  $\underline{l}'$  and the spin of the residual nucleus is  $\underline{I}'$ . For simplicity, Ericson considers the case of a zero spin target nucleus. Then since  $\underline{J} = \underline{l}$ , the angular momentum of the emitted particle is restricted by the condition  $\underline{l}' = \underline{l} - \underline{I}'$ . We can therefore regard  $\underline{l}'$  as aligned to  $\underline{l}$  but for the decoupling angle  $\nu_0$  due to the fact that  $\underline{I}' \neq 0$ . Since the emergent particle is emitted in a plane perpendicular to  $\underline{l}'$  there will be a 'piling-up' effect of particles in cones along the incident particle axis of half angle  $\approx \nu_0$ . Thus the angular distribution will be smeared out over a cone in the forward and backward directions. Outside the cones, Ericson shows that an averaging over the direction of  $\underline{l}$  perpendicular to the beam gives an angular distribution  $W(\theta)$  of the form  $\frac{2}{\pi} \arcsin \frac{I'}{l \sin \theta}$ . Thus, the angular distribution is of the form

$$W(\theta) \propto \begin{cases} 1 & \text{for } \sin \theta < \sin \nu_0 = I'/l \\ \frac{2}{\pi} \arcsin \frac{I'}{l \sin \theta} & \text{for } \sin \theta > \sin \nu_0 = I'/l \end{cases}$$

Ericson and Strutinski, 1958, have considered the case of many levels in the residual nucleus. In this case, the exponential cut-off factor in the expression, for the spin distribution (I.6)

will again tend to align  $\underline{l}$  and  $\underline{l}'$  to within a decoupling angle  $\nu_0$ . Since the decay of the compound nucleus leads to a high density of states in the residual nucleus, it is very probable that the decoupling between  $\underline{l}$  and  $\underline{l}'$  is quite large. In this case, the 'weak coupling limit', Ericson and Strutinski show the angular distribution of particles of energy  $E^Z$  to be of the form

$$W(\theta, E') \approx 1 + \frac{\langle l^2 \rangle \langle l'^2 \rangle}{12 \sigma^4} P_2(\cos \theta)$$

where the average values of  $l^2$  and  $l'^2$  are obtained by the use of weighing factors derived from the penetrabilities of the incident and emergent particles. From this form of the angular distribution one may determine the spin cut-off parameter (Chapter VI.). Douglas and MacDonald, 1959, have carried out exact quantal calculations of the angular distributions. Their results indicate that the classical approximation of Ericson and Strutinski produces results which agree closely with the exact solution.

#### I.8. Direct Interactions and Angular Distributions.

Considerable evidence has accumulated which suggests that the compound nucleus theory is an over simplification of the facts. The activation studies of the (n,p) reaction at 14 Mev by Paul and Clarke, 1953, are in violent disagreement with the statistical theory. The latest measurements of Blosser et al, 1955, Coleman, 1959, and Weigold, 1960, have also shown the existence of discrepancies. Following some initial work by M<sup>C</sup>Manus and Sharp, 1952, Austern, Butler and M<sup>C</sup>Manus, 1953, provided a theoretical model to explain the discrepancies. They showed that a small contribution of surface direct interactions, i.e. interactions involving only a

few degrees of freedom on the surface of the nucleus, could account for the observed discrepancies. Other theories of volume direct interaction have been provided by Hayakawa et al, 1955, Lamarsh and Feshbach, 1956, and Brown and Muirhead, 1957, and explain effects such as those observed in the  $(n,n')$  results of Rosen and Stewart, 1955.

In general, direct interactions cause the angular distributions to be forward peaked (Rosen and Stewart, 1955, Ahn and Roberts, 1957, and Coon et al, 1958).

The presence of direct interaction mechanisms in low energy ( $\sim 3 - 4$  Mev) experiments (c.f. Chapter III) is unlikely because of the influence of the coulomb barrier. The cross section for a direct interaction process is proportional to the absolute square of the transition Matrix  $T_{fi} \propto \int \psi_f^* \phi_f^* V \phi_i \psi_i d\mathbf{r} d\mathbf{r}'$  where  $\psi_i$  and  $\psi_f$  are wave functions of the target and residual nucleus,  $\phi_i$  and  $\phi_f$  are wave functions of the incident and emergent particles,  $V$  is the interaction potential, and the integral is evaluated at the position of the nucleus. Hence, the cross section is proportional to the product of squares of wave functions, which is essentially just the product of the barrier penetrabilities  $T T'$ . The work of Hauser and Feshbach shows that the compound nuclear cross section is proportional to  $T T' / \sum \epsilon T''$  where  $\epsilon$  is a channel spin factor. Thus  $\frac{\sigma_{DI}}{\sigma_{CN}} \propto \frac{T T'}{\sum \epsilon T''} = \sum \epsilon T''$ . This factor is close to zero when the incident energy is below the Coulomb barrier height and increases rapidly as the incident energy increases above the Coulomb barrier. The results of Taketani et al, 1962,

Hausman et al, 1960, and Seward, 1959, on (p. p<sup>6</sup>) angular distributions at 6~7 Mev corroborate the above result.

### 1.9. Fluctuations of Cross Sections and Angular Distributions.

The concept of averages plays a central rôle in the statistical model. The assumption of a smoothly varying cross section with energy is one of the premises of the compound nuclear theory. However, when dealing with averages, one must be able to say something about the evaluation of the fluctuations which are inevitably associated with the averages. Ericson, 1960, has considered the fluctuations which are present in the cross section of a process in which a beam of microscopically fine energy resolution is incident upon a target nucleus, the intermediate state decaying to specific states of the residual nucleus. Knowing these fluctuations, he has estimated the fluctuations when the resolution of the beam is finite and when transitions take place to many states. The total cross section,  $\sigma_{\alpha\alpha'}$ , for a reaction going via a compound nucleus in which  $N$  non-overlapping compound states are formed, each of which decays to  $n$  different states in the final nucleus over which an average is also taken, may be expressed as

$$\sigma_{\alpha\alpha'} = \langle \sigma_{\alpha\alpha'} \rangle \left( 1 \pm 1/\sqrt{N} \pm 1/\sqrt{Nn} \right)$$

The averaging process may be performed experimentally by using an incident beam with an energy spread greater than the level spacing in the compound nucleus.

Ericson also shows that fluctuations result in an angular distribution of the form

$$W(\theta) = \langle W(\theta) \rangle \left( 1 \pm 1/\sqrt{Nn} \right)$$

Agodi and Pappalardo, 1963, in an analysis of neutron total cross section data in the energy range 2.5 to 5 Mev obtained by Cuzzocrea et al, 1960, and Agodi et al, 1962, suggest the fluctuations may also be present as a result of statistical deviations from the average of the compound nucleus level density. Such fluctuations, which differ from the Ericson interference fluctuations, were used by Konijn and Lauber, 1963, to explain their excitation curve for the (n,p) reaction in  $\text{Ni}^{58}$  in the region of 3 Mev.

CHAPTER II.Previous Experimental Work on (n,p) Reactions in Medium Weight Elements, in the Neutron Energy Range 1Mev to 10 Mev.II.1. Introduction:

The study of charged particle emission induced by neutrons of energy less than  $\sim 5$  Mev in medium weight nuclei has been carried out by few workers. At the beginning of the present programme of work described in this section of the thesis, all information on the (n,p) reactions had been obtained indirectly by the activation technique (II.3.). However, before the completion of the author's experimental work, a similar approach to the study of the (n,p) reactions was reported (II.5.). The technique utilised in the experimental work of the author involved the detection of protons emitted into a known solid angle from a target material in the form of a thin foil.

Before we discuss the experiments on (n,p) reactions that have been performed, we shall consider some of the difficulties involved as these have a direct bearing on the methods used and the results obtained.

II.2a. Neutron Flux.

The yield of charged particle reactions is limited by the yield of the neutron source, by geometrical considerations and by the magnitude of the cross section for the reaction. A flux of neutrons of energy of the order of 3 Mev may be obtained using the reaction  $H^2(d,n) He^3$ ,  $Q=3.27$  Mev. This reaction exhibits an increasing yield as the deuteron energy is increased above the

threshold of approximately 100 Kev. For a bombarding energy of 500 Kev the energy of the emitted neutron varies between  $\sim 2.5$  Mev and  $\sim 3.5$  Mev at  $0^\circ$  at  $90^\circ$ . With a deuteron beam of  $40 \mu$  amp on a thick deuterium target (i.e. a target in which the incident deuteron is completely stopped) it is possible to obtain a flux of neutrons of the order of  $2 \times 10^7$  neutrons per second per steradian at  $90^\circ$  to the deuteron beam. The difficulties involved in neutron experiments are realised when this figure is compared with directed beam of  $10^{12}$  particles per second in the case of accelerated charged particle beams used in charged particle experiments.

#### II.2b. Background Problems.

The extreme penetrability of fast neutrons require the operation of a charged particle detection system in a large flux of neutrons. The problem of the relatively high number of background counts obtained in an experimental assembly placed in a neutron flux render the detection of emitted protons difficult. This problem does not obtain in the case of the activation technique since the detection system is operated after the target material is withdrawn from the neutron flux.

#### II. 2c. Detection Efficiency.

Because of the presence of the Coulomb barrier, the cross section of (n,p) reactions will be much reduced in comparison with that of (n,n') reactions. Also, the low energy of the emitted protons require the use of a thin target in order that sufficient energy resolution is obtainable. This will, therefore, cause a further reduction in the yield of the emitted protons. In order

to increase the detection efficiency one can decrease the target-detector and target-neutron source separations. However, these distances are limited by the angular resolution required in a given experiment. In practice, a suitable balance between detection efficiency, angular resolution and energy resolution must be chosen. The problems associated with the detection efficiency and resolution are much simplified by the use of an activation technique.

### II.3. Activation Technique.

There are several methods<sup>of</sup> studying the emission of charged particles from medium weight elements bombarded with neutrons of energy less than  $\sim 10$  Mev. The most common method is that of the activation technique.

This technique requires the detection and counting of gamma rays emitted from the residual nuclei which are left in unstable states as a result of the emission of a proton. Because of the relatively large penetrability of gamma rays in comparison with that of low energy protons, a large volume of target material may be used, thus giving a high yield. Also, the target may be made to subtend a small solid angle at the neutron source giving good energy resolution. However, the technique gives no indication of the energy or angular distribution of the emitted protons since it only requires the detection of the secondary gamma rays.

A series of experiments which resulted in the absolute cross-section and excitation function for (n,p) reactions in various target materials have been carried out by several workers using the

activation technique. Rapaport and Van Loef, 1959, have studied the reaction  $Zn^{64}(n,p)Cu^{64}$  in the neutron energy range 2 Mev to 3.4 Mev. Gonzalez, Rapaport and Van Loef, 1960, have carried out a similar investigation into the reaction  $Ni^{58}(n,p)Co^{58}$ , the neutron energy varying between 2.2 Mev and 3.6 Mev. Van Loef, 1961, using the results of the previous two papers and additional results on the (n,p) reactions in  $Fe^{54}$ ,  $Ni^{61}$ , and  $Zn^{67}$  has sought to verify the existence of some of the systematics of nuclear reactions which have been found to hold for (n,p) reactions at 14 Mev. (Bullock and Moore, 1960). And, finally, in the same series of experiments, Gonzalez, Van Loef, and Trier, 1962, have obtained the excitation function for the reaction  $Ti^{47}(n,p)Sc^{47}$  in the range 2 Mev to 3.6 Mev. Absolute cross-sections were determined by comparison of the activity of the residual nuclei with that of  $Si^{31}$  resulting from the reaction  $P^{31}(n,p)Si^{31}$ . Their neutron source was a self generating deuterium target.

In an attempt to give an explanation of the excitation functions obtained, recourse was made to the compound nucleus theory of nuclear reactions. Rapaport et al, 1959, derived an excitation function for the reaction  $Zn^{64}(n,p)Cu^{64}$  by means of the statistical theory using a black square well nuclear model with  $r_0 = 1.5$  Fermis and level densities derived from a) the charged particle data of Buechner et al, 1954, and b) a Fermi degenerate gas model. However, both of these approaches lead to cross-sections which are smaller than the experimental cross-sections by a factor of approximately five.

Similarly, Gonzalez et al, 1960, have derived theoretical excitation functions for the reaction  $\text{Ni}^{58}(n,p)\text{Co}^{58}$  using a) a square well potential with  $r_0 = 1.5$  fermis and experimental level densities, b) a diffuse edge potential with Saxon-Woods parameters and experimental level densities, and c) a square well potential with  $r_0 = 1.5$  fermis and a Weinberg and Blatt, 1953, expression for the level densities (an exponential level density formula based upon the Fermi degenerate gas model.). Energy corrections for the pairing energy of even numbers of protons and neutrons were made; also, the effect of the closed proton shell in  $\text{Ni}^{58}$  was considered in a manner similar to that of Kaufman, 1960, in a study of the  $(p,\alpha)$ ,  $(p,2p)$  and  $(p,pn)$  reactions in  $\text{Ni}^{58}$  near threshold. Agreement between experimental and theoretical cross-sections was somewhat better in the case of the Weinberg and Blatt approach than in the other two cases, although again as in the case of the reaction  $\text{Zn}^{64}(n,p)\text{Cu}^{64}$  no satisfactory explanation for the cross-sections could be given.

Van Loef, 1961, has found that the cross-sections for the  $(n,p)$  reactions in the even nuclei  $\text{Fe}^{54}$ ,  $\text{Ni}^{58}$  and  $\text{Zn}^{64}$  were much greater than those for the reactions in the odd nuclei  $\text{Ni}^{61}$  and  $\text{Zn}^{67}$ . This is an agreement with the results of Bullock and Moore, 1960, and may be explained as due to the decreased level density in even nuclei targets - a result of the pairing of nucleons - minimizing the competition of  $(n,n')$  reactions. Van Loef also showed that the  $(n,p)$  cross-sections for even-even nuclei, allowing for different  $Q$ -values, i.e. at equivalent energies, showed large variations.

Thus, the cross sections for the reactions  $Zn^{64}(n,p)Cu^{64}$  and  $Fe^{56}(n,p)Mn^{56}$  are an order of magnitude less than those for the reactions  $Fe^{54}(n,p)Mn^{54}$  and  $Ni^{58}(n,p)Co^{58}$ . Van Loef suggests that this may be due to shell effects,  $Fe^{54}$  having a closed shell of 28 neutrons and  $Ni^{58}$  having a closed shell of 28 protons.

Meadows and Whalen, 1963, have measured the excitation function for the reaction  $Ni^{58}(n,p)Co^{58}$  within the neutron energy range 1.04 Mev to 2.67 Mev using the activation technique. They have also determined the isomeric ratio i.e. the ratio of the cross sections for the emission of protons leading to the  $2^+$  ground state and the  $5^+$  meta-stable state at 25 Kev in  $Co^{58}$ . Their results are not in agreement with the results of Gonzales, 1960; the values of Meadows and Whalen for the cross sections are 30% to 60% lower than those of Gonzales in the energy region in which the experiments overlap. These authors have calculated the excitation function of the  $Ni^{58}(n,p)Co^{58}$  reaction using a diffuse edge potential with a spin orbit coupling term and surface absorption by considering the emission of protons leading to the  $2^+$  ground state and  $5^+$  metastable state of  $Co^{58}$  in competition with neutron emission leading to the ground state and  $2^+$  rotational state at 1.45 Mev in  $Ni^{58}$ . It was found that the calculated excitation function was lower than the experimental curve by a factor of approximately 2. Similarly, the isomeric ratio was too low. They suggest that this discrepancy may be corrected by postulating a  $4^+$  level at an excitation energy of approximately 0.2 Mev in  $Co^{58}$ .

Two further studies of the  $Ni^{58}(n,p)Co^{58}$  reaction with low

energy neutrons using the activation technique have been carried out by Barry, 1962, and Nakai, Gotoh and Amano, 1962. The latter workers have found the cross-sections of the  $\text{Ni}^{58}(\text{n,p})\text{Co}^{58}$  and  $\text{Zn}^{64}(\text{n,p})\text{Co}^{64}$  reactions for neutron energies from 1.8 Mev to 4.8 Mev. Absolute cross sections were obtained by monitoring the neutron beam by means of detecting recoil pulses in a plastic scintillator and by direct calculation from the known  $\text{H}^2(\text{d,n})\text{He}^3$  cross-section. Both excitation functions increase monotonically with neutron energy. The experimental results were compared with theoretical calculations which were performed using an evaporation model with a semi empirical level density obtained from magnetic spectograph data. In the case of the  $\text{Zn}^{64}(\text{n,p})\text{Cu}^{64}$  reaction the experimental values agree with the theoretical values of the cross-sections fairly well, but in the case of  $\text{Ni}^{58}(\text{n,p})\text{Co}^{58}$  there is a discrepancy of a factor of two, the theoretical values being the lower.

Barry, 1962, has determined the  $\text{Ni}^{58}(\text{n,p})\text{Co}^{58}$  cross section at several energies between threshold at 1.8 Mev by irradiating a nickel sample in a known flux of monoenergetic neutrons and measuring the amount of  $\text{Co}^{58}$  formed. Flux monitoring was carried out by placing a  $\text{U}^{235}$  fission counter behind the samples to be irradiated; the fission counter was calibrated in a known flux of 14 Mev neutrons from the D-T reaction, the 14 Mev neutron flux being determined by detection of the associated alpha particle from the D-T reaction. Barry finds that the excitation curve increases monotonically with energy to a maximum at 8 Mev; it then drops to the values obtained

at 14 Mev. Near threshold <sup>the</sup> values for the cross-sections agree approximately with those of Gonzales, 1960.

#### II.4. Nuclear Emulsion Technique.

This technique has been extensively applied to the study of (n,p) reactions induced by neutrons in the 14 Mev range. (Brown et al, 1957; Allan, 1957, '58, '59, '61; March and Morton, 1958, a,b,c; Peck, 1957,61; Haling et al, 1957; Armstrong and Rosen, 1960; and Kumabe and Fink, 1960). Since angular and energy distributions are obtained simultaneously, the technique is very useful, giving the maximum information from relatively few events. However, this advantage is offset by the time and labour involved in the analysis of the plates. Protons of energies down to 1 Mev may be detected, although some difficulty may be encountered in distinguishing low energy protons and alpha particles. (Cevolani et al, 1960).

Very little use has been made of the emulsion technique in the study of (n,p) reactions at low neutron energies. Urech, Jeannet, and Rossel, 1961, have measured the energy and angular distribution of the (n,p) and (n, $\alpha$ ) reactions in Ca<sup>40</sup> bombarded with neutrons of energy 6Mev. Their experimental arrangement consisted of Ilford K2 emulsion plates which were loaded with grains of Ca Si<sub>2</sub> (diameter 5 $\mu$ ) and SiO<sub>2</sub> as a clinical stabiliser. However, they experienced difficulty in the separation of the proton and alpha particle tracks because the Ca Si<sub>2</sub> grains upset the homogeneity of the development of the plates. The most interesting fact of their results was the lack of any evidence of direct reactions, i.e. there is no evidence

of forward peaking in the angular distribution of the reaction products.

## II.5. Counter Techniques.

The accumulation of information under adverse conditions of background can best be realised by use of counter telescope techniques. This technique was first applied to the study of (n,p) reactions by Colli et al, 1956, using 14 Mev neutrons; their telescope consisted of two or three proportional counters and a CsI(Tl) detector. The counter technique has been successfully used in Glasgow by Lynch (private communication) and by Irfan and Jack, 1963, in a study of (n,p) and (n, $\alpha$ ) reactions respectively; both studies were carried out at 14 Mev.

During the course of the present programme, work on the  $\text{Ni}^{58}(n,p)\text{Co}^{58}$  was published by Konijn and Lauber, 1963,. These workers, using an experimental arrangement consisting of a  $\text{Ni}^{58}$  target foil placed in close proximity to a semiconductor detector, have investigated the variation of the  $\text{Ni}^{58}(n,p)\text{Co}^{58}$  and  $\text{Si}^{29}(n,\alpha)\text{Mg}^{24}$  cross-sections in the neutron energy region 2.2 Mev to 3.8 Mev. During the course of their experiment they changed the geometry of their detector system. Initially, the distance between the target foil and the surface of the semiconductor counter was 7 mm, and the nickel target to neutron source distance was 3 cms. The final target-counter distance was 2.22 mm. and the target-neutron source was 1.75 cm. During the first series of irradiations all collimators were tantalum, and the target backing material was platinum. No absolute cross section measurements were made during

these irradiations. During the final irradiations all shields and collimators that 'viewed' the detector were replaced by gold.

Absolute monitoring was obtained by means of the detection of the recoil protons from a polythene foil placed in the flux of neutrons. The neutron source consisted of a  $\text{Li}^7$  target bombarded with protons ( $\text{Li}^7(\text{p},\text{n})\text{Be}^7$ , threshold 1882 Kev). The use of this neutron source required a correction for a second neutron group present when the energy of the incident proton was greater than 2.37 Mev. The total energy spread of the neutrons was of the order of 30 Kev due to the target thickness, while the energy spread due to geometrical considerations was approximately 60 Kev. The total energy spread was  $\pm 30$  Kev at  $E_n = 2.3$  Mev and  $\pm 38$  Kev at 3.8 Mev. For the main part of the experiment, the target consisted of a natural nickel target having a thickness  $7.1 \mu\text{m}$ , while in a subsidiary experiment the target consisted of 99.5%  $\text{Ni}^{58}$ ,  $1 \mu\text{m}$  thick. The semiconductor counter was 1030 ohm-cm silicon with a sensitive area, of 12 mm diameter.

The excitation function obtained by Konijn and Lauber for the reaction  $\text{Ni}^{58}(\text{n},\text{p})\text{Co}^{58}$  showed marked fluctuations. The  $\text{Si}^{29}(\text{n},\alpha)\text{Mg}^{24}$  reaction in the semiconductor counter also showed fluctuations with varying neutron energy. Using a level density formula (Ericson, 1960) for the equidistant spacing model, and pairing energies from Gardner, 1962, an attempt was made to correlate the fluctuations with that of the levels in compound nucleus in a manner similar to that of Agodi, et al, 1962. The latter have found that similar strong fluctuations in excitation curves may be attributed to level density fluctuations

in the compound nuclei  $Al^{28}$ ,  $P^{32}$  and  $S^{33}$ . The relative deviation of the cross sections from the average cross sections, assuming a Poisson distribution for the levels, was estimated. However, Konijn and Lauber were unable to explain their results on these grounds. The possibility of Ericson fluctuations (Ericson, 1960) have been considered. However, it was found that the fluctuations could not be due to this effect.

## II.6. Conclusion.

Near the reaction threshold a quantitative explanation of the  $Ni^{58}(n,p)Co^{58}$  cross section has been given by Trier, 1962. He calculated the excitation function for the reaction by considering particle emission to individual levels in the residual nuclei. Proton emission to the ground state and 25 Kev state of  $Co^{58}$  and neutron emission to the ground state of  $Ni^{58}$  was considered. The calculation was based on the theory of Hauser and Feshbach (1952), and Wolfenstein, 1951, and used a diffuse edge nuclear potential to determine the penetrabilities of the protons and neutrons. His results agree quite well with the results of Barry, but not with those of Gonzalez. The results of Nakai et al. show an excitation curve having a different slope from that calculated by Trier. In general, the results of the measurement of the excitation curves for the  $Ni^{58}(n,p)Co^{58}$  reaction show a wide variation in magnitude and slope, although there is a general tendency to increase with incident neutron energy.

In theoretical calculations the assumptions are usually made that the reaction mechanism through which low energy neutron

reactions proceed is of the compound nuclear type, and, in the case of the  $\text{Ni}^{58}(n,p)\text{Co}^{58}$  reaction, that proton emission leads solely to the known  $2^+$  ground state and metastable  $5^+$  state in  $\text{Co}^{58}$ . With these points in mind an investigation into the energy spectrum and the ratio of the yield of protons into the forward and backward hemisphere for the  $(n,p)$  reaction in nickel, has been carried out. Also, for comparison with the results of other workers, a determination of the absolute cross section at various incident neutron energies was also made. Similar investigations were carried out on the target nuclei  $\text{Fe}^{54}$  and  $\text{Cu}^{63}$  in order that some insight into the influence of shell effects on nuclear reactions might be obtained.

### CHAPTER III.

#### Determination of the Absolute Cross-section, Energy Spectra, and Forward to Backward Yields of Protons from (n,p) Reactions in Ni<sup>58</sup>, Fe<sup>54</sup>, Cu<sup>63</sup>.

##### III.1. Introduction

The chief aims of the experimental work described in this section are :-

a) the determination of the energy spectra and absolute cross-section of the (n,p) reactions in the medium weight targets Ni<sup>58</sup>, Fe<sup>54</sup>, and Cu<sup>63</sup> bombarded with approximately monoenergetic neutrons within the energy range of 2.4 Mev. to 3.2 Mev. and

b) the comparison of the cross-sections for the emission of protons in the forward and in the backward direction, with respect to the incident neutron beam, at a neutron energy of 2.4 Mev.

##### III. 2. General Considerations.

Since the Q - value for (n,p) reactions in medium weight elements is generally of the order of zero, the energies of the emitted protons are of the order of that of the incident neutrons i.e. 2 to 3 Mev. One would expect, therefore, that the yield of such (n,p) reactions would be very low, since the energies of the emitted protons are much less than 7 Mev., the approximate Coulomb barrier height in medium weight nuclei. Hence, for the success of the present study, a main requirement is the design of a suitable charged particle ~~particle~~-detection system capable of operation in a high flux of neutrons, and having maximum efficiency and resolution. In practice, a compromise has to be made between the

requirement of adequate resolution and efficiency.

### III.3. Development of a charged-particle detection system.

A preliminary study of the (n,p) reaction produced in a nickel foil bombarded with 3 Mev neutrons was carried out by detecting the emitted protons in a CsI(Tl) crystal. Protons emitted in a small angle ( $\pm 6^\circ$ ) about the direction of the incident neutrons were detected. In order to decrease background produced by neutrons and  $\gamma$ -ray interactions in the crystal, the crystal was made as thin as possible. With a crystal of thickness 0.009" (the range of a  $\sim 5$  Mev proton) it was possible to detect protons of energy greater than  $\sim 1$  Mev. This lower limit was proved by the use of a thin  $de/dx$  proportional counter between the CsI(Tl) crystal and nickel foil, operating in coincidence with the energy counter. The proportional counter was rectangular in cross-section, 1 cm. deep, and filled to a pressure of 10 cm Hg with a mixture of 10%  $Co_2$  and 90% Argon.

However, this detection system had several disadvantages:-

- a) The method of grinding down the crystal to the required thickness produced non-uniformities in the crystal surface.
- b) The resolution for the detection of 3 Mev protons was of the order of 25% F.W.H.M. (Full Width Half Maximum) i.e. some difficulty would be experienced in distinguishing between proton groups of energy in the region of 3 Mev, and separated by 750 Kev.
- c) The use of a proportional counter increases the maximum

distance between the target and the energy counter, thus decreasing the efficiency of the system.

To overcome the difficulties associated with the use of a CsI(Tl) crystal, it was decided to investigate the possibility of using a silicon semiconductor counter as an energy detector. Since part of the background effect in the detecting system is due to electrons formed by gamma-ray interactions in the energy counter, (gamma-rays always being present as a result of neutron reactions, and from the neutron source) the use of a detector of low atomic mass serves to lower this source of background.

It was found that, in general, commercially available semiconductor counters were encapsulated in a material of low atomic weight in such a way that charged particles produced in the material as a result of neutron reactions could enter the counter and give rise to unwanted pulses. To avoid this difficulty one would have to place a  $dE/dx$  counter between the solid state counter and the target, so that only those charged particles coming from the direction of the target would register as a coincidence pulse. In order to avoid the necessity of using a coincidence system, the semiconductor counter was developed in the laboratory at Glasgow University in such a way that the amount of material in front of the sensitive area of the counter was a minimum. The method of manufacture of the counters from silicon slices was that developed by Dearnley, 1961. The counters consisted of a slice of 2,000 ohm-cm silicon having a diameter 0.75" and thickness 1 mm. approximately.

The sensitive region of the counter was defined by a gold evaporation of diameter 1.2 cm. The gold layer had a thickness of the order of  $50 \mu\text{g}/\text{cm}^2$  i.e. the energy lost by a 3 Mev proton passing through the gold surface is negligible. Electrical contact to the front surface of the counter was made through a gold filament fixed to the edge of the gold evaporation by means of a small amount of silver paste. An aluminium evaporation on the rear surface of the counter was held at earth potential by means of a brass rod attached to the centre of the rear surface with a silver paste. The brass rod, diameter  $\frac{1}{8}$ " , was perpendicular to the counter face, and served as a support for the counter.

The advantages of using a semiconductor counter as a charged particle detector may be stated as :-

- a) The resolution obtainable with the semiconductor counter was of the order of 1% F.W.H.M. for charged particles of energy 3 Mev. (c.f. Fig. III.6.). Thus, such a detector, unlike a CsI(Tl) crystal, is ideally suited to the study of (n,p) reactions leading to separated levels in the residual nucleus.
- b) The pulse height output from the semiconductor counter depends solely on the energy dissipated in the depletion<sup>region</sup> of the counter, and is independent of the type of charged particle incident upon the counter. The fact that the pulse height output is proportional to the energy of the charged particle stopped in the counter greatly assists in the analysis of results.
- c) The depletion depth of the counter (i.e. the sensitive volume)

can be controlled easily by means of the applied bias voltage. Thus, the sensitive volume of the counter can be minimized so that the range of the most energetic particle to be detected is less than the depletion depth. This procedure has the advantage of keeping the background count rate in the counter to a minimum.

d) Since the surface of the counter is formed by etching, a uniform surface is formed. Also, the gold evaporation serves to define accurately the sensitive area of the counter.

e) The semiconductor counter is capable of high stability of operation. It was found possible to operate the counter system for long periods of time without any appreciable drift in gain of the system.

#### III.4. Design of Apparatus for Measurement of Excitation Functions and Forward to Backward Yields.

Preliminary studies of the yield of the  $^{58}\text{Ni}(n,p)^{58}\text{Co}$  reaction using a detection system consisting of a  $\frac{dE}{dx}$  proportional counter and a solid state energy counter, and a typical neutron flux of  $1.6 \times 10^7$  neutrons per second per steradian showed that the yield was very low, especially when one was dealing with neutrons of energy less than 3 Mev. Since the measurement of the excitation curve required studying the reactions at several different neutron energies, a process which could involve a large amount of machine time, it was decided to increase the efficiency of the detector system at the expense of resolution. (The investigation of the energy spectra of the

emitted protons was carried out with a detection system having increased resolution.) Because of the corresponding decrease in efficiency the energy spectra were obtained at only 1 neutron energy.

A schematic diagram of the apparatus designed for the measurement of the excitation functions and forward to backward yield is shown in fig. III.1. Basically, the apparatus consists of an experimental target, in the form of a thin foil, situated close to, and parallel to, a semiconductor counter (A, Fig.III.1). The target assembly consisted of a target foil clamped between two gold foils of thickness  $0.002''$ , and two bismuth plates (B, Fig.III.1). The effective area of the target was defined by the aperture, diameter 1.2 cm. in one of the gold foils in contact with the target material. One of the bismuth plates had a corresponding aperture of diameter 1.7 cm. The target assembly was firmly held together by means of three countersunk screws. The target and semiconductor counter were mounted accurately parallel in such a position that the line joining their centres was perpendicular to the planes of the target foil and counter. The separation of the targetfoil and the front face of the semiconductor counter was 3 m.m., giving a mean solid angle of  $2.409$  steradians for the detection of charged particles emitted from the target. A brass rod supporting the semiconductor counter was fixed rigidly to a brass base-plate. Electrical contact between the counter and the electronic system was made through a 'kovar' seal (C, Fig. III.1) in the base-plate.

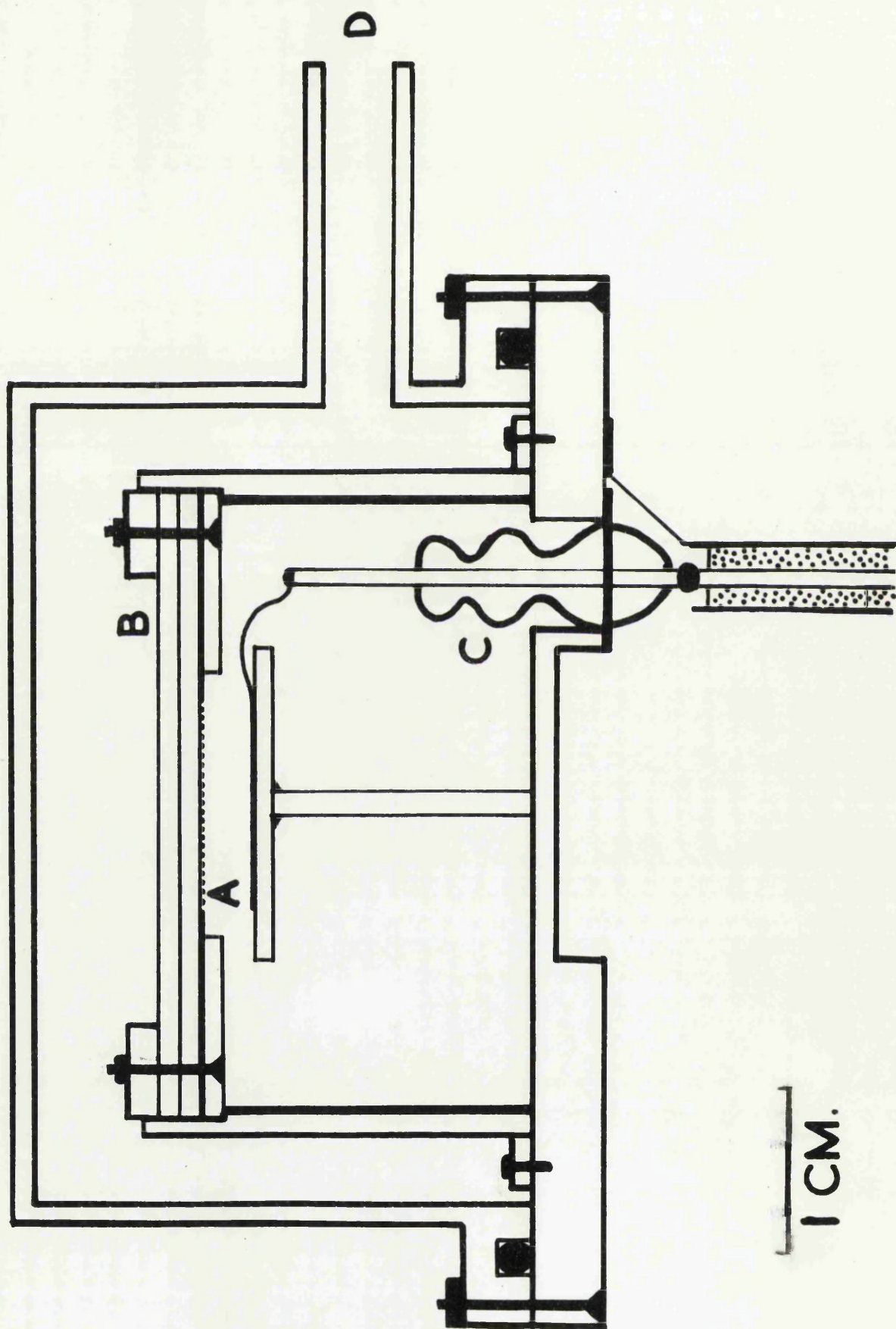


Figure 111.1. Apparatus for measurement of excitation curves.

Also, attached to the base-plate was a brass cylinder, coaxial with the line joining the centres of the counter and target, which served as a support for the target assembly. The target assembly was held in position on a ledge inset into the cylinder wall by means of spring clips. This arrangement enabled the easy removal of the target assembly, and ensured that the target-counter separation could always be <sup>re</sup>produced accurately. The target-counter assembly was housed in a brass can attached to the base-plate by an O-ring seal. The apparatus could be evacuated through the port D (Fig. III.1)  $\frac{1}{4}$

Several steps were taken in the design of the apparatus to minimize the effect of background. Evacuation of the apparatus was considered necessary since the pressure of air would give rise to charged particles and would also cause an appreciable energy loss in the passage of the protons from the target to the counter. Also, all materials that could be 'seen' by the semiconductor counter were materials of high atomic mass, and, hence, had a low (n,p) cross-section. Thus, the target assembly consisted of bismuth plates and gold foils, both materials having higher atomic mass than the medium weight target nuclei being studied. The inner surface of the brass cylinder was lined with lead of sufficient thickness (0.02") to stop protons produced in the brass. In order to minimize the effect of neutron attenuation and scattering those parts of the brass container that lay between the neutron source and the target foil were machined to a thickness of  $\frac{1}{16}$ ".

### III.5. Development of the Neutron Source.

Neutrons of energy varying from 2.4 Mev to 3.5 Mev were obtained using the reaction  $H^2(d,n)He^3$ ,  $Q=3.268$  Mev. A beam of deuterons of energy 500 Kev was obtained from the Glasgow University Cockcroft-Walton set. The  $H^2(d,n)He^3$  reaction exhibits a forward peaked angular distribution; the ratio of the neutron yield at  $0^\circ$  to that at  $90^\circ$  as measured by various workers, varies between 3.2 to 5.3 for an incident deuteron energy of 0.6 Mev. (Hunter et al, 1949, Rreston et al, 1954, Cagnon et al, 1956, Fuller et al, 1957, Gonzalez et al, 1960.). The neutron energy also depends upon the angle of emission, being 2.41 Mev at  $100^\circ$  and 3.45 Mev at  $0^\circ$  for an incident (500 Kev) deuteron beam. In order to obtain a neutron yield of suitable intensity, three types of deuteron targets were investigated.

a) A deuterium target was formed by bombarding a piece of copper with a beam of low energy (100 Kev) deuterons. After bombardment for an hour with a beam of 40 micro-amps, it was found that when the beam energy was increased to 500 Kev, the neutron flux had an intensity of  $8 \times 10^4$  neutrons / $\mu$ a emitted into unit solid angle at  $90^\circ$  with respect to the direction of the incident beam. This figure might be compared with a typical flux,  $5 \times 10^6$  neutrons / $\mu$ a steradian, used in a study of (n, $\alpha$ ) reactions at 15 Mev (Chapter VI.). Apart from the low neutron yield, a disadvantage of this type of target is that the thickness (i.e. the depth to which the deuterium layer is formed in the copper) is undefined and is continually changing by diffusion of deuterium into the

copper.

b) A second type of target consisted of a deuterium layer in a thin titanium foil supported on a copper backing. This target, supplied by the Atomic Energy Research Establishment, Harwell, had the advantage of being thin, the incident deuteron beam losing a fraction of its energy in passing through the deuterium layer and, thus, giving a small energy spread in the emitted neutron beam. However, the intensity of the neutron flux obtained was low, being of the order of  $5 \times 10^4$  neutrons /  $\mu\text{r}$ . steradian at  $90^\circ$  to the incident beam direction for a deuteron energy of 500 Kev.

c) With a view to increasing neutron yield, a  $\text{D}_2\text{O}$  ice target was developed. The 'heavy' ice was formed on a horizontal flat surface close to one end of an L-shaped copper rod, the other end of the rod passing through a vacuum seal of the Cockcroft - Walton Set into a bath of liquid nitrogen. The copper bar could be rotated so that the surface on which the deuterium target was to be formed was positioned opposite an inlet in the wall of the accelerator beam pipe. A controlled amount of vapour from an evacuated flask of 'heavy' water passing through the inlet formed a layer of heavy ice on the cold copper bar. The area of the target thus formed was approximately 5 mm x 8 mm. To avoid condensation on the target of impurities from the pumping system of the accelerator, the deuteron beam passed through a copper tube of length 10" which was cooled to a low temperature by means of a liquid ~~by~~ nitrogen bath.

With this target a neutron yield of  $8 \times 10^5$  neutrons /microamp into unit solid angle at  $90^\circ$  to the incident beam direction was obtainable. It was found that the maximum flux was obtained if the deuterium target was renewed after a period of five hours, and the liquid nitrogen bath replenished every hour. A deuterium target formed in this way is a thick target, the deuterium beam losing all its energy in the layer of heavy ice. Thus, there was a large spread in the neutron energy. A large energy spread insures that a large number of states are excited in the compound nucleus, a necessary condition for the application compound nuclear statistical theory. (Chapt. I.) The neutron energy spreads were calculated using the data of Wenzel and Whaling, 1952, for energy loss of deuterons in heavy ice. Values of the differential cross-section for  $H^2(d,n)He^3$  reaction used in calculation were taken from Preston et al, 1954. The dependence of the neutron energy spread on the angle of emission of the neutron is a result of the kinematics of the  $H^2(d,n)He^3$  reaction. It will be noted from Fig. III.2. that the neutron energy spread decreases as the angle of emission,  $\psi_n$ , is increased. The areas under the curves shown in Fig. III.2. are a measure of the number of neutrons emitted at each angle for a constant beam current. A correction for the effect of the neutron energy width on the excitation curves can be made, as shown later. (Appendix A.)

### III. 6. Neutron Flux Monitoring.

Having obtained a neutron flux of sufficient intensity, the

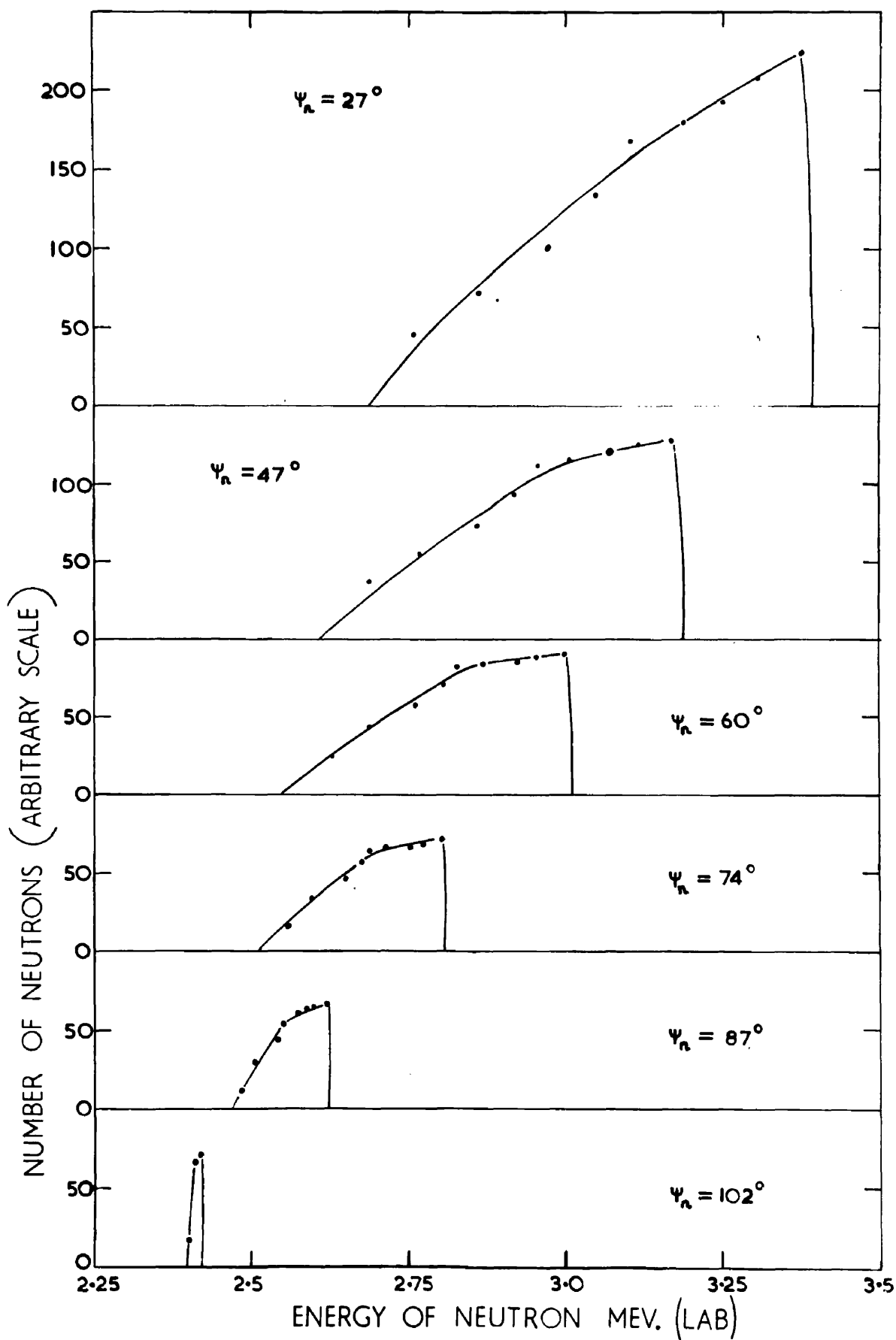


Figure 111.2. Dependence of energy spectrum of neutrons on angle of emission.

problem of monitoring the flux remains. Since one of the chief aims of the experiment was to obtain absolute cross-sections, it was necessary to know the magnitude of the flux accurately.

If the neutron flux at a neutron monitor is known, one can calculate the neutron flux at the position of the experimental target provided that the distances of the neutron monitor and the target from the neutron source are known and are constant. During preliminary investigations of the neutron flux obtainable from a deuterium target, it was found that the deuteron beam could strike the deuterium target at different positions during the course of several irradiations. Since the 'heavy' ice target was rectangular in shape with dimensions 5 mm  $\times$  8 mm, the beam drift could give rise to an error of 20% in the determination of the neutron flux at a detector situated at 2 cm. from the centre of the neutron source. To avoid this difficulty, two neutron monitors were used. One monitor, situated at a distance of 13.3 cm. from the neutron source, and detecting neutrons emitted at an angle of  $64^\circ$ , was relatively insensitive to fluctuations in the position of the source of neutrons. The second neutron monitor was placed behind, and on the same axis as, the experimental apparatus. The latter monitor was sensitive to variations in the position of the neutron source, especially when the neutrons to be detected were emitted in the plane of the 'heavy' ice target. The ratio of the counting rates in the two monitors enabled

the mean position of the neutron source to be determined, which, when combined with the counting rate with the monitor behind the experimental apparatus, gave the absolute value of the neutron flux at the target foil being studied. It was estimated that the error in determining the neutron flux was reduced to  $\pm 6\%$  with the use of the two neutron monitors.

Both neutron monitors operated on the principle of detecting the recoil protons from a thin polythene foil ( $3.8 \text{ mg/cm}^2$ ) bombarded with neutrons. The recoil protons were detected by means of a CsI(Tl) crystal. In both cases the diameter of the polythene and the CsI(Tl) crystal was  $0.75 \text{ cm}$  and the separation between them was  $3.4 \text{ cm}$ . The efficiency of the monitors for the detection of neutrons was  $3.02 \times 10^{-7}$  counts per number of neutron / unit solid angle subtended at the neutron source. The efficiency was calculated using the tables of Bame et al, 1957. The spectrum obtained from the neutron monitors bombarded with neutrons of energy  $2.41 \text{ Mev}$  and  $3.17 \text{ Mev}$  are shown in Fig.III.3. It can be seen that even in the worst case, the detection of neutrons emitted at  $102^\circ$  ( $E_n = 2.41 \text{ Mev}$ ), it was possible to set accurately a discriminator level in the dip between the proton peak and the rapidly rising background. Allowing for the errors in the (n,p) scattering cross section in hydrogen, and in the measurement of the dimensions of the monitor etc, the intrinsic accuracy of the neutron monitors was calculated to be  $\pm 3\%$ . Combined with the estimated accuracy in the determination of the position of the neutron source, the overall accuracy in

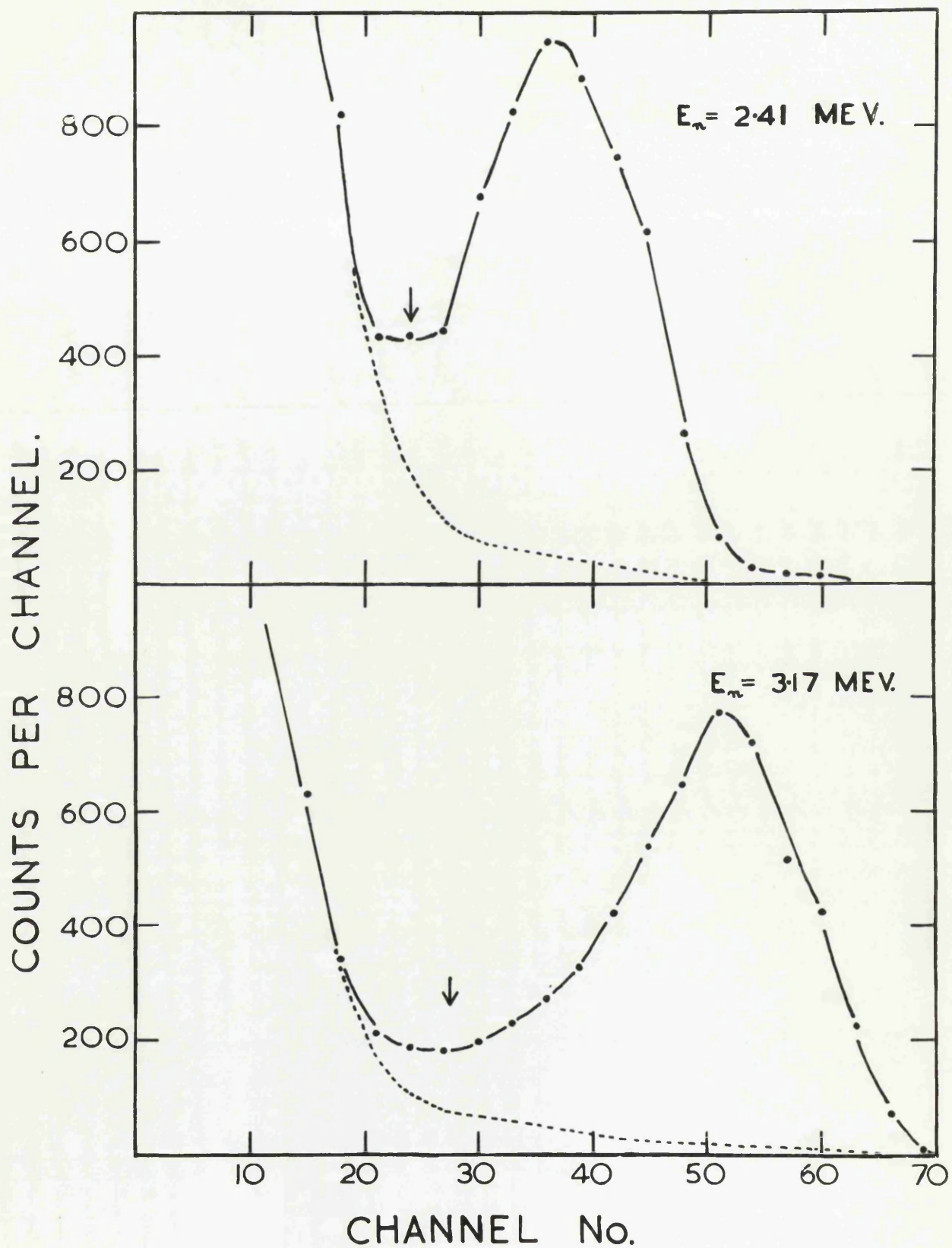


Figure 111.3. Typical energy spectra from the proton recoil neutron monitor. Background spectra shown by dotted lines. Arrows show biasing position.

neutron monitoring was  $\pm 7\%$

### III.7. Arrangement of Apparatus.

The relative positions of the experimental apparatus, neutron monitors and neutron source are shown in schematic form in figure III.4. A particular view of the apparatus is shown in figure III.5.

The distance between the centre of the neutron source and the target foil was  $3.8 \pm 0.1$  cms, the polythene foil of the neutron monitor I (fig:III.4.) being  $4.45$  cms. behind the target foil. The mean solid angle subtended by the target material at the centre of the 'heavy' ice target was  $\pi \times 0.076$  steradians. The experimental apparatus and the neutron monitor behind the apparatus were clamped rigidly on a stand which could rotate in the plane containing the beam pipe and the neutron monitor I about an axis through the centre of the neutron source, allowing the use of neutrons emitted into an angle between  $0^\circ$  and  $150^\circ$ . The experimental apparatus was clamped on the stand in such a manner that it could easily be rotated about an axis in the plane of the target foil and through the centre of the foil. Thus, the apparatus could be set up with the target foil either between the counter and the neutron source or behind the counter, the neutron source-target separation remaining constant. This arrangement allowed the study of the emission of protons from the (n,p) reaction into the forward or backward hemisphere with respect to the direction of the incident neutrons.

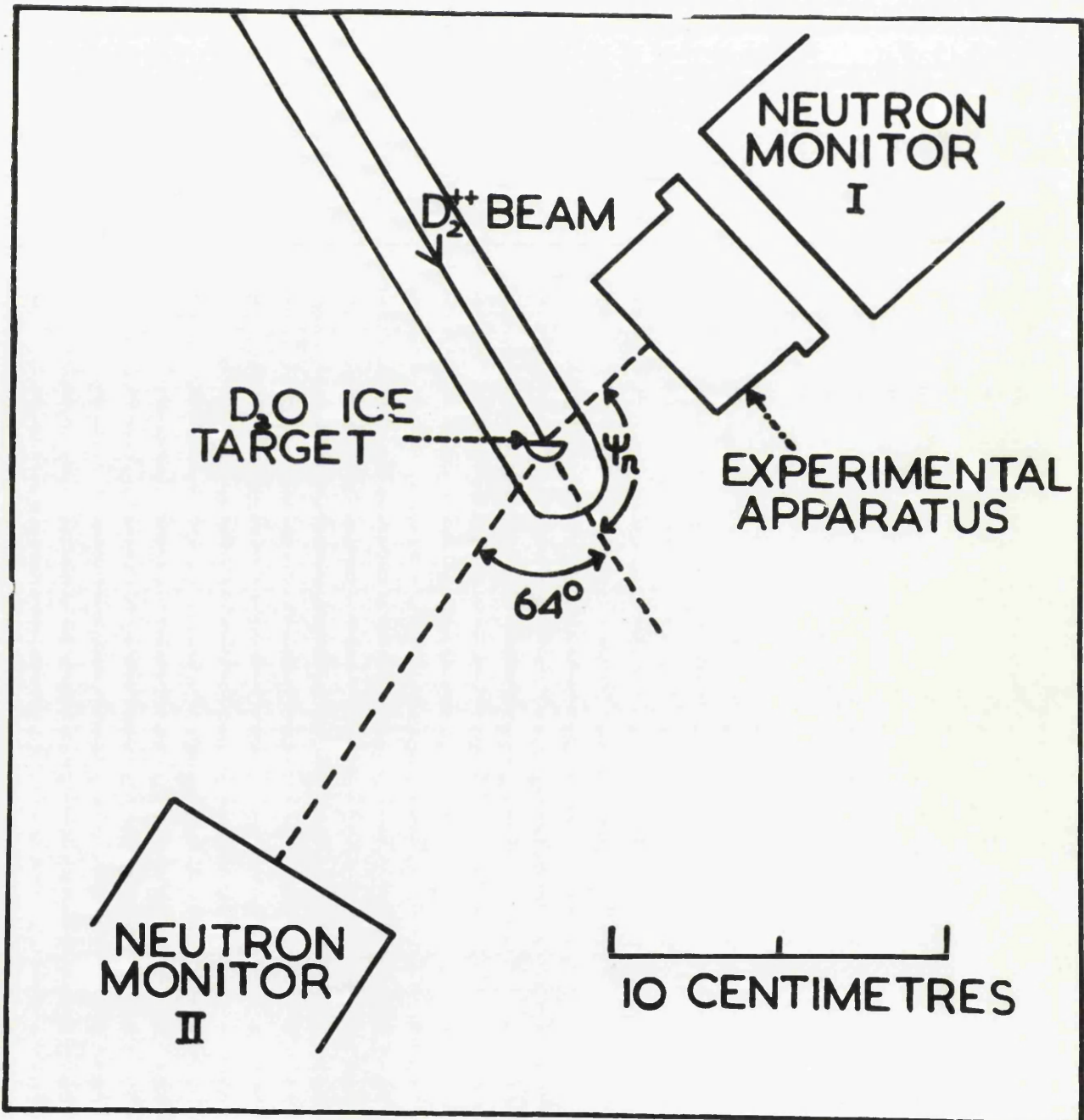


Figure 111.4. Showing relative positions of apparatus in the measurement of the excitation curves.

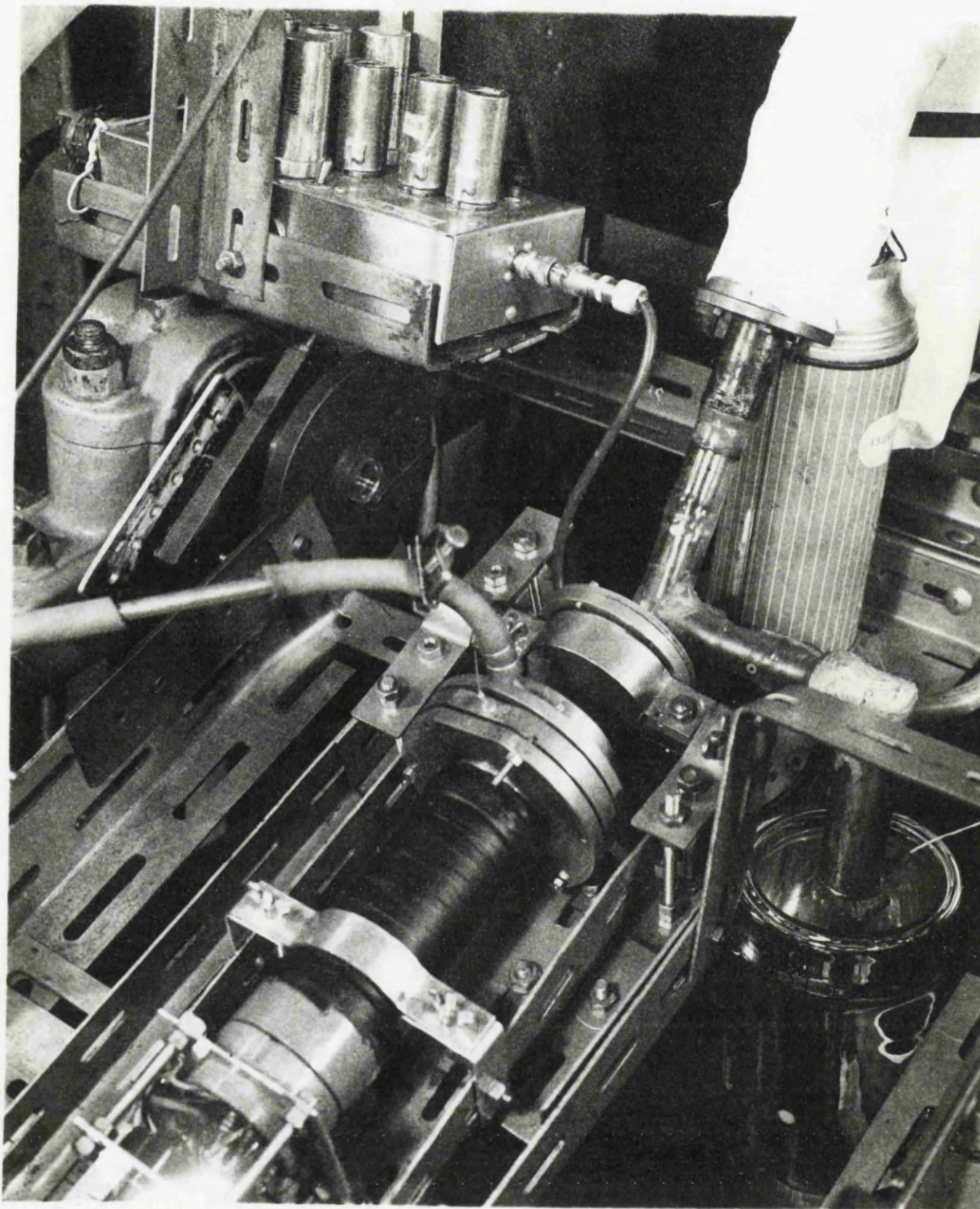


Figure 111.5. A general view of the experimental assembly used in the determination of the excitation curves.

### III. 8. Calibration.

The linearity of the semiconductor counter and the electronics system (described in III.9.) and the magnitude of the output pulse for a given energy loss in the counter were determined using protons and alpha particles from the reactions  $H^2(d,p)H^3$ ,  $B^{10}(d,p)B^{11}$ , and a  $Po^{210}$  alpha source. Figure III.6. shows the energy spectrum obtained from the counter using a combination of these sources (the deuterium target was present as an impurity in the boron target). The separation of the peaks in Fig: III.6. agreed with the calculated energy difference of the various proton and alpha groups. The counter and associated electronic system was found to be linear, and the pulse output dependent on the energy loss in the counter and independent of the type of particle incident upon the counter. Because of this, the stability of the gain of the complete system could be checked quickly during the course of the experiment using a  $Po^{210}$  alpha source.

### III. 9. Accumulation of Data.

Trial irradiations at various neutron energies and with the apparatus in the forward and backward positions showed that the number of background counts obtained when the apparatus was set to detect protons emitted into the forward hemisphere was much greater than when the apparatus was set in the backward direction configuration. This was found to be due to recoil protons originating in the small amount of paste binding the gold filament to the gold surface of the semiconductor counter. Since

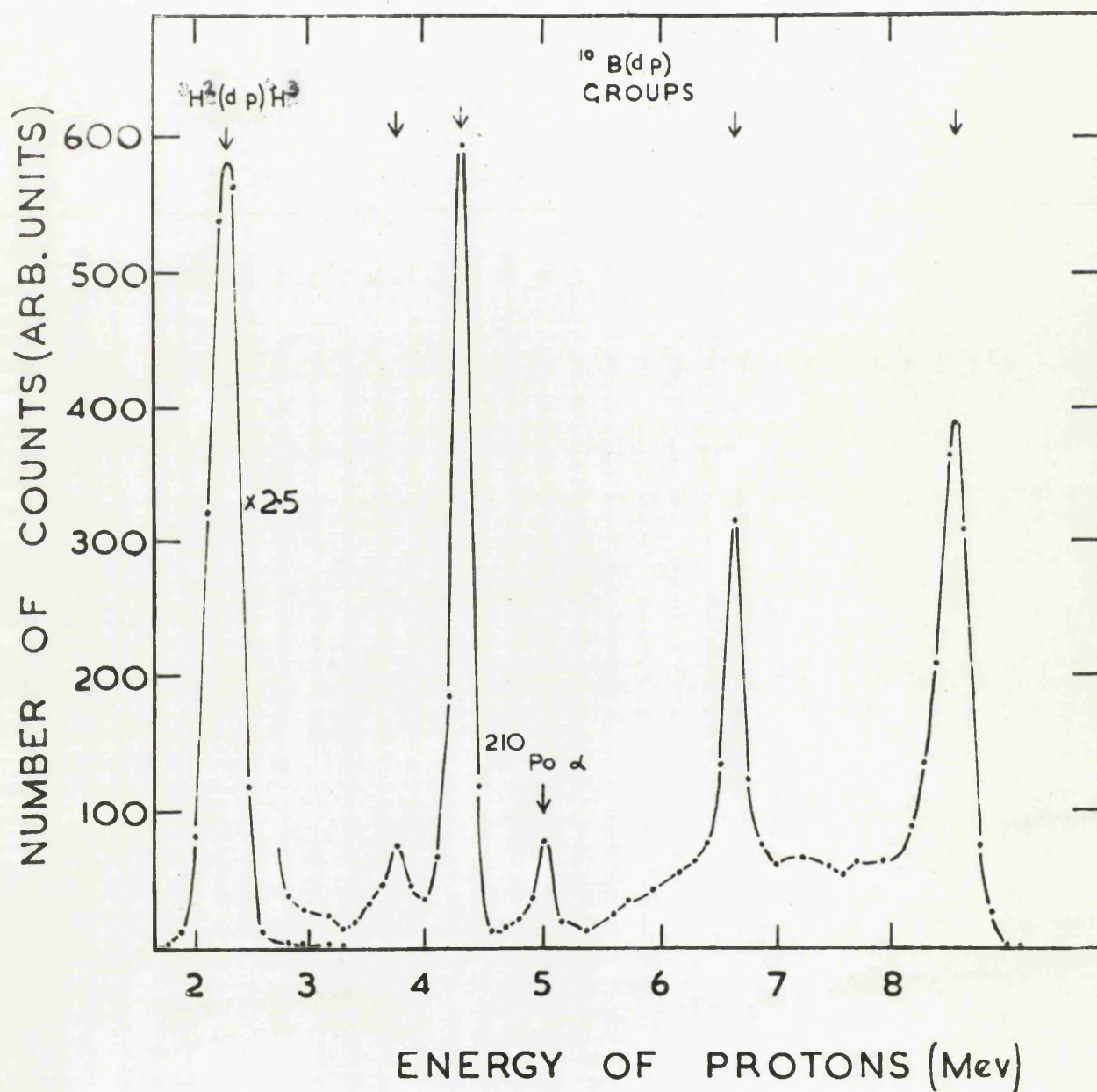


Figure 111.6. Typical semiconductor energy spectrum obtained with a combination of sources.

the measurement of the excitation function required a large number of irradiations at different neutron energies, it was decided to carry out the determination of the excitation function by detecting the protons emitted into the backward hemisphere. This procedure enabled a quicker accumulation of data. A check on the ratio of the proton yield in the forward and backward directions was made at one neutron energy.

The measurement of the absolute cross-section for the emission of protons into the mean solid angle of 2.41 steradians in the backward hemisphere was carried out at 6 angles,  $\psi_n = 102^\circ, 87^\circ, 74^\circ, 60^\circ, 47^\circ$  and  $27^\circ$ . The ratio of the yield of protons into the forward and backward directions was carried out at one angle  $\psi_n = 102^\circ$ . Two target holder assemblies were used, one containing the target material on a 0.002" gold backing foil and the other containing a similar gold foil for background measurements. Target-in and target-out irradiations were alternated during the course of the experiment. To ensure that the true background was measured, irradiations were carried out with the target material in both target holders. One irradiation in general, required irradiation of the target or background assembly for a period of approximately one hour. The liquid nitrogen coolant for the 'heavy' ice target was replenished, and the stability of the counter and electronics checked using a  $\text{Po}^{210}$  alpha source between each irradiation. The  $\text{Po}^{210}$  alpha source was mounted on a brass plate of the same dimensions as the target assembly, thus allowing the  $\text{Po}^{210}$  alpha

to be placed in the experimental apparatus and close to the semiconductor counter. It was found that the detector and associated electronics were stable to less than 1% during the course of an irradiation. At the beginning of each irradiation, the apparatus was evacuated.

The signal from the semiconductor counter was amplified by means of a high gain low noise preamplifier and amplifier, type Ortec, (601 System). The amplified pulses were analysed by means of a C.D.C. multichannel analyser. The bias voltage to the semiconductor counter was applied by means of a facility in the main amplifier. It was found that a bias voltage of approximately 40 volts was required to give the necessary depletion depth in the counter. The depletion depth was adjusted to be greater than the range of the maximum energy of proton expected from a consideration of the neutron energy and Q - value of the (n,p) reaction. It was found that after a period of about 100 hours irradiation in a flux of  $2 \times 10^7$  neutrons/sec. steradian, the detector current increased and the resolution of the counter gradually decreased. Konijn and Lauber, 1963, have also reported a similar effect and suggest that it is due to radiation damage in the counter. The semiconductor counter was replaced by a similar non-irradiated counter before the series of irradiations were completed. A check on the reproducibility of the accumulated data was made and was found to be satisfactory.

### III. 10. Experimental Targets.

Information of the (n,p) reaction was collected for three isotopes:- Ni<sup>58</sup>, Fe<sup>54</sup> and Cu<sup>63</sup>.

a) Ni<sup>58</sup>:- Naturally occurring nickel is composed of five isotopes. The Q - values for the (n,p) and (n, $\alpha$ ) reactions and the isotopic abundance are shown in table III.1. below:

	% Abundance.	(n,p) Q-value.	(n, $\alpha$ ) Q-Value.
Ni <sup>58</sup> :	67.88.	399 Kev.	2888 Kev.
Ni <sup>60</sup> :	26.23.	- 2030 Kev.	1351 Kev.
Ni <sup>61</sup> :	1.19.	- 507 Kev.	3575 Kev.
Ni <sup>62</sup> :	3.66.	- 4437 Kev.	- 429 Kev.
Ni <sup>63</sup> :	1.08.	- 7000 Kev.	—————

For neutrons of energy in the range 2 Mev to 3.5 Mev the only possible (n,p) reactions occurring in natural nickel are Ni<sup>58</sup>(n,p)Co<sup>58</sup> and Ni<sup>61</sup>(n,p)Co<sup>61</sup>. Since Ni<sup>61</sup> is an odd-even nuclei, it is expected that the Ni<sup>61</sup>(n,p)Co<sup>61</sup> cross section would be small due to competition from the Ni<sup>61</sup>(n,n')Ni<sup>61</sup> reaction; Van Loef, 1961, reports that the cross section for the reaction Ni<sup>61</sup>(n,p)Co<sup>61</sup> is only 3.3 Millibarns at 3.3 Mev, the ratio of the (n,p) cross section in Ni<sup>58</sup> to that in Ni<sup>61</sup> being 60:1. Because of the influence of the Coulomb barrier, no appreciable yield for the (n, $\alpha$ ) reactions in the nickel isotopes is to be expected. Thus, it is possible to use a natural nickel target in the study of the Ni<sup>58</sup>(n,p)Co<sup>58</sup> reaction. The target thickness was 1.11 mg/cm<sup>2</sup>.

b)  $\text{Fe}^{54}$ :- Since  $\text{Fe}^{54}$  is only 5.9% abundant in natural iron, an enriched  $\text{Fe}^{54}$  target was used. The target consisted of an evaporation on a gold backing foil and had a thickness of  $1.39 \text{ mg/cm}^2$ .

c)  $\text{Cu}^{63}$ :- Naturally occurring copper occurs as two isotopes,  $\text{Cu}^{63}$  and  $\text{Cu}^{65}$ , with isotopic abundance 69% and 31% respectively. In the absence of any knowledge of the  $\text{Cu}^{65}(\text{n,p})\text{Ni}^{65}$  reaction, an enriched  $\text{Cu}^{63}$  target was used. The target in the form of an evaporation on a 0.001" gold foil had a thickness of  $2.96 \text{ mg/cm}^2$ .

### III.11. Spectra of Emitted Protons.

The spectra of protons emitted into the forward hemisphere as a result of the (n,p) reaction in  $\text{Ni}^{58}$ ,  $\text{Cu}^{63}$ , and  $\text{Fe}^{54}$  are shown in Fig:III.7. The experimental points joined by the continuous solid line are obtained by subtracting the target-out spectra from the target-in spectra. The errors shown are statistical errors allowing for the background subtraction. The spectra shown as dashed lines were obtained by target-out irradiations i.e. background spectra. It will be noticed that the background spectra rise steeply below 2.4 Mev, the energy of the incident neutrons, as one would expect if the background was due to 'knock-on' protons. Each spectra exhibits a large peak with the suggestion of a smaller peak at a lower energy. The energies of the protons forming the peak agree with the calculated energies of protons leading to the ground state of the residual nucleus in each case.

The spectra of protons from the  $\text{Ni}^{58}(\text{n,p})\text{Co}^{58}$  emitted into

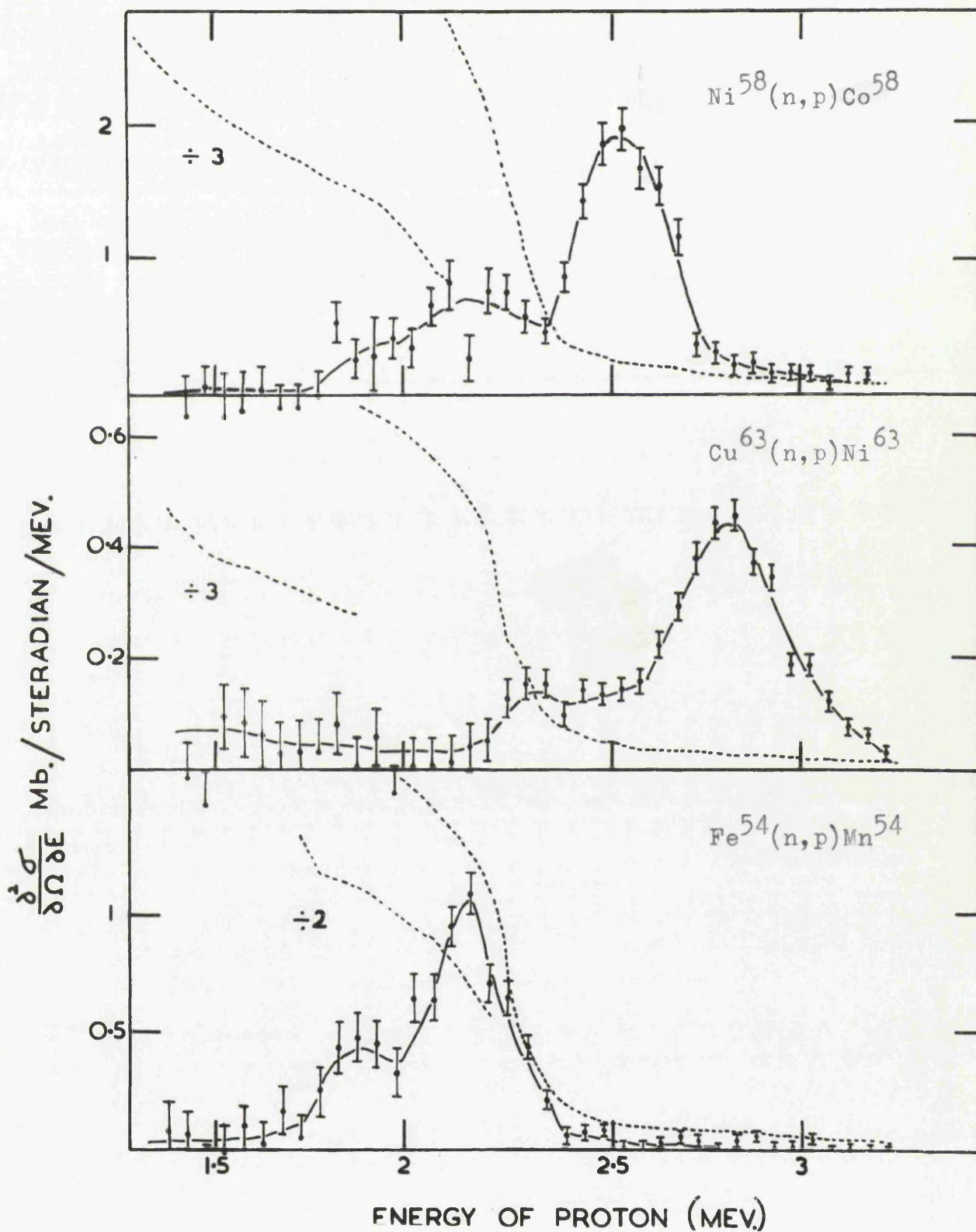


Figure 111.7. The energy spectra of protons emitted into the forward direction from the (n,p) reactions in  $\text{Ni}^{58}$ ,  $\text{Cu}^{63}$  and  $\text{Fe}^{54}$ . Background spectra shown by dotted lines.

the backward hemisphere are shown in Figs: III.8. and III.9. The spectra are for six neutron energies in the range 2.41 Mev to 3.17 Mev. The solid lines represent the target-in spectra less the target-out spectra and the dashed lines are the background spectra. The error bars are statistical. Similarly, figs: III.10. to III.13. show the spectra of protons obtained from the reactions  $\text{Fe}^{54}(n,p)\text{Mn}^{54}$ , and  $\text{Cu}^{63}(n,p)\text{Ni}^{63}$ .

It will be noticed that the background spectra obtained in these cases are much less than those obtained in the forward direction measurements. The presence of the peak in the background is probably due to the reaction  $\text{Si}^{29}(n,\alpha)\text{Mg}^{26}$  in the silicon of the semiconductor counter. This reaction, having a Q - value of -36 Kev, is the only possible charged particle reaction in silicon bombarded with neutrons of energy in the region of 3 Mev. The peak is not present in spectra obtained by means of a detection system incorporating a  $dE/dx$  proportional counter, (chapter IV), showing that the peak is due to charged particle reactions in the semiconductor counter.

The subtracted spectra exhibit similar characteristics to the forward direction spectra, especially at the lower energies, (2.41 Mev and 2.57 Mev). With increasing neutron energy, the width of the main peak increases due to the greater energy spread of the beam. (Fig. III.2.).

### III. 12. Experimental Results.

Absolute cross sections were determined for the emission of

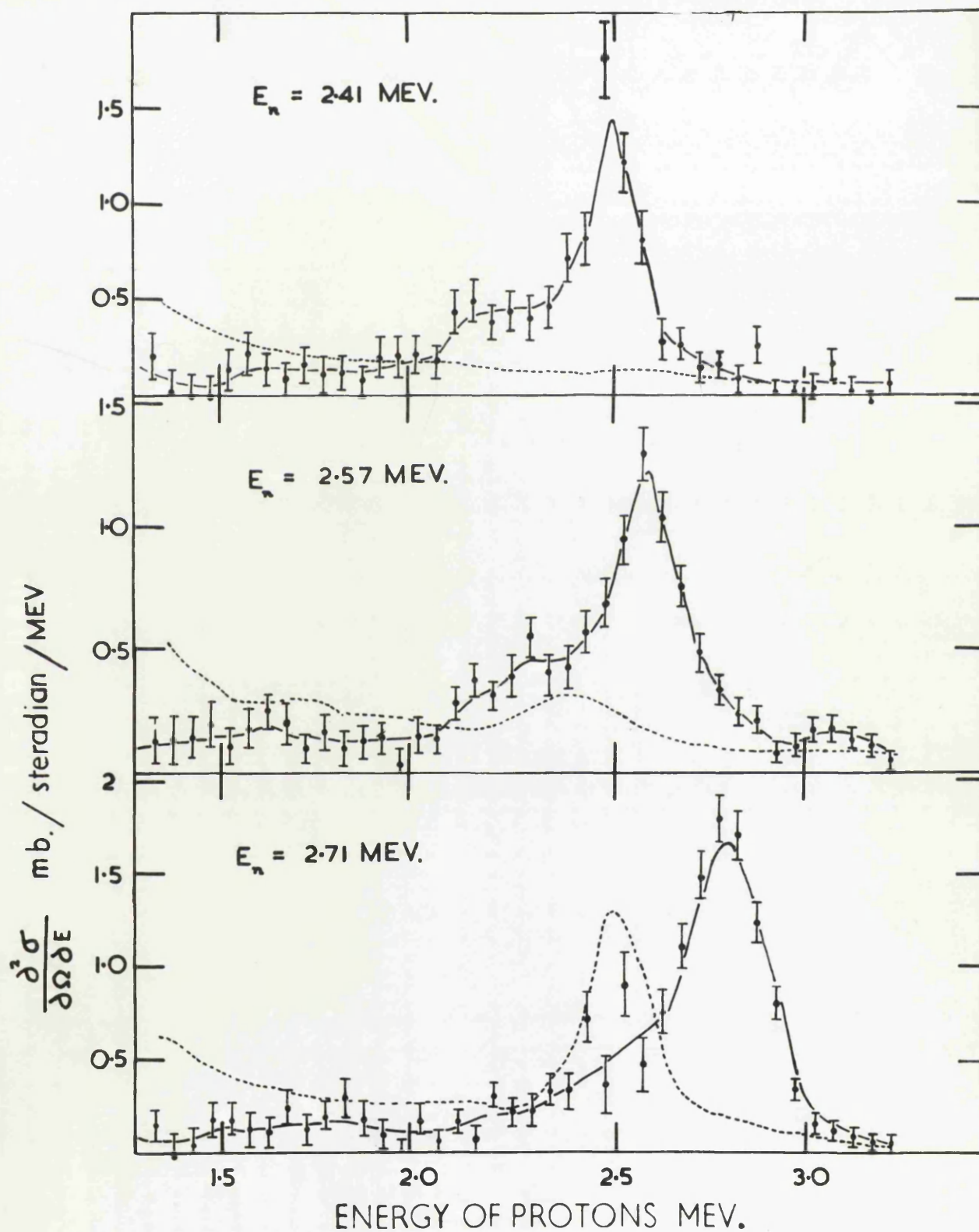


Figure 111.8. The energy spectra of protons emitted in the backward direction from the  $\text{Ni}^{58}(n,p)\text{Co}^{58}$  reaction. Background spectra shown by dotted lines.

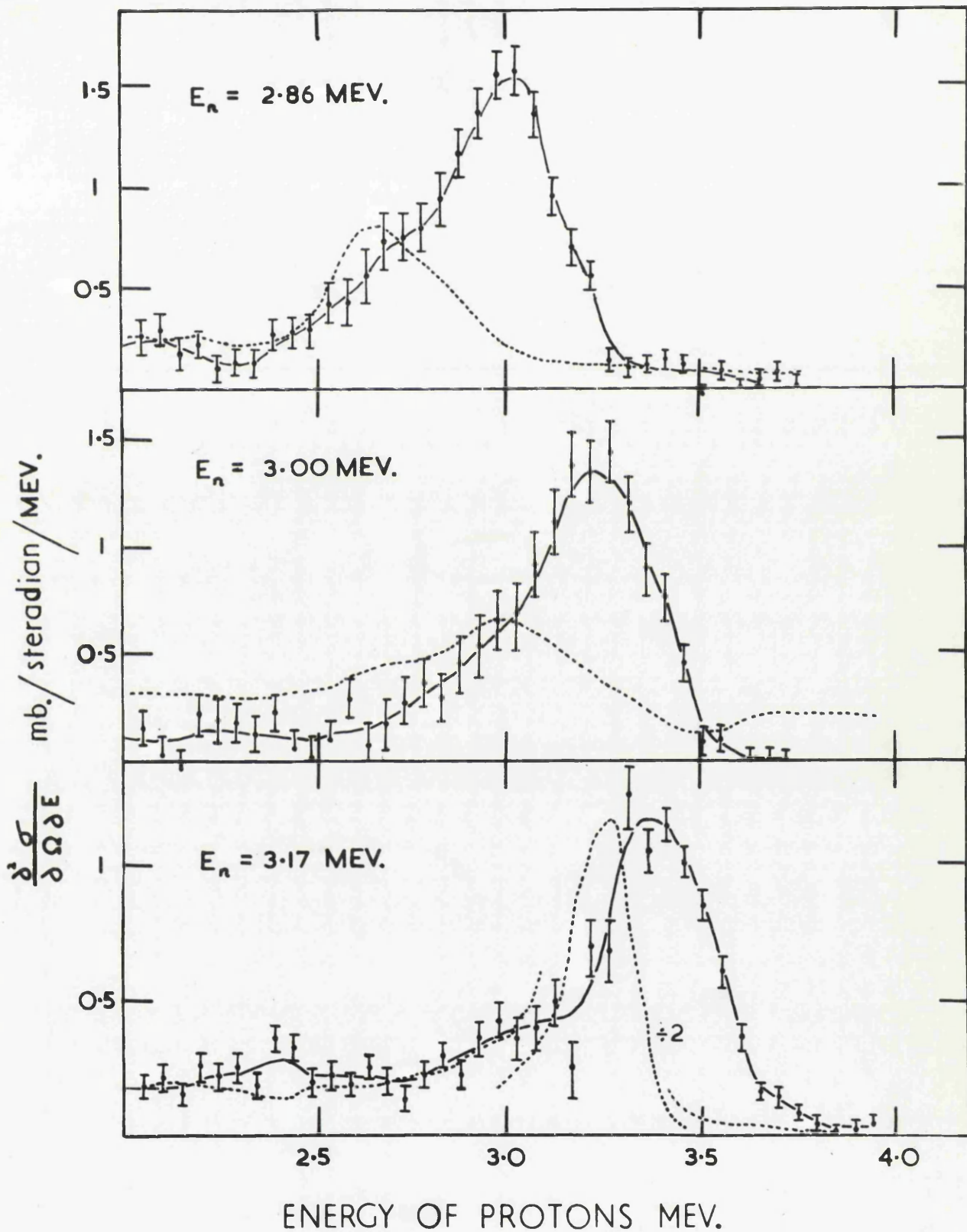


Figure 111.9. Energy spectra of protons from the  $\text{Ni}^{58}(n,p)\text{Co}^{58}$  reaction emitted into the backward direction.

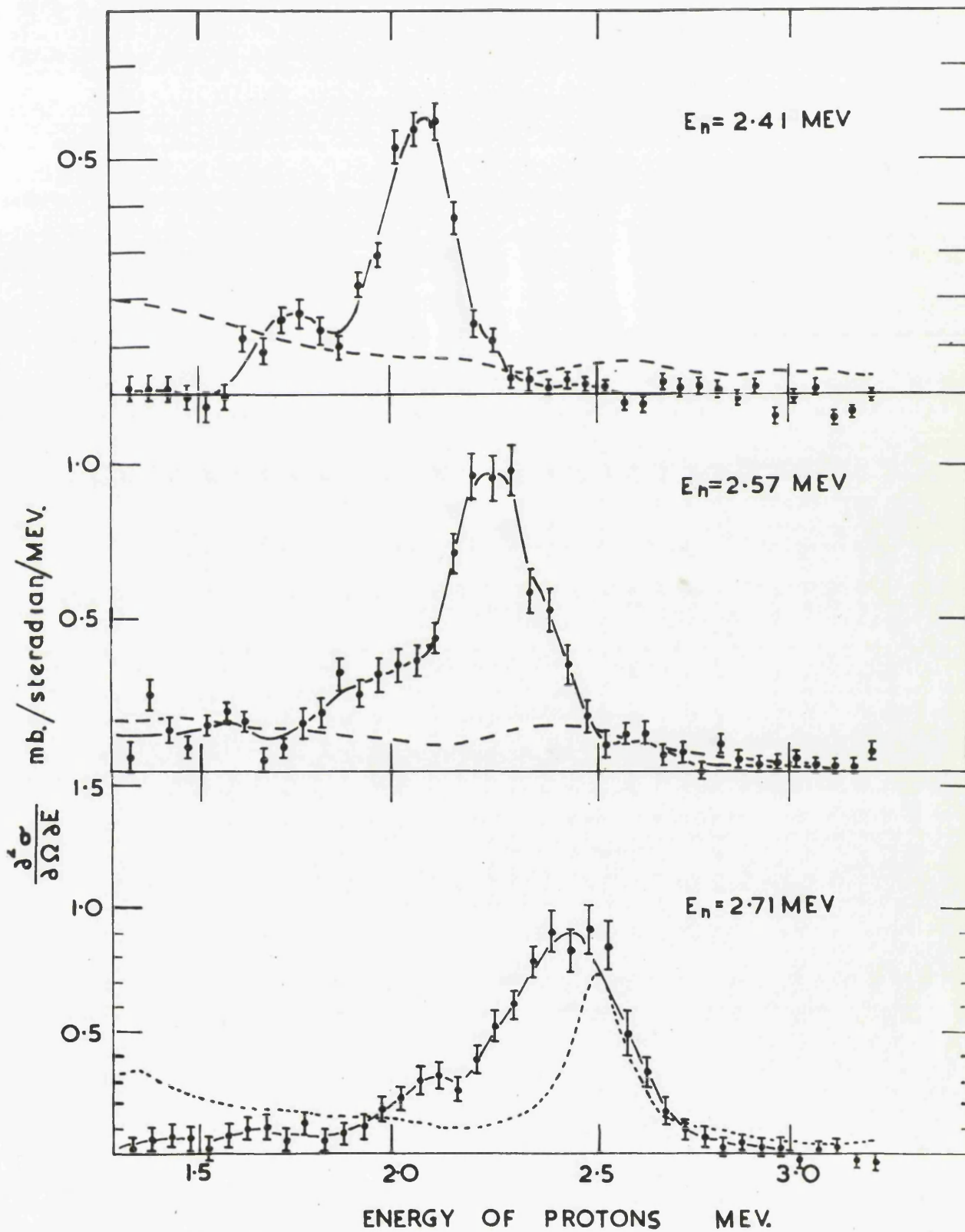


Figure 111.10. Energy spectra of protons from the  $Fe^{54}(n,p)Mn^{54}$  reaction emitted into the backward direction.

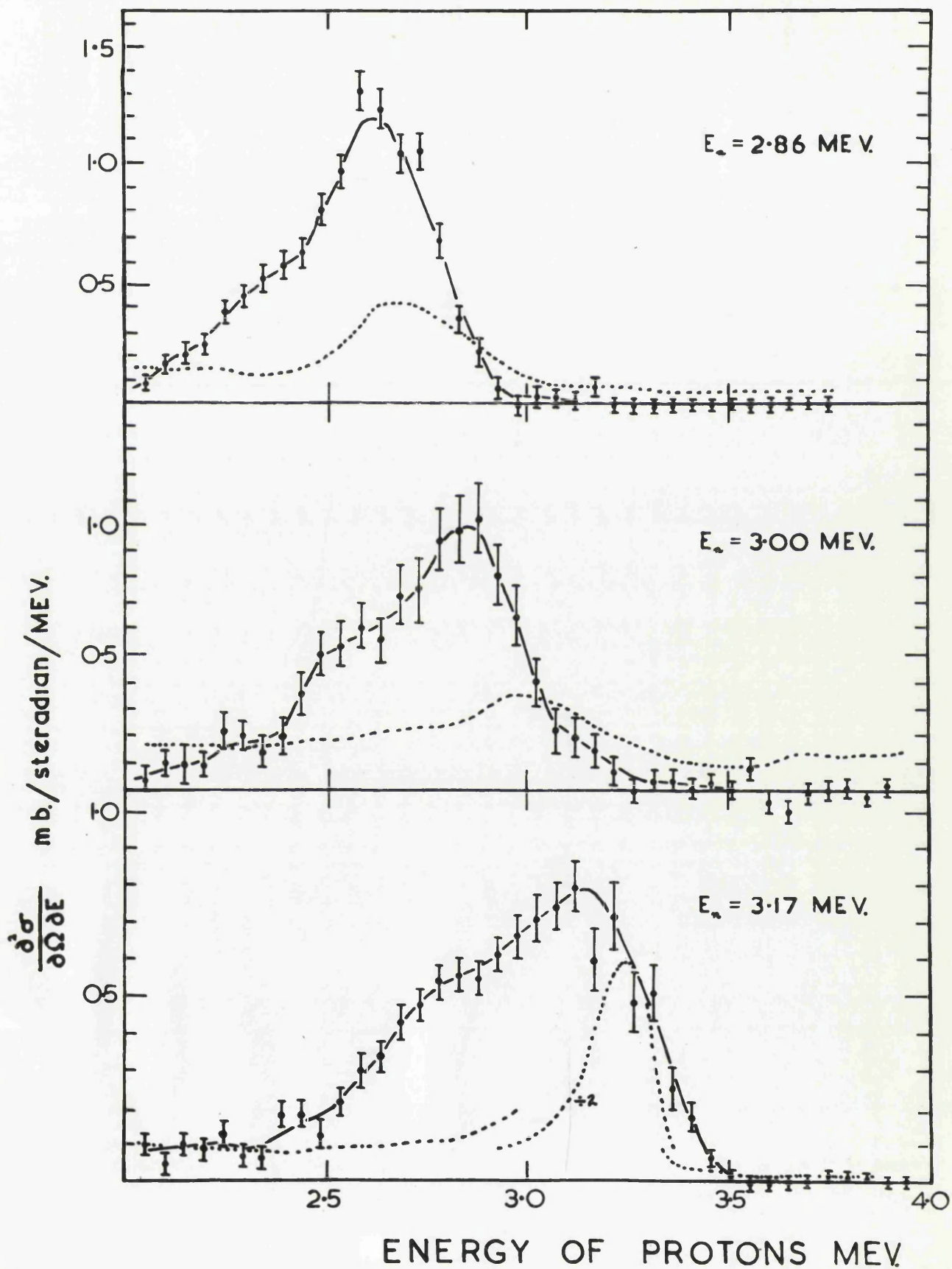


Figure 111.11. Energy spectra of protons emitted into the backward direction from the  $\text{Fe}^{54}(n,p)\text{Mn}^{54}$  reaction.

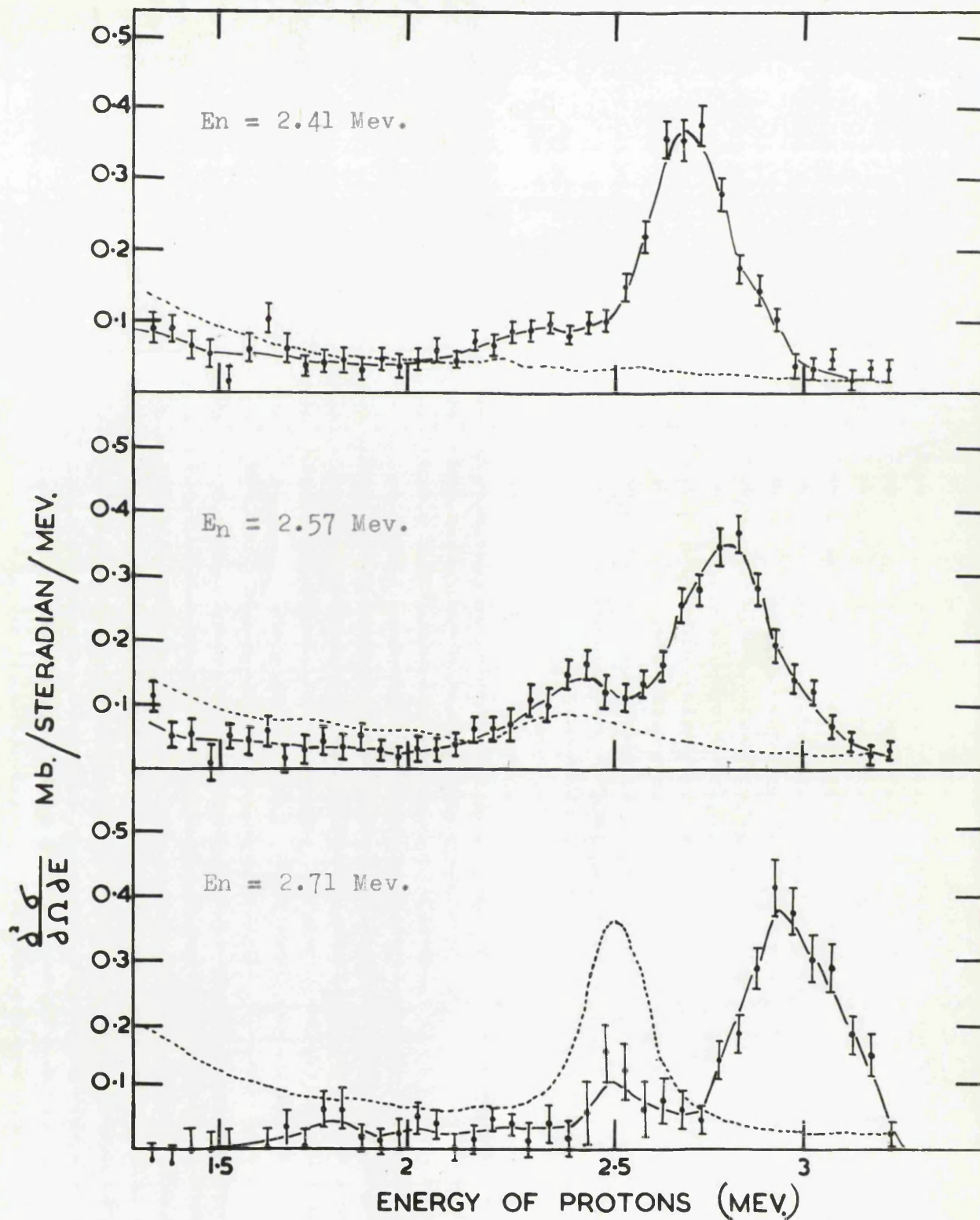


Figure 111.12. Energy spectra of protons, from the  $\text{Cu}^{63}(n,p)\text{Ni}^{63}$  reaction, emitted into the backward direction.

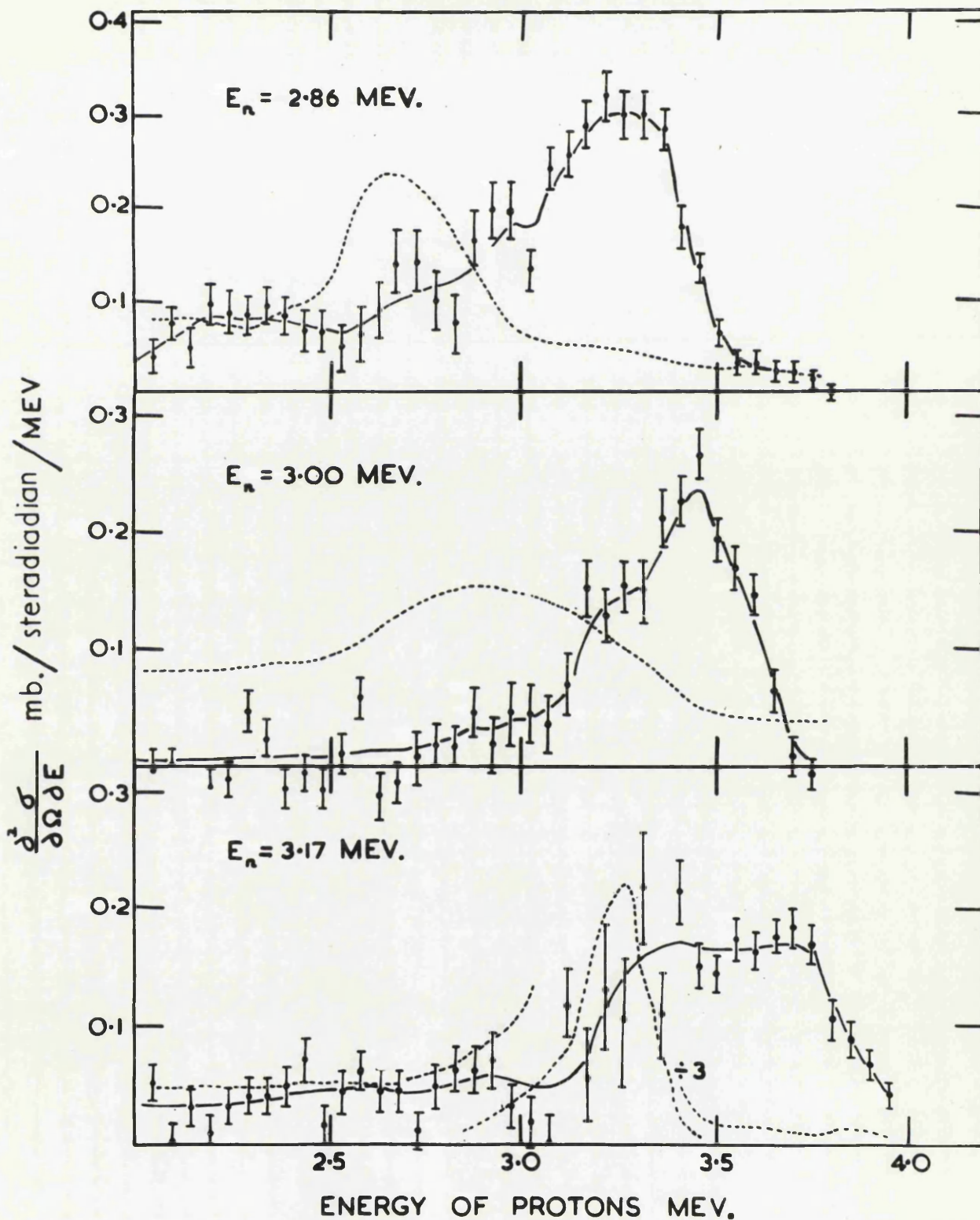


Figure 111.13. Energy spectra of protons emitted into the backward direction from the reaction  $\text{Cu}^{63}(n,p)\text{Ni}^{63}$ .

protons which were within the energy limits of the peaks in the spectra. The cross sections were, therefore, for the (n,p) reaction leading to the ground state or states close to the ground state of the residual nuclei. Total cross sections were determined on the assumption that the emission of protons was isotropic in each case studied. Corrections were applied for the attenuation and scattering of neutrons using the cross-section compilation of Hughes and Schwartz, BNL-325. Centre of mass corrections were evaluated and were found to be small. The cross-sections obtained at various energies for the (n,p) reactions in Ni<sup>58</sup>, Cu<sup>63</sup> and Fe<sup>54</sup> are tabulated in tables III.2., and III.3. The errors in the cross-sections are a combination of statistical errors ( $\leq 5\%$ ) and errors in the neutron monitoring. The spread in neutron energy is due to a) -the 'heavy' ice target thickness and b) -the finite solid angle of acceptance of the target foil for neutrons emitted at different angles  $\psi_n$ .

The average irradiation time required for the accumulation of the data for each target varied between 16 hours for  $\psi_n = 102^\circ$  and 12 hours for  $\psi_n = 27^\circ$  in the backward direction; 25 hours per target were required for the forward hemisphere measurement at  $\psi_n = 102^\circ$ . The total irradiation time, including the initial trial irradiations was of the order of 450 hours.

a)

$\psi_n$	$\text{Ni}^{58}(n,p)\text{Co}^{58}$				$\text{Fe}^{54}(n,p)\text{Mn}^{54}$				$\text{Cu}^{63}(n,p)\text{Ni}^{63}$			
	$E_n$ (Mev)	$\pm\Delta E_n$	$\sigma$ (mb)	$\pm\Delta\sigma$	$\sigma$ (mb)	$\pm\Delta\sigma$	$\sigma$ (mb)	$\pm\Delta\sigma$	$\sigma$ (mb)	$\pm\Delta\sigma$		
$102^\circ$	2.41	0.09	80.2	8.1	44.1	4.5	36	3.7				
$87^\circ$	2.57	0.10	100	10	77.7	7.8	35.4	3.7				
$74^\circ$	2.71	0.11	128	13	83	8.5	29	3.2				
$60^\circ$	2.86	0.12	143	14.5	109	11	33.6	3.5				
$47^\circ$	3.00	0.14	145	14.8	128	13.2	24.2	2.7				
$27^\circ$	3.17	0.18	155	16	135	14	33.6	3.6				

Cross-sections for emission of protons into backward direction  
(integrated over  $4\pi$  ster., assuming isotropy.)

b)

$E_n$ (Mev)	2	3	4
$\sigma$ (mb)	42	120	222

Theoretical cross-section for  $\text{Ni}^{58}(n,p)\text{Co}^{58}$  reaction.

TABLE 111.2.

a)			$\text{Ni}^{58}(n,p)\text{Co}^{58}$		$\text{Fe}^{54}(n,p)\text{Mn}^{54}$		$\text{Cu}^{63}(n,p)\text{Ni}^{63}$	
$\psi_n$	$E_n(\text{Mev})$	$\pm\Delta E_n$	$\sigma(\text{mb})$	$\pm\Delta\sigma$	$\sigma(\text{mb})$	$\pm\Delta\sigma$	$\sigma(\text{mb})$	$\pm\Delta\sigma$
$102^\circ$	2.41	0.09	94	10	44	5	36	4
b)			$\text{Ni}^{58}(n,p)\text{Co}^{58}$	$\text{Fe}^{54}(n,p)\text{Mn}^{54}$	$\text{Cu}^{63}(n,p)\text{Ni}^{63}$			
$\frac{\sigma(n,p)}{\sigma(n,p)}$ forward			$1.15 \pm 0.17$	$1 \pm 0.13$	$1 \pm 0.14$			
$\frac{\sigma(n,p)}{\sigma(n,p)}$ backward								

Cross-sections for emission of protons in forward directions  
(integrated over  $4\pi$  ster., assuming isotropy.)

TABLE 111.3.

## CHAPTER IV.

### Determination of Energy Spectra, and Absolute Cross- Sections for (n,p) Reactions in Ni<sup>58</sup> and Fe<sup>54</sup> at E<sub>n</sub> = 3.45 Mev, with Improved Resolution.

#### IV.1. Introduction.

A further measurement of the (n,p) energy spectra and absolute cross section was made for the target nuclei Ni<sup>58</sup> and Fe<sup>54</sup> with improved resolution. From a consideration of the low resolution experiment described in Chapter III, the resolution may be improved by decreasing the energy spread of the neutron beam and by suitable adjustments to the geometry of the detection system. Since the increased resolution must be made at the expense of the efficiency of the detection system and the neutron yield, the measurements were carried out at only one neutron energy and for two target materials; Cu<sup>63</sup> was not used because of its low (n,p) cross section (III.12).

#### IV.2. Design of Telescope.

The basic design of the apparatus consisted of target and background foils mounted on a rotating wheel, and a detection system. The latter was comprised of a  $dE/dx$  proportional counter and a semiconductor energy counter. Fig. IV.1. shows a schematic drawing of the apparatus, and also its position relative to the neutron source, D. The diameter of the target foil and the semiconductor counter was 1.2 cm and their separation was 1.78 cm. Thus the mean solid angle for

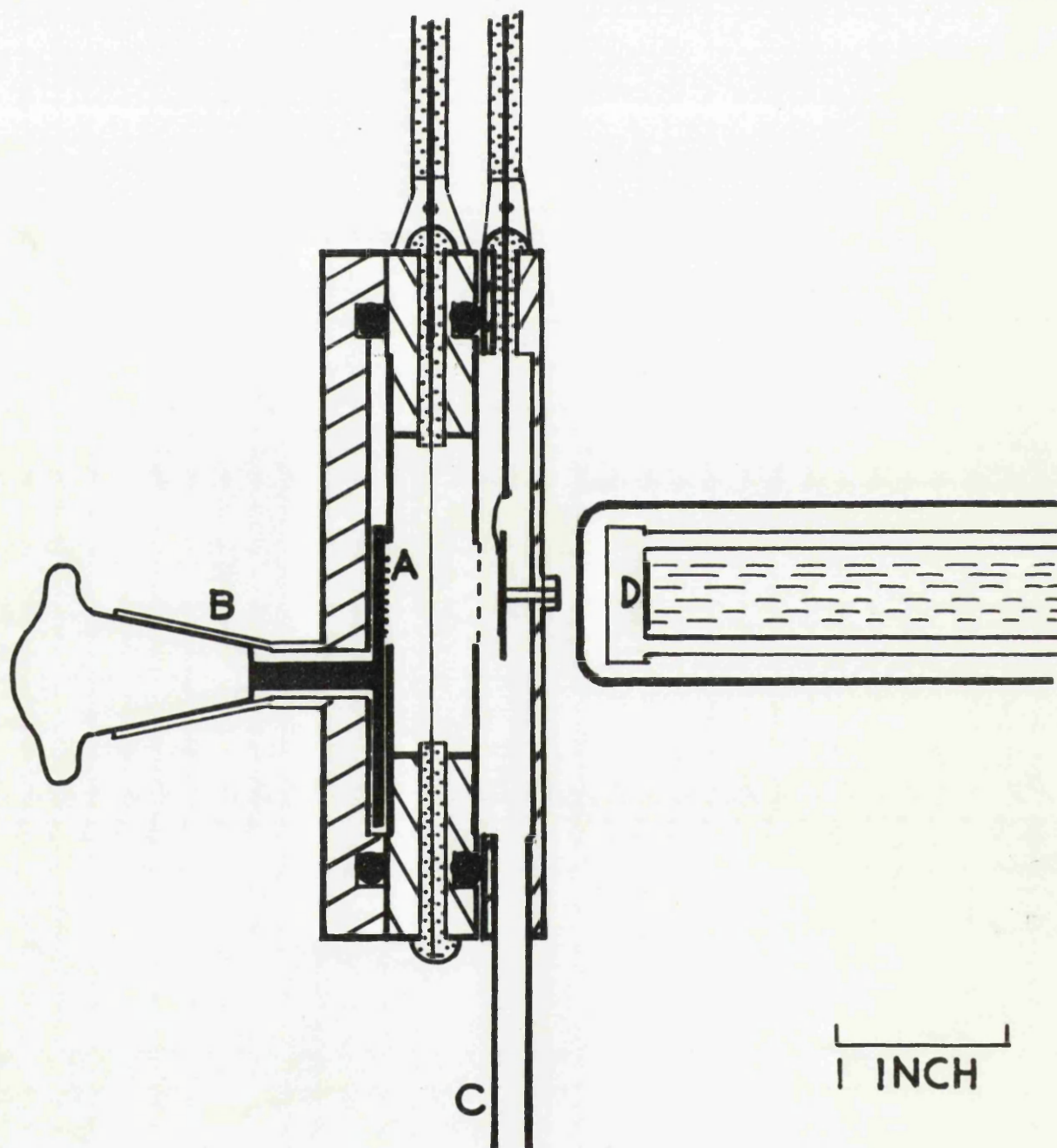


Figure 1V.1. Apparatus for the measurement of energy spectra and absolute cross sections for the (n,p) reaction in  $\text{Ni}^{58}$  and  $\text{Fe}^{54}$ .

the detection of charged particles originating at the target foil was 0.41 steradians, a factor of six less than that of the low resolution apparatus.

The semiconductor counter was identical to that described in III.3., and was fixed to a brass end plate by means of a short brass rod. The gold filament from the front surface of the counter was attached, through a 'kovar' seal in the side wall of the brass plate, to an external coaxial cable. The proportional counter was formed out of a flat cylindrical piece of brass of the same diameter as the end plate (4INS) and depth 1.2 cm. The proportional counter was rectangular in shape with dimensions  $1\frac{1}{2}$ " by 2", and depth 1 cm. The central electrode, which was parallel to the long dimension of the counter was a tungsten wire of diameter 0.005". The wire passed through a 'kovar' seal to a coaxial cable, the other end being sealed in a glass rod in the wall of the counter to prevent electrical discharge from the sharp ends.

The target assembly contained a target foil (A, Fig IV.1.), a target backing material, a polythene foil, a  $\text{Po}^{210}$  alpha source and an aperture for the passage of protons produced externally in the H.T. set. The target wheel was attached to a brass front plate of similar dimensions to the end plate, in an off-centre position; This allowed the target foil etc., to be placed opposite and parallel to the semiconductor counter. The target wheel could be rotated, while the apparatus was evacuated, by means of a glass cone joint (B, Fig. IV.1.).

In order to prevent the passage of charged particles, produced in the brass target plate and in the kovar seals, through the proportional counter into the semiconductor counter, 0.03" lead plates with a central aperture of diameter 1.5 cm were attached to each 'face' of the proportional counter. The inner surfaces of the proportional counter which could be 'viewed' by the semiconductor counter were lined with 0.002" gold foil. A thin ( $0.26 \text{ mg/cm}^2$ ) aluminium window placed across the aperture in the face of the proportional counter next to the semiconductor counter prevented capacitative effects between the two counters.

The three units of the apparatus were held together by means of six rods placed around the circumference (not shown in Fig: IV.1.) and two O-ring seals made evacuation possible by means of the port C (Fig: IV.1). The proportional counter was filled with a mixture of 10%  $\text{CO}_2$  and 90% Argon at a pressure of 10 cm Hg.

#### IV.3. Neutron Source and Monitoring.

Because of the requirement of good energy resolution, a 'thick'  $\text{D}_2\text{O}$  ice target was not used as a neutron source. Instead a thin deuterium target supplied from the Atomic Energy Research Establishment, Harwell, was used. The target consisted of a thin layer of titanium, impregnated with deuterium, and having a copper backing. The target was soldered onto the water coolant tube in the beam pipe of the H.T. Set. With an incident beam of  $40 \mu$  amp. at an energy of 500 Kev. a neutron flux of  $\sim 8 \times 10^7$  neutrons/sec. into unit solid angle about  $0^\circ$  was obtainable. The energy loss of

the 500 Kev deuteron beam in passing through the deuterium layer was  $\sim 75$  Kev, giving a beam spread of  $\pm 40$  Kev. The mean energy of the neutron beam emitted at  $0^\circ$  to the deuteron beam was 3.45 Mev for a 500 Kev incident deuteron beam.

Monitoring of the neutrons was carried out as described in III.6. However, since the apparatus was arranged to detect neutrons emitted at  $0^\circ$ , the effect of the deuteron beam drift was to cause the effective neutron source to move in a plane perpendicular to the axis of the apparatus. Thus, the beam drift effect was only a second order effect, and only one neutron monitor was required. The neutron flux was measured by means of the monitor behind the apparatus, while the second monitor, set at  $64^\circ$  to the incident beam direction, served as a check on the counting rate of the main neutron monitor. The error involved in the neutron monitoring as a result of the error in the  $H'(n,p)$  scattering cross section and the error in measuring the various dimensions of the monitor was  $\pm 3\%$ .

#### IV.4. Arrangement of Apparatus.

The apparatus was positioned to detect protons emitted into a solid angle around an angle of  $180^\circ$  to the direction of the neutron beam; this procedure was adopted for reasons of consistency with previous measurements. The target foil-neutron source separation was 3.86 cm. Thus, since the diameter of the target foil was 1.2 cm, the mean solid angle for acceptance of the neutrons was 0.075 steradians. The mean angular spread of

the neutrons incident on the target was  $0^\circ \pm 6^\circ$ , and the maximum angular spread was  $0^\circ \pm 9^\circ$  (the number of neutrons incident upon the target and emitted within a cone of half angle  $6^\circ$  being half that number emitted within the cone of half angle  $\sim 9^\circ$ ). The mean angular spread of  $\pm 6^\circ$  corresponded to mean energy spread of  $\pm 35$  Kev, on the assumption that the neutrons were emitted isotropically into the cone of half angle  $9^\circ$ . The total spread, allowing for the effect of target thickness, was  $\pm 55$  Kev. This spread is a factor of three smaller than the maximum energy spread ( $\sim \pm 160$  Kev at  $\psi_n = 27^\circ$ ) of the neutron beam in the low resolution experiment.

#### IV.5. Associated Electronics.

A block diagram of the electronic system associated with the detector system is shown in Fig: IV.2. The output pulses from the semiconductor counter were amplified by a high gain, low noise amplifier - pre amplifier system, ( Ortec 601 ) The proportional counter pulses were amplified by means of a 'Ring 0' Three' preamplifier and a main amplifier, (I.D.L. type 652). Discriminator pulses corresponding to the pulses from both amplifying units were obtained by means of discriminator units of the type in the third stage of the I.D.L. amplifier; two discriminator pulses were obtained from the  $\frac{dE}{dx}$  pulses. The energy discriminator pulse and the lower  $\frac{dE}{dx}$  discriminator pulse operated a coincidence - gateing unit (Fig: IV.3.). The presence of an upper discriminator pulse from the proportional counter amplifier operated an anti coincidence-gate

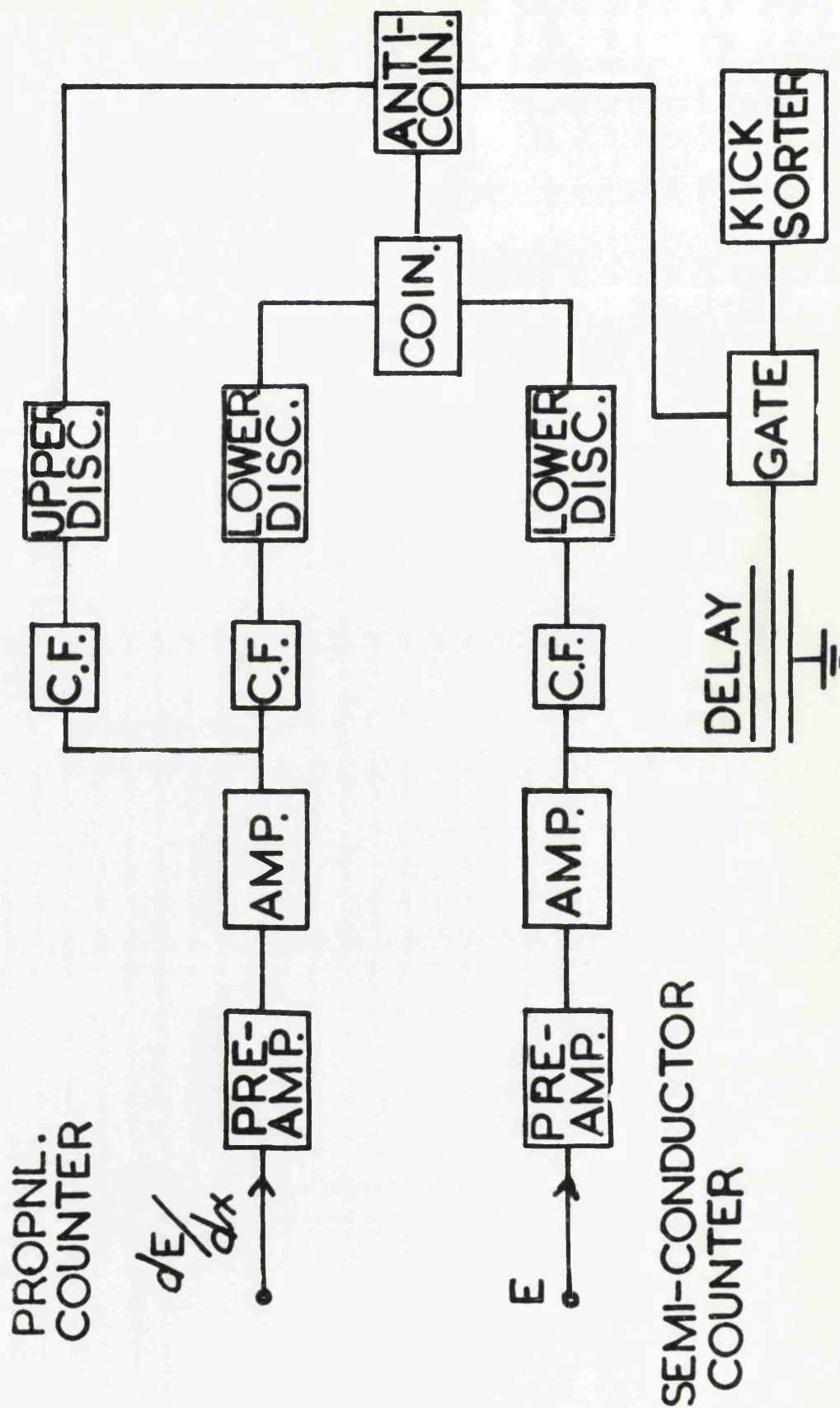


Figure 1V.2. Block diagram of electronics used in determination of the energy spectra.



unit. (The criteria for the <sup>d</sup>adjustment of the discriminator levels is discussed in the following section, IV.6.). The final 'gated' energy pulses were analysed on a C.D.C. 100 channel analyser.

#### IV.6. Calibration.

Initially, the response of the semiconductor counter and the proportional counter for the passage of protons of various energies was found. As in the case of the low resolution experiment (Chapter IV.), the source of protons was the reactions  $H^2(d,p)H^3$ ,  $B^{10}(n,p)B^{11}$  and the  $(n,p)$  scattering in polythene. The ungated spectrum from the semiconductor counter was similar to that shown in Fig: III.6. A calculation of the energy losses of the protons passing through the 0.0005" mylar windows of the accelerator beam pipe and the front plate, and the gas in the proportional counter, showed a linear variation of pulse height with energy lost in the semiconductor counter. The setting of the discriminator levels on the proportional counter required the accurate calibration of the counter. The setting of the lower discriminator level, corresponding to the most energetic protons to be detected, was carried out by observing the effect of variation of the discriminator setting on the gated semiconductor counter spectrum of the proton groups. As the discriminator level was increased, the higher energy proton groups were unable to register a coincidence pulse because of the anti-coincidence unit, and were thus absent from the spectrum. Since the Q-values for the  $Ni^{58}(n,p)Co^{58}$  and  $Fe^{54}(n,p)Mn^{54}$

reactions are 0.399 Mev and 0.092 Mev, respectively, and the mean neutron energy is 3.45 Mev, the most energetic proton to be detected was  $\sim 3.5$  Mev. The final adjustment of the lower proportional counter setting was such that all protons of energy greater than 5 Mev were rejected. This procedure has the effect of decreasing the number of small electron background pulses, and also pulses arising from charged particle reactions in the silicon. The upper discriminator level, corresponding to a high  $dE/dx$  pulse caused by low energy protons or alpha particles was adjusted arbitrarily to reject alpha particles of energy less than 5 Mev (from the  $Po^{210}$  alpha source.). In particular, alpha particles which may arise as a result of  $(n, \alpha)$  reactions in the nickel or iron targets were rejected in the accumulation of data. The upper discriminator setting also set a limit on the lowest proton energy that could be detected, viz;- 1 Mev. Since the presence of the Coulomb barrier will cause a large reduction in the emission of low energy protons, this procedure is justifiable.

The stability of the gain of the counter - electronic system was checked before and after each irradiation by means of the  $Po^{210}$  alpha particles. The gain of the  $dE/dx$  amplifier was decreased for this purpose to allow the detection of the alpha particles in coincidence.

#### IV.7. Experimental procedure.

The spectra of the emitted protons and background counts were obtained in a series of irradiations on the target-in and

target-out positions. The target-in and target-out irradiations were alternated during the course of the experiment. Regular checks on the stability of the counter-electronic system and the neutron monitor showed, again, a stability of less than 1% during each irradiation ( 2 hours). By suitable adjustments of the proportional counter discriminator levels, a measure of the yield of the  $(n,\alpha)$  reactions in the nickel and  $\text{Fe}^{54}$  targets was obtained; there was no measurable  $(n,\alpha)$  cross section in each case. The targets used were those used in the low resolution experiment (III.10.) i.e. a natural nickel target and an enriched  $\text{Fe}^{54}$  target. In both cases the backing material was 0.002" gold.

#### IV.8. Experimental Spectra.

The energy spectra of the emitted protons obtained for both the nickel and iron targets are shown in Figs. IV.4. and IV.5. respectively. The solid lines represent the spectra of protons with the background subtracted; the background spectra are shown as a dashed line. The lines joining the points merely show the general trend of the spectra. The error bars are statistical errors, due allowance being made for the effect of the background separation.

##### a) $\text{Ni}^{58}(n,p)\text{Co}^{58}$ .

The spectrum exhibits two broad peaks at 3.49 Mev and 2.21 Mev. The widths of the peaks suggest the presence of more than one unresolved proton group leading to energy levels in the residual nucleus in the neighbourhood of the ground state and

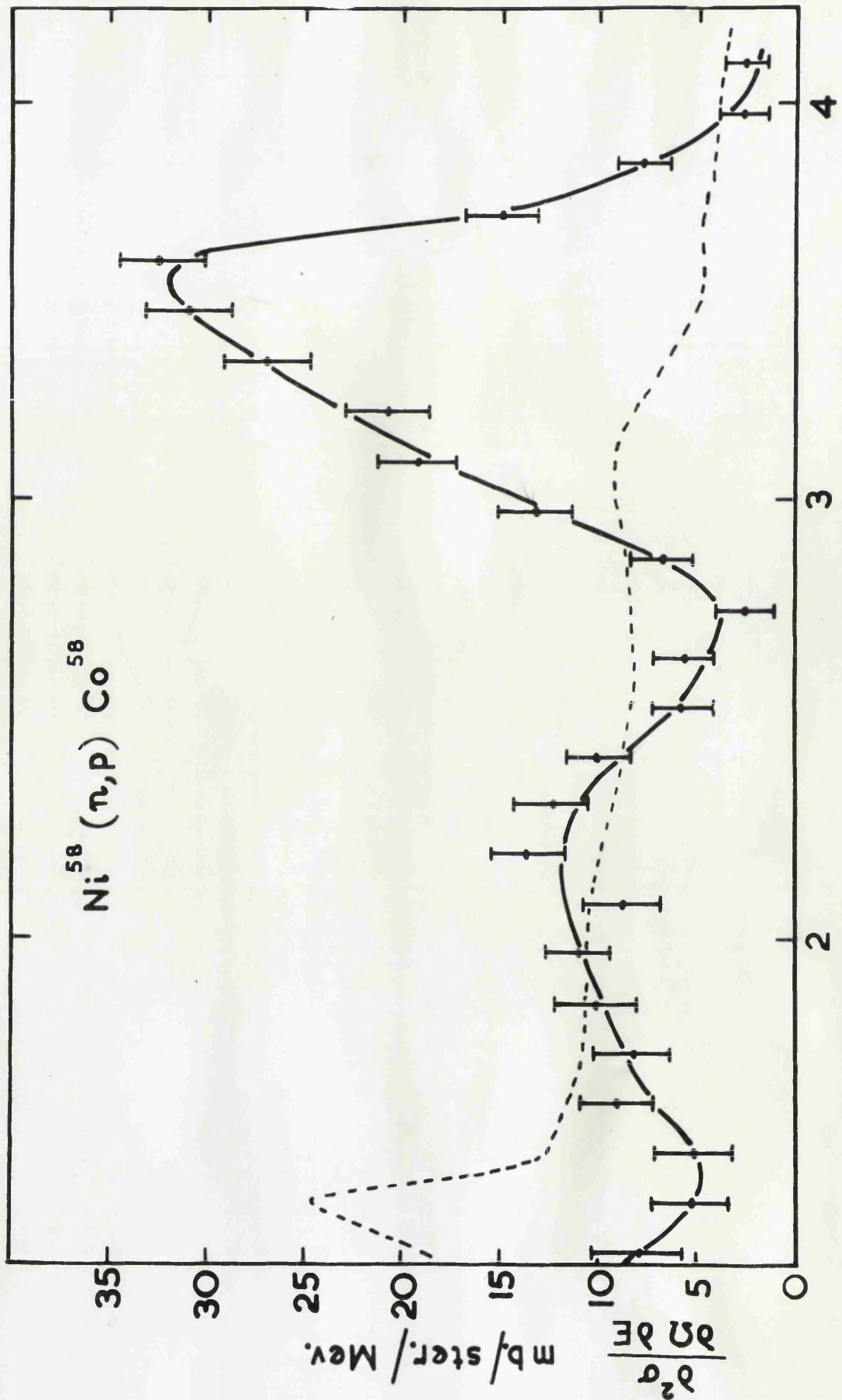


Figure 1V.4. Energy spectrum of protons from the reaction  $^{58}\text{Ni}(n,p)\text{Co}^{58}$   
Background spectrum shown as a dotted line.

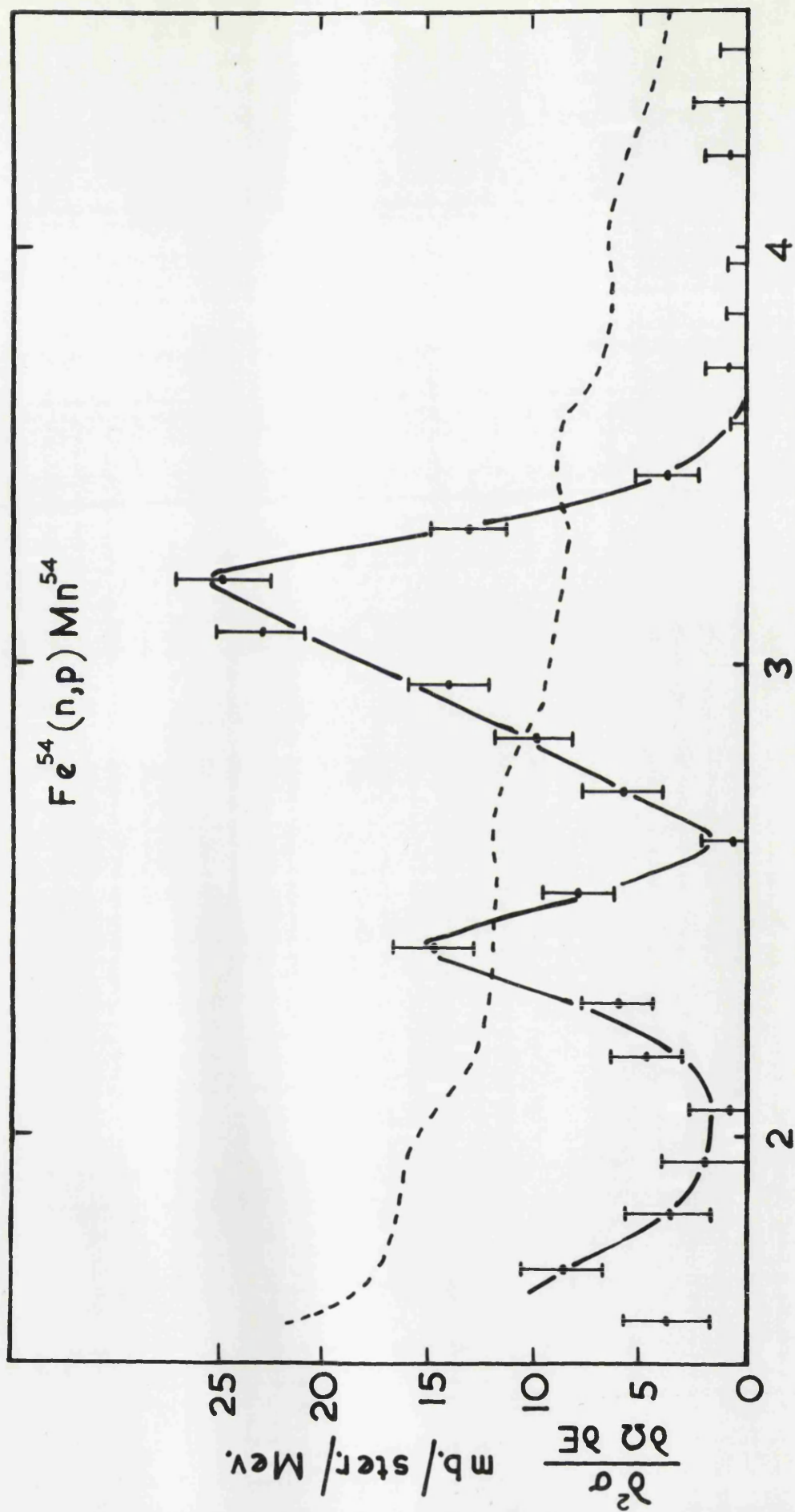


Figure IV.5. Energy spectrum of protons from the reaction  $Fe^{54}(n,p)Mn^{54}$ .  
Background spectrum shown as a dotted line.

1.3 Mev excitation. The background spectrum is comparatively flat; the peak present in the background spectrum of the low resolution experiment (Fig. III.8,9.) is not present in this case because of the coincidence arrangement.

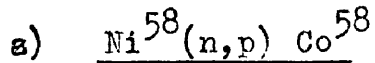
b)  $\text{Fe}^{54}(\text{n,p})\text{Mn}^{54}$ .

Again, two proton peaks are present in the spectrum at energies of 3.2 Mev and 2.45 Mev, corresponding to excitation of the ground state and a level at 0.75 Mev in the residual nucleus. The slowly falling tail of the upper peak may be due to a smaller proton peak in the region of 3.1 Mev i.e. corresponding to an excitation of  $\sim 100$  Kev of the residual nucleus. However, there is no direct evidence as to the presence of a level in this region.

TABLE IV.1. gives the cross-sections for the emission of protons from the reactions studied. The cross sections quoted are calculated on the assumption that the angular distribution of the emitted protons is isotropic in each case. i.e. the tabulated cross sections are total (n,p) cross sections. Cross sections have been corrected for the effect of neutron attenuation and scattering using the cross section compilation of BNL-325 (Hughes & Schwarz.)

$$E_n = 3.45 \text{ Mev.}$$

$$\Delta E_n = \pm 0.06 \text{ Mev.}$$



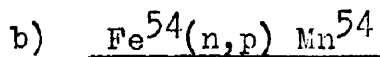
Cross-section for emission of protons >1 Mev.

$$= 364 \text{ millibarns } \pm 31 \text{ mb.}$$

Mean energies of protons peaks = 3.49 Mev., 2.21 Mev.

Cross-section for emission of protons leading to "upper" peak (3.49 Mev.) = 238 mb.

Cross-section for protons leading to "lower" peak  
= 126 mb.



Cross-section for emission of protons >1 Mev.

$$= 175 \text{ millibarns } \pm 15 \text{ mb.}$$

Mean energies of proton peaks = 3.2 Mev., 2.45 Mev.

Cross-section for emission of protons leading to "upper" proton peak (3.2 Mev.) = 129 mb.

Cross-section for emission of protons leading to "lower" proton peak = 46 mb.

---

TABLE 1V.1.

## CHAPTER V.

### Discussion and Conclusions.

#### V.1. Neutron Beam Width.

Having obtained the cross sections for the (n,p) reactions in Ni<sup>58</sup>, Fe<sup>54</sup> and Cu<sup>63</sup> for an incident neutron beam produced by a 'thick' neutron target, one may enquire into the effect of the neutron beam width on both the magnitude of the cross section and its variation with neutron energy. It was found that, in the approximation that the measured excitation function and the theoretical excitation function in the limit of narrow neutron energy spread, can be represented as a polynomial of degree three in the mean energy and energy respectively, the measured excitation function is a good representation of the 'true' excitation function. (Appendix A). The procedure adopted in Appendix A cannot account for any cross section fluctuations which may arise as a result of having a neutron beam spread comparable to the average level spacing at the energy of excitation in the compound nuclear state. Thus a fluctuating excitation curve of the type obtained by Konijn and Lauber, 1963, cannot be deduced from the present measurements.

#### V.2. Comparison of Present Results with other (n,p) Results.

Before comparing the present results with those of other workers, two points can be made.

- a) The proton spectra were obtained by detection of the protons

emitted into a solid angle about  $180^\circ$  with respect to the incident neutron beam direction. The cross sections are, therefore, essentially differential cross sections. To compare with the results of other workers (which have been arrived at mainly by the activation technique), one requires total (n,p) cross sections. Total cross sections were determined by assuming an isotropic angular distribution of emitted protons.

b) The cross sections were obtained by detection of protons leaving the residual nucleus in or close to its ground state. Since the activations technique does not require the detection of protons away from their source, but only the de-excitation gamma rays, all emitted protons are necessarily detected. With these points in mind, the present measurements may be compared with the results of other workers.

V.2.a. Ni<sup>58</sup>(n,p)Co<sup>58</sup>

Figs. V.1.a,b,c show plots of the results obtained by other workers on the Ni<sup>58</sup>(n,p)Co<sup>58</sup> excitation curve. It can be seen that there is a wide discrepancy in the various measurements. The present measurements agree, within experimental error, with those of Meadows and Whalen, 1963, and Nakai et al, 1962. The results of Meadows and Whalen are approximately 10% higher than the author's results in the energy region of overlap, although the slope of the excitation curve of the former compares favourably with that of the author. Unfortunately, Meadows and Whalen's measurements do not extend above an energy of 2.66 Mev. There is an excellent agreement with the results of

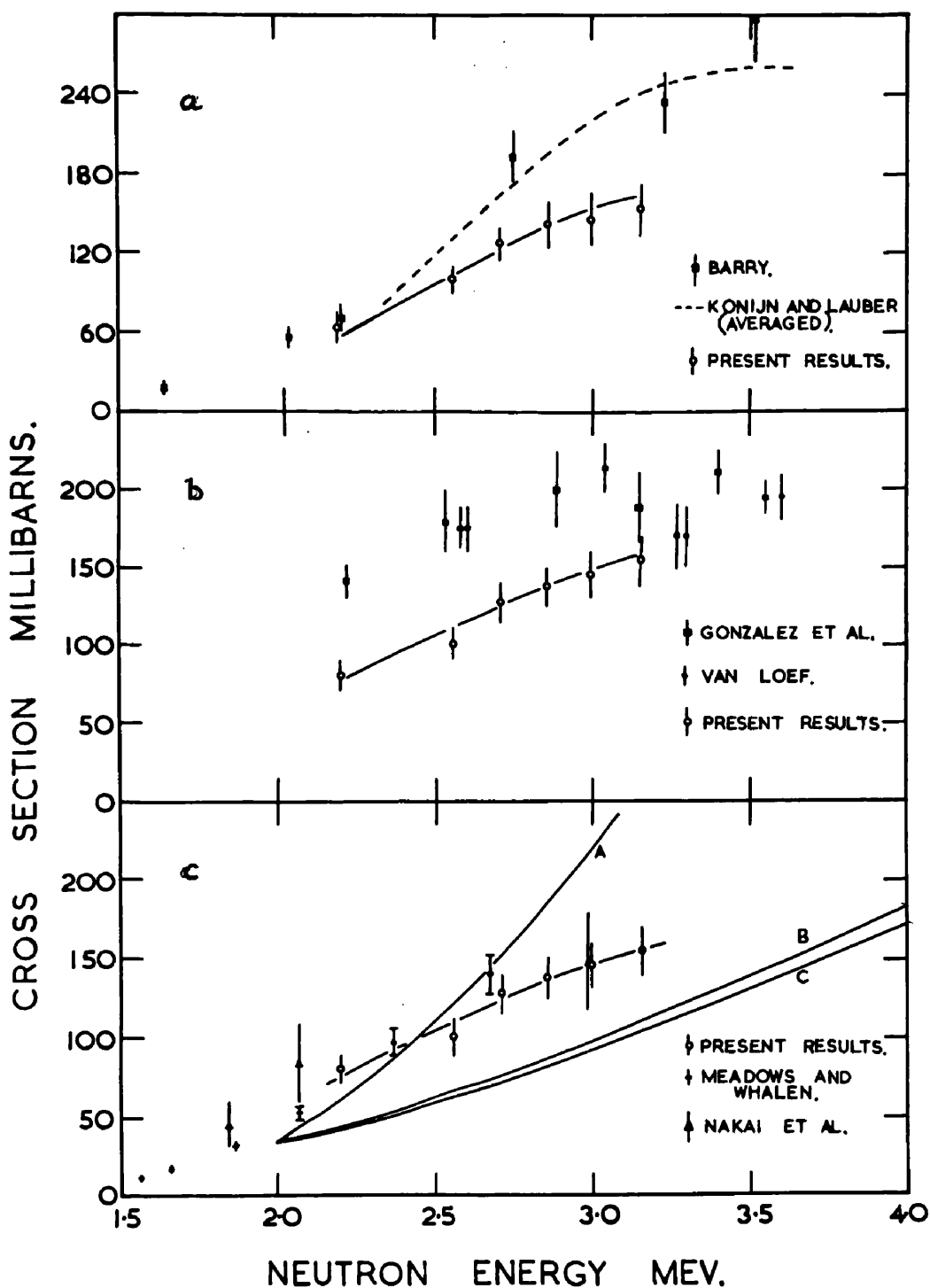


Figure V.1a,b,c. Excitation curves for the reaction  $\text{Ni}^{58}(n,p)\text{Co}^{58}$ , experimental and theoretical.

Nakai et al. The comparatively large errors quoted by the latter workers ( 30%) do not allow any detailed knowledge of the slope of their excitation curve. The neutron energy spread quoted by Nakai et al. is comparable to the energy spread found in the present work; Nakai et al quote an energy spread in the region of 8% while the estimated energy spread in the low resolution experiment varies from 6% at  $\psi_n = 102^\circ$  to 11% at  $\psi_n = 27^\circ$ .

The measurements of the cross sections by Gonzalez et al, 1960, and Van Loef, 1961 , are shown in Fig. V.1.b. (The results of Gonzalez, 1960, are too high by about 9% due to a systematic error. (Gonzalez et al., 1962.)). The results of Gonzalez et al and Van Loef are not independent since the absolute cross sections determined by Van Loef are based on the  $\text{Ni}^{58}(n,p)\text{Co}^{58}$  activation cross section at 3.55 Mev as measured by Gonzalez. The cross sections determined by Gonzalez et al and Van Loef are 20% to 50% larger than the present measurements. The excitation curve of these workers has the same slope as that of the authors in the energy region less than  $\sim 2.8$  Mev; however, above 2.8 Mev, the cross sections obtained by Gonzalez et al and Van Loef remain approximately constant with increasing energy.

The results of Barry, 1962, plotted in Fig. V.1.a, do not agree with the results of the low resolution experiment. Barry's excitation curve, although of the same magnitude in the energy region about 2.2 Mev rises steeply to a maximum of 657 mb at  $E_n = 8.3$  Mev.

All the previously discussed measurements of other workers

have been obtained by the activation technique i.e. they measure the  $(n,p)$  cross sections integrated over the energy of the emitted proton and over the angle of emission. Konijn and Lauber, 1963, have measured the emission of protons of energy greater than 1 Mev emitted into a solid angle about  $0^\circ$  (Chapter II.). Typical spectra obtained and the resultant excitation curve are shown in Figs. V.2.a,b. respectively. The solid line 'a' is the spectrum of protons and background, while the lower spectrum 'b' is that obtained in a background irradiation. The peak due to the emission of protons leading to the ground state of  $\text{Co}^{58}$  lies on the high energy tail of the  $\text{Si}^{29}(n,\alpha)\text{Mg}^{29}$  peak. The background present in the spectrum is quite high, being 30% to 50% of the recorded number of protons; Konijn and Lauber attribute the background to residual hydrogen in the detector and surroundings. A main difference in the experimental technique of Konijn and Lauber and the low resolution experiment lies in the energy width of the neutron beam. The narrow neutron energy spread ( $\pm 30 \sim 40$  Kev) used by Konijn and Lauber make a comparison with the results of other workers, including the present results, extremely doubtful, since the neutron energy spread of the latter is of the order of  $\pm(100 \sim 200)$  Kev. The narrow energy spread used by Konijn and Lauber is reflected in their excitation curve, (Fig. V.2.b.) which shows an number of peaks. For the purpose of comparison with excitation functions obtained with a wide energy spread, an average excitation curve has been obtained by calculating

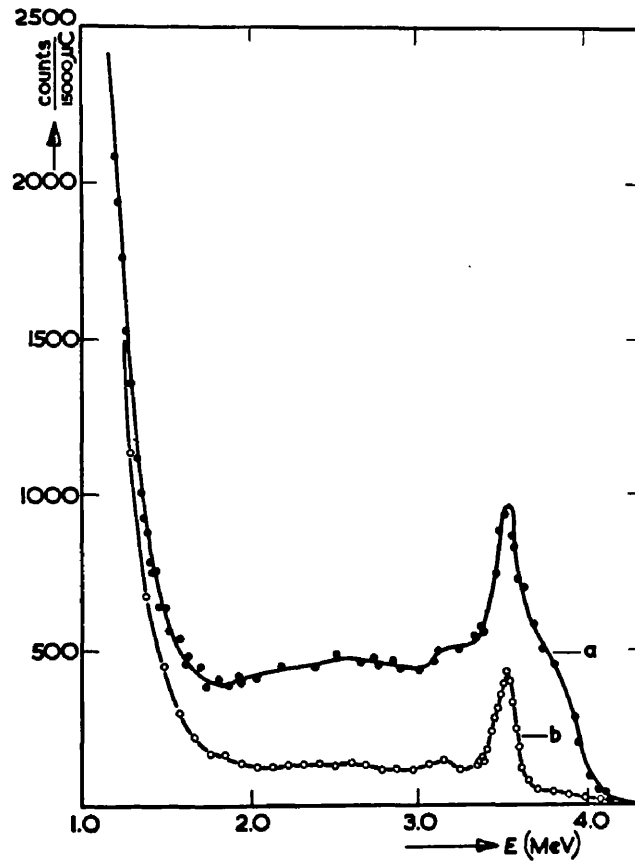


Figure  
V.2a.

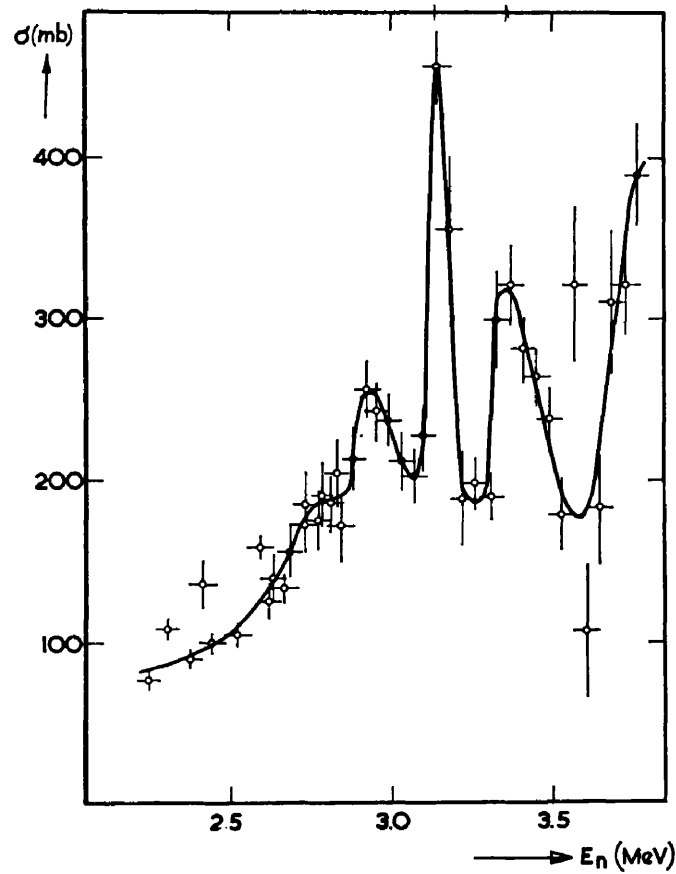


Figure  
V.2b.

Results of KoNijn and Lauber.

the mean cross section in each of 36 energy regions, between 2.24 Mev and 3.77 Mev, from Konijn and Lauber's excitation curve. A smooth curve, shown in Fig. V.1.a. was obtained, which agreed with that obtained by Barry, up to an energy of 3.4 Mev, above which the curve tends to decrease with increasing energy.

In conclusion, to the extent that the type of measurement made by the author may be compared with other types of measurements, there is agreement within experimental error with the results of Meadows and Whalen, and Nakai et al., while those of Barry, Gonzalea et al, Van Loef and Konijn and Lauber are 30% to 60% greater than the author's measurements; the results of the latter group of workers do not agree within themselves.

V.2.b. Fe<sup>54</sup>(n,p)Mn<sup>54</sup>

The only reported work on the (n,p) reaction in Fe<sup>54</sup> at low energies (< 5 Mev) is that of Van Loef, 1961. Their measurements were carried out by the activation technique at three neutron energies, 2.6±0.2, 3.3±0.1, and 3.6±0.1 Mev. The excitation curve of Van Loef and the present measurements are shown in Fig. V.3. The cross section values obtained by Van Loef are approximately a factor of 2 greater than the author's measurements at a neutron energy of 2.6 Mev. However, the excitation curve of Van Loef does not rise with energy as steeply as that obtained in the present work; at 3.1 Mev, Van Loef's measurement is a factor of 1.3 greater than the author's measurements. Van Loef obtained the absolute values of the (n,p) cross sections by comparison with the Ni<sup>58</sup>(n,p)Co<sup>58</sup>

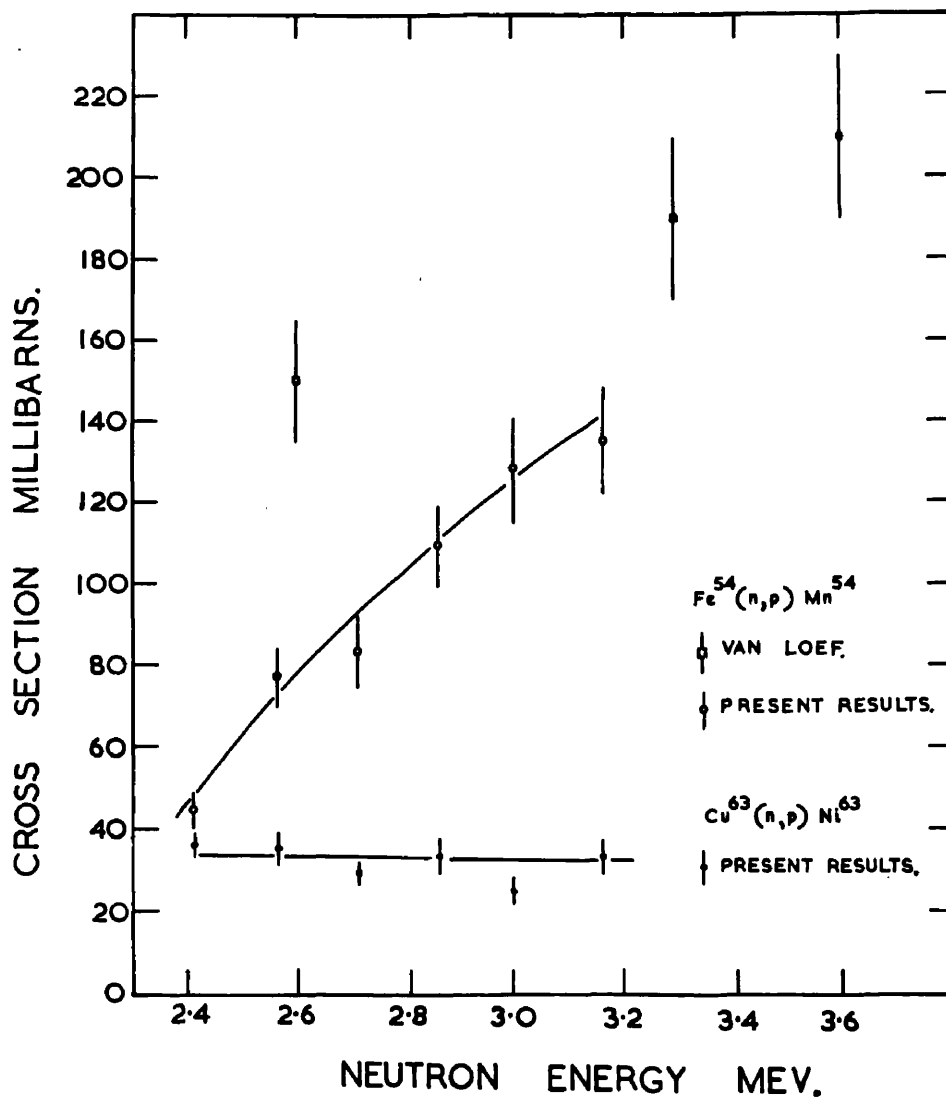


Figure V.3. Excitation curves for the reactions  $^{54}\text{Fe}(n,p)^{54}\text{Mn}$  and  $^{63}\text{Cu}(n,p)^{63}\text{Ni}$ .

at 3.55 Mev obtained by Gonzalez et al, 1960. Since the latter results are too large by  $\sim 9\%$  (Gonzalez et al, 1962) it is to be expected that Van Loef's results are too large by the same amount. Since Gonzalez's measured cross section for the  $\text{Ni}^{58}(n,p)\text{Co}^{58}$  reaction is greater than the author's value, a similar discrepancy will be reflected in Van Loef's measurement. However, the different slopes of the two excitation curves as obtained by Van Loef and in the present programme of work remains unexplained.

#### V.2.c. $\text{Cu}^{63}(n,p)\text{Ni}^{63}$ .

The excitation curve for the  $\text{Cu}^{63}(n,p)\text{Ni}^{63}$  reaction is plotted on the lower part of Fig. V.3. There is no other reported work on this reaction with which to make a comparison. However, a similar reaction i.e. an  $(n,p)$  reaction with an odd mass target, has been studied by Gonzalez et al. 1962, who obtained the excitation curve for the reaction  $\text{Ti}^{47}(n,p)\text{Sc}^{47}$ , ( $Q = 182.6$  Kev.) in the energy range 2 to 3.6 Mev. The variation of the cross section with energy was similar to that of the  $\text{Cu}^{63}(n,p)\text{Ni}^{63}$  reaction, in that the cross sections were small ( $\sim 50$  millibarns) and did not rise rapidly with energy.

#### V.3. Theoretical variation of Cross Section with Neutron Energy.

A calculation of the theoretical excitation function for the reaction  $\text{Ni}^{58}(n,p)\text{Co}^{58}$  was carried out using the semi-statistical theory of Hauser and Feshbach, 1952, and Wolfenstein, 1951, (Chapter I,4.). Proton and neutron penetrabilities were taken from the tables of Mani et al., 1963.

These penetrabilities were calculated using an optical model potential with a real part of the Saxon - Wood form, an imaginary gaussian part and a spin-orbit potential. The parameters used in the penetrability calculation were taken from an extensive survey made by Bjorklund and Fernbach, 1959, using proton scattering data. The parameters obtained were an average fit over a range of energy and nuclei of the experimental data. The calculation of the cross sections, using the Hauser - Feshbach theory were carried out at three neutron energies, 2, 3, and 4 Mev. Neutrons and Protons of orbital angular momentum up to  $\ell = 4$  were included in the calculation. Cross sections for the emission of protons leading to the  $2^+$  ground state and the 25 Kev  $5^+$  metastable state in  $\text{Co}^{58}$ , in competition with:-

- a) neutron emission leading to the ground state in  $\text{Ni}^{58}$
- b) neutron emission leading to the  $0^+$  ground state, the  $2^+$  state at 1.452 Mev and the  $4^+$  state at 2.458 Mev in  $\text{Ni}^{58}$ , and
- c) as in b) together with proton emission to a hypothetical  $4^+$  state at 0.3 Mev in  $\text{Co}^{58}$ .

The variation of the cross section with neutron energy for the competition as in cases a), b) and c) are plotted on Fig. V.1.0, and labelled A, B and C respectively.

Several interesting points may be noted in the results of the calculations. The calculated cross sections are very dependent upon the neutron competition assumed but are relatively independent of the additional proton competition.

This is presumably due to the influence of the Coulomb barrier on the emission of the low energy protons. The excitation curves B and C agree well with the theoretical calculations of Meadows and Whalen, and Nakai et al, but not with those of Trier or Gonzalez. (These workers calculated the total proton emission). The results of Trier agree with curve A, the competition being the same in each case.

The cross sections for the  $\text{Ni}^{58}(n,p)\text{Co}^{58}$  reaction obtained by means of the low resolution experiment lie between the theoretical calculations A, B and C. (Fig. V.1.C.). A possible reason for this discrepancy may lie in the fact that average optical model parameters have been used. Since  $\text{Ni}^{58}$  has a closed shell of protons it is to be expected that the optical model parameters associated with  $\text{Ni}^{58}$  will not conform with the average. However, the main part of the discrepancy may be due to the detection of protons which lead to a level (or levels) in  $\text{Co}^{58}$  at an excitation energy above the 25 Kev state, as suggested by Meadows and Whalen. Because of the neutron beam width in the low resolution experiment, the proton peak extended over an energy range of  $\sim 0.5$  Mev, especially for the higher neutron energies. Thus, emitted protons causing the excitation of a level at, say, 0.3 Mev in  $\text{Co}^{58}$  will contribute to the experimental excitation curve. The Hauser - Feshbach calculation for the emission of protons to the two known states in  $\text{Co}^{58}$  and a hypothetical  $4^+$  state at 0.3 Mev in competition with neutron emission to the three low lying states

in  $\text{Ni}^{58}$  yields theoretical cross sections which are a factor of 1.3 greater than the case C above, although they are still approximately 20% less than the experimental values. The theoretical values for the cross section obtained by this method are those tabulated on TABLE III.2. A better fit to the experimental data could probably be achieved by assuming the  $4^+$  level to be at a lower excitation energy or by assuming the type of the level to be, say,  $3^+$ .

Because of the considerable amount of computation involved, and the average nature of the optical model parameters, no attempt was made to apply the Hauser-Feshbach formula to the (n,p) reactions in  $\text{Fe}^{54}$  and  $\text{Cu}^{63}$ .

#### V.4. Ratio of Forward to Backward Proton Yield.

The ratio of the cross sections for the emission of protons into a solid angle about  $0^\circ$  and  $180^\circ$  is, within experimental error, unity for each type of target nucleus. (Tables III.2,3.). Since a direct interaction mechanism will generally give rise to an excess of protons emitted in the forward direction ( e.g. results of Rosen and Stewart at 14 Mev.) and also, the work of Hauser and Feshbach, and Ericson, shows that compound nuclear theory predicts a symmetrical angular distribution (c.f. Chapter I.), the measured ratios of unity suggest that the direct interaction mechanism is not present in 3 Mev neutron reactions. Such a result is in agreement with the fairly good ( $\sim 25\%$  discrepancy) theoretical fit of the excitation curve (for a nickel target) using the

compound nucleus theory. Although no other work on the angular distribution of protons from (n,p) reactions in the energy range studied has been reported, there have been some investigations into (p,p') and (n,n') reactions. Taketani et al, 1962, Sen Gupta et al, 1964, and Seward, 1959, have studied the angular distribution of inelastically scattered protons or neutrons in the energy range 4 to 7 Mev for various targets. They have found that in the case of medium weight targets, there is no assymetry in the angular distributions for incident particle energies less than 6 Mev, but have appreciable direct interaction mechanism contribution at above 7 Mev, the approximate Coulomb barrier height.

#### V.5. Systematics of (n,p) Reactions.

The three (n,p) reactions studied may be classified according to whether the target nucleus contains an odd or even number of protons or neutrons. Thus, the reactions  $\text{Ni}^{58}(n,p)\text{Co}^{58}$  and  $\text{Fe}^{54}(n,p)\text{Mn}^{54}$  are of the type



whereas the reaction  $\text{Cu}^{63}(n,p)\text{Ni}^{63}$  is of the type



The level density at an excitation energy E in a nucleus may be described in terms of an effective excitation energy U (e.g. level density formula of Ericson, 1960.), where  $U = E - \Delta$ ,  $\Delta$  being a factor to account for the pairing energy of two protons or neutrons (Cameron, 1958, Newton, 1956). Dostrovski et al, 1959, use  $\Delta = 0$  for an 0 - 0 nucleus, and

$2\Delta_{O-E} = \Delta_{E-E}$  where  $\Delta$  is given in terms of the atomic mass  $A$  by the empirical rule:-  $\Delta \approx 3.4 (1 - A/400)$  Mev,  $A \geq 40$ .

Thus,  $(n,p)$  reactions in an  $E - E$  nucleus leading to an  $O - O$  nucleus will be enhanced at the expense of  $(n,n')$  reactions leading to an  $E - E$  nucleus with a smaller level density.

On the other hand  $(n,p)$  reactions in an  $O - O$  nucleus will be suppressed by the competition of  $(n,n')$  reactions leading to an  $O - O$  residual nucleus. This has been found to be the case.

The cross section for the  $Cu^{63}(n,p)Ni^{63}$  reaction is lower than the cross sections for the  $(n,p)$  reactions in  $Fe^{54}$  and  $Ni^{58}$ , although the  $Q$  value for the former reaction (  $0.716$  Mev) is higher than those for the latter (  $0.092$  Mev and  $0.399$  Mev, respectively.). This is in agreement with the work of Bulloch and Moore, 1960, and with the low energy work of Van Loef, 1961.

#### V.6. Energy Spectra obtained with 'Good' Energy Resolution.

##### V.6.a. $Ni^{58}(n,p)Co^{58}$ .

The cross section for the  $Ni^{58}(n,p)Co^{58}$  reaction as measured by the 'good' resolution apparatus described in Chapter IV, was found to be 364 Millibarns ( assuming an isotropic emission of protons ) for an incident neutron energy 3.45 Mev. The spectrum of emitted protons consists of two peaks (Fig. IV.4. ), the energies of which correspond to excitation of regions about the ground state and 1.3 Mev in the  $Co^{58}$  residual nucleus. The cross sections for emission of protons leading to the upper and lower energy proton peaks are 238 mb.

and 126 mb. respectively. The cross section obtained by extrapolation of the excitation curve ( Fig. V.1. ) (obtained under 'poor' resolution conditions) was 180 mb. This latter figure may be compared with that of 238 mb., the cross section for emission of protons leading the higher energy proton peak (Fig. IV.4. ) since the excitation curve was obtained for a similar proton energy band. The discrepancy in the cross sections may be attributed to the difference in the neutron energy spread used in the two experiments. The narrow neutron energy spread used in the measurement of the cross section at 3.45 Mev, i.e.  $\pm 60$  Kev throws some doubt on the application of a compound nuclear statistical mechanism as a description of the reactions under consideration ( c.f. Chapter I. ). The results of Konijn and Lauber who measured the excitation curve with a narrow neutron energy spread ( $\pm 30-40$  Kev) comparable to the energy spread of the 'good' resolution experiment show a fluctuating cross section with incident neutron energy. These authors suggest that the rapidly varying cross section may be due to the fluctuations in the level density of the compound nucleus away from the average level density, similar to that found by Agodi et al, 1960.

The spectrum of emitted protons obtained by Konijn and Lauber (Fig. V.2.a) does not show any evidence of a second peak, centred on a proton energy of 2.21 Mev as found in the present experiment. However, the high background rate ( $\sim 50\%$ ) obtained by Konijn and Lauber in their work make the

observation of such a peak very difficult. (Konijn and Lauber show only the 'target-in' and 'target-out' spectra in their paper, rather than the subtracted spectrum; also, their method of analysis involved an integration of all detected particles having energy greater than 1 Mev, i.e. they offer no information as to the presence of a second proton peak.)

The width of each of the proton peaks in the 'good' resolution experiment is greater than was calculated from the resolution of the system ( 9%). This increased width may be due to the excitation of several levels in the residual  $\text{Co}^{58}$  nucleus. For example, if the higher energy proton peak is due to the excitation of the two known levels in  $\text{Co}^{58}$  ( $2^+$  ground state and  $5^+$ , 25 Kev metastable state) and another level, then allowing for the resolution of the system the width of the peak may be explained as being due to the excitation of a third level at 0.26 Mev in the residual  $\text{Co}^{58}$  nucleus. However, the excitation energy of such a level cannot be determined accurately in the present experiment but would require a further study with improved resolution. The presence of a third level in the region of 0.26 Mev excitation energy in the  $\text{Co}^{58}$  nucleus justifies to a certain extent, the type of Hauser-Feshbach calculations carried out ( V.3. ). The width of the lower energy proton peak corresponding to an excitation energy at approximately 1.3 Mev in the residual nucleus, is also suggestive of the presence of more than one level. However, again the resolution of the system does not allow an accurate

determination of the number or position of the levels.

The excitation curve for the (n,p) reaction in Ni<sup>58</sup> was determined by detecting protons leading to a region of approximately 0.5 Mev excitation energy above the ground state in the Co<sup>58</sup> residual nucleus. Therefore, the presence of proton groups leading to an excitation energy of approximately 1.3 Mev would not be considered in the determination of the excitation curve. These proton groups would have the effect of increasing the gradient of the excitation curve, bringing it into better agreement with the measurements of Barry, 1962, and Gonzalez et al, 1960, who measured the total proton emission by the activation technique. The increase in gradient would be such as to increase the cross section at a neutron energy of 3.45 Mev by a factor of 1.5. (This factor has been determined from the 'good' resolution experiment and hence the remarks made previously in this section on the non-applicability of a compound nuclear statistical mechanism throw some doubt on the application of the factor 1.5 to the 'poor' resolution experiment.). The presence of the Coulomb barrier will have the effect of decreasing the cross section for the emission of the lower energy protons by a greater amount than that for the emission of the higher energy protons at neutron energies less than 3.45 Mev i.e. the factor 1.5 is a maximum value.

V.6.b. Fe<sup>54</sup>(n,p)Mn<sup>54</sup>.

The spectrum of the protons (Fig. IV.5) emitted in the study of the Fe<sup>54</sup>(n,p)Mn<sup>54</sup> reaction is in many respects

similar to that obtained for the reaction  $\text{Ni}^{58}(\text{n,p})\text{Co}^{58}$  (Fig IV.4.). The spectrum consists of a broad peak with a narrow width peak at lower energy, corresponding to excitation of the  $\text{Mn}^{54}$  residual nucleus in the region of the ground state and 0.75 Mev respectively. The cross sections for the emission of protons to the higher and lower energy peaks are respectively 129 mb. and 46 mb., (assuming an isotropic emission of the protons). The value of the cross section for the reaction obtained by extrapolation of the excitation curve (Fig.V.1.a.) is 165 millibarns. This latter value may be compared to the cross section for the emission of protons leading to a region of excitation energy 0.5 Mev above the ground state of the manganese nucleus i.e. 129 millibarns. As in the case of the 'good' resolution measurement of the  $\text{Ni}^{58}(\text{n,p})\text{Co}^{58}$  cross section the applicability of a compound nuclear statistical mechanism is in some doubt and hence, the comparison of the cross sections may not be justified.

One possible explanation for the broad peak at the higher proton energy is that it is due to the emission of two groups of protons leading to the ground state and to an excitation energy of 0.35 Mev in the residual nucleus (each 9% Full Width half maximum height), the ratio of the cross sections for the emission of the former group to the latter group being of the order of 5 : 1. The lower energy peak present in the spectrum is not as wide as that formed in the  $\text{Ni}^{58}(\text{n,p})\text{Co}^{58}$  spectrum, its width suggesting that it is due to the excitation

of a single level at 0.75 Mev in the manganese nucleus.

However, as stated previously, the resolution of the system is not sufficient to give accurate information as to the number and energy of the levels in the residual nucleus.

#### V.7. Conclusion.

The excitation curves for the emission of protons leading to a region of excitation near the ground state of the residual nucleus have been measured for the (n,p) reactions in  $\text{Ni}^{58}$ ,  $\text{Fe}^{54}$  and  $\text{Cu}^{63}$  and have been found to be in reasonable agreement with the results of other workers. In the case of  $\text{Ni}^{58}(\text{n,p})\text{Co}^{58}$ , the excitation curve has been predicted to within 25% by means of Hauser-Feshbach calculations, assuming the existence of a  $4^+$  level at 0.3 Mev excitation energy in the residual  $\text{Co}^{58}$  nucleus. Measurements at one neutron energy with improved resolution on the emission of protons from the (n,p) reactions in  $\text{Ni}^{58}$  and  $\text{Fe}^{54}$  show the presence of previously unknown levels in the residual nucleus. However, the resolution of the experiments was not sufficient to make an accurate determination of the number and energies of the levels. Further experiments with improved resolution would be of value in making an accurate determination of these quantities, and also, possibly, spins and parities by comparison with theoretical calculations. The existence of other levels in the cobalt-58 and manganese-54 nuclei have not been proven by other workers in the field of low energy (n,p) reactions but have been predicted as an explanation of the discrepancy

between experimental results and theoretical Hauser -  
Feshbach calculations (e.g. Meadows and Whalen, 1963, for  
the case of the cobalt-58 nucleus).

Chapter VI.

The Angular Distribution of Alpha Particles emitted from  
Medium Weight Targets bombarded with 14.8 Mev Neutrons.

VI.1. Introduction.

The study of the angular distribution of particles resulting from nuclear reactions thought to proceed mainly through a compound nuclear statistical mechanism, has the twofold objective of a) verifying the nuclear mechanisms of the reaction and b) obtaining a measurement of the spin dependence of the level density of the residual nucleus.

Bloch, 1954, has shown on general grounds that most models describing level density spin dependence lead to the form

$$\omega(I) \propto \frac{(2I+1)}{2\sigma^2} \exp\left[-\frac{(I+\frac{1}{2})^2}{2\sigma^2}\right] \quad (I)$$

(c.f. Chapter I), where  $\sigma^2$  is an energy dependent parameter known as the 'spin-cut-off' parameter. When  $\sigma^2$  is such that  $2\sigma^2 \gg (I + \frac{1}{2})^2$ , the above expression reduces to the form  $\omega(I) \propto (2I+1)$ . Most methods of deriving  $\sigma^2$  are indirect. The best method would be to count levels of a given spin in an energy interval; however, such a procedure would be difficult. The most frequently employed method is that of the study of angular distributions of nuclear reactions. Wolfenstein, 1951, Hauser and Feshbach, 1952, and Lane and Thomas, 1958, have shown that the angular distribution of particles emitted through compound nuclear processes is isotropic when the level density has a spin dependence  $\omega(I) \propto (2I+1)$  i.e.  $\sigma^2 \rightarrow \infty$ .

Ericson and Strutinski, 1958, have given classical arguments to show that, in the general case of  $\omega(I)$  given by equation VI.1., the angular distribution of the emitted particles should be peaked in the forward and backward directions while having symmetry about  $90^\circ$ . The treatment of the latter authors leads to an approximate expression for the angular distribution of the form

$$W(\theta) = 1 + \frac{\langle l^2 \rangle \langle L^2 \rangle}{12\sigma^4} P_2(\cos \theta) + \frac{3 \langle L^4 \rangle \langle l^4 \rangle}{560\sigma^8} P_4(\cos \theta)$$

where  $L$  and  $l$  are the angular momenta of the incident and emitted particles, respectively. The expression for  $W(\theta)$  is applicable within the approximation of  $\frac{Ll}{\sigma^2} \ll 1$  (the weak coupling approximation). Hence a determination of the anisotropy of the angular distributions, bearing in mind the possible effects of reaction mechanisms other than compound statistical mechanisms (e.g. direct interaction effects), leads to an estimation of the spin cut-off parameter which, in turn, gives a further understanding of nuclear level density spin dependence.

#### VI.2. Previous Studies of $(n, \alpha)$ Reactions.

A large amount of work has been carried out in the measurement of the cross sections of  $(n, \alpha)$  reactions produced by neutrons in the energy range 12 to 17 Mev. The first and most extensive general survey was made by Paul and Clarke, 1953, who used an activation technique. Their results show little agreement with the Weisskopf-Ewing statistical theory of nuclear reactions, especially in the mass region  $80 \leq A \leq 110$ .

The cross sections obtained by Paul and Clarke were, in general, several orders of magnitude greater than the predicted values. Later measurements obtained lower values for the cross sections in better agreement with theory. (Blosser et al, 1955, '58, Coleman et al, 1959, and Weigold, 1960). Facchini et al, 1964, have computed  $(n, \alpha)$  cross sections for a number of target nuclei by means of the statistical theory making use of the level density formula of Lang and Le Couteur, 1964, in which allowance for the odd-even effect in level densities has been made. Their calculated cross sections agree to within 30% with the known experimental values in the mass region  $A < 90$ . Chatterjee, 1963, has published a survey of measured  $(n, \alpha)$  cross sections. By plotting the  $(n, \alpha)$  cross sections versus neutron and proton number ( Fig. VI.1), he has demonstrated the influence of shell effects. He found that there were minima at all major proton shell closure positions of the residual nuclei; there was no evidence for corresponding minima due to neutron shell closures.

The energy spectrum and angular distribution of emitted alpha particles has been studied by several workers for a variety of targets using emulsion and counter techniques. Kumabe et al, 1957, '58, have obtained the energy spectra and angular distribution for the  $(n, \alpha)$  reactions in the target nuclei  $Al^{27}$ ,  $Co^{59}$ ,  $Mn^{55}$ ,  $V^{51}$  and  $S^{32}$  using an emulsion technique. The target foils formed a thin layer on each side of a thick platinum foil, sandwiched between two 200 micron

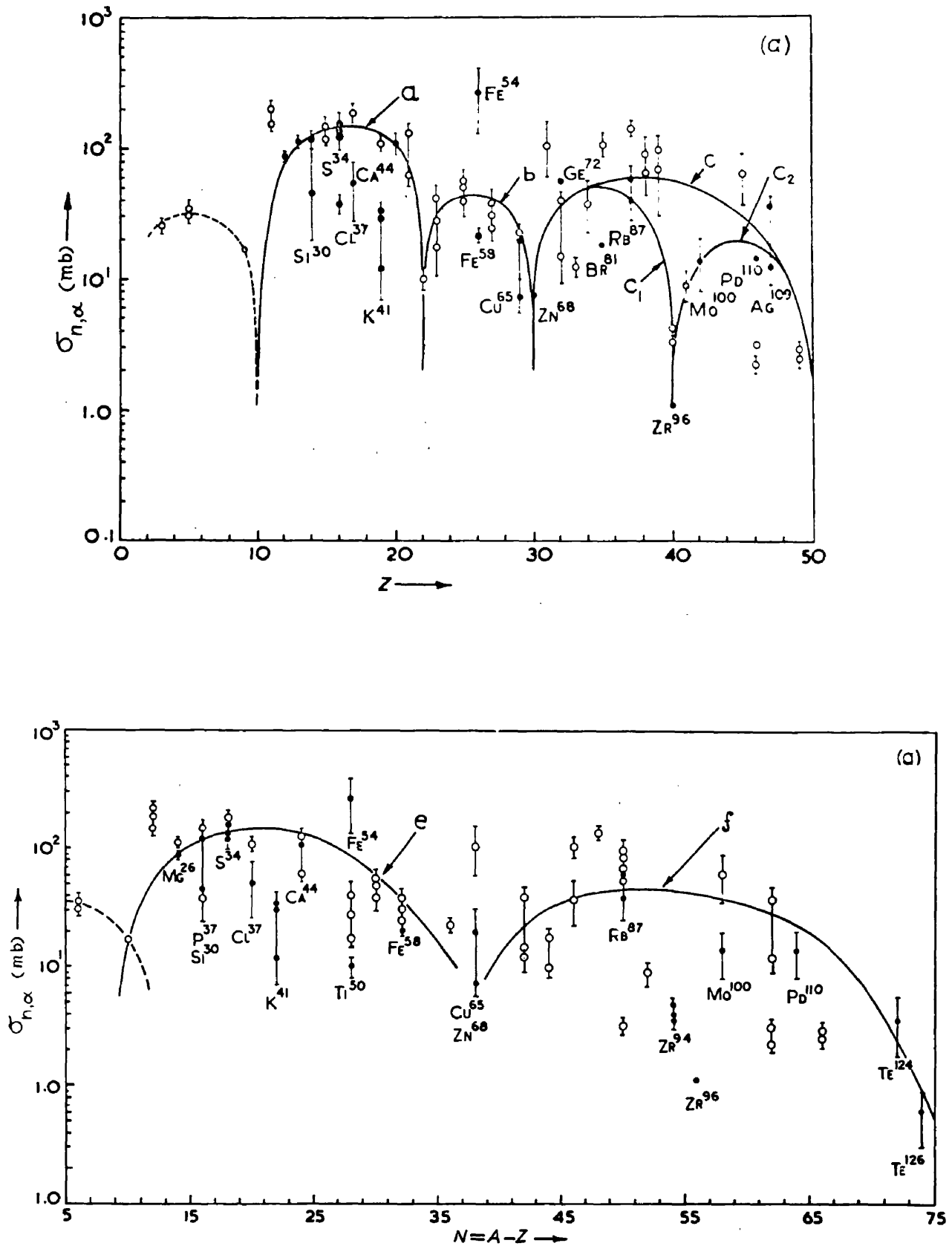


Figure V1.1. Showing results of survey by Chatterjee.

nuclear emulsions. The target assembly was mounted such that the mean angle of incidence of 14.8 Mev neutrons on the target foils was  $45^\circ$ . Ilford C2 and K2 plates were used with a temperature development method; the method of development lead to some difficulty in discriminating between alpha particles originating close to the surface of the plate and external alpha particles. Typical results obtained by Kumabe et al for the target nuclei  $\text{Co}^{59}$  and  $\text{Mn}^{55}$  are shown in Fig.VI.2. The angular distributions show a large degree of anisotropy, the ratio of the cross sections at  $0^\circ$  and  $90^\circ$  being of the order of 3. However, there is symmetry about  $90^\circ$  suggesting the lack of a direct interaction mechanism in the  $(n, \alpha)$  reactions. Their results are in contrast to the results generally found in the study of  $(n, p)$  reactions at 14 Mev (Less anisotropy and preferential forward peaking). Kumabe et al found that low energy alpha particles were emitted in excess of what was expected ; They suggest that such an excess of low energy particles may be indicative of a diffuse nuclear boundary. Sen, 1962, in an investigation of the  $(n, \alpha)$  reaction in Indium using the emulsion technique has obtained similar angular distributions to those of Kumabe et al. However, Sen has shown that alpha particles of energy greater than 13 Mev are preferentially peaked forward, suggesting the presence of a direct interaction mechanism. Sen estimated that the direct interaction mechanism accounted for 12% of the total  $(n, \alpha)$  cross section. Kaul, 1962, '64, has also obtained angular

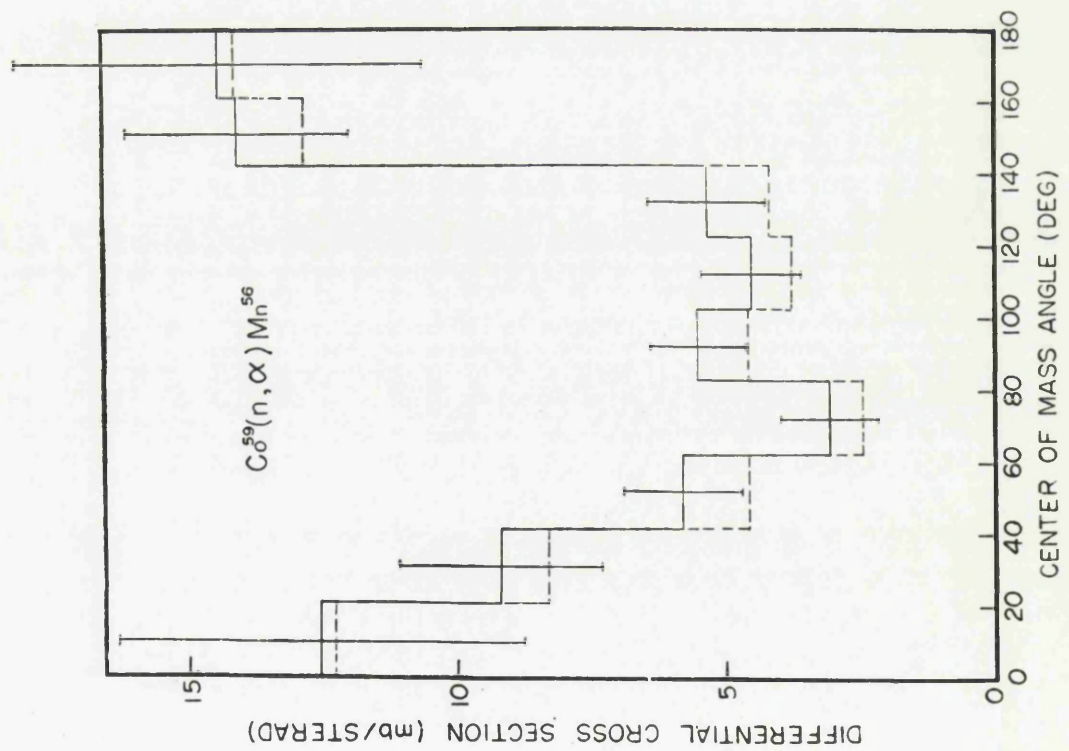
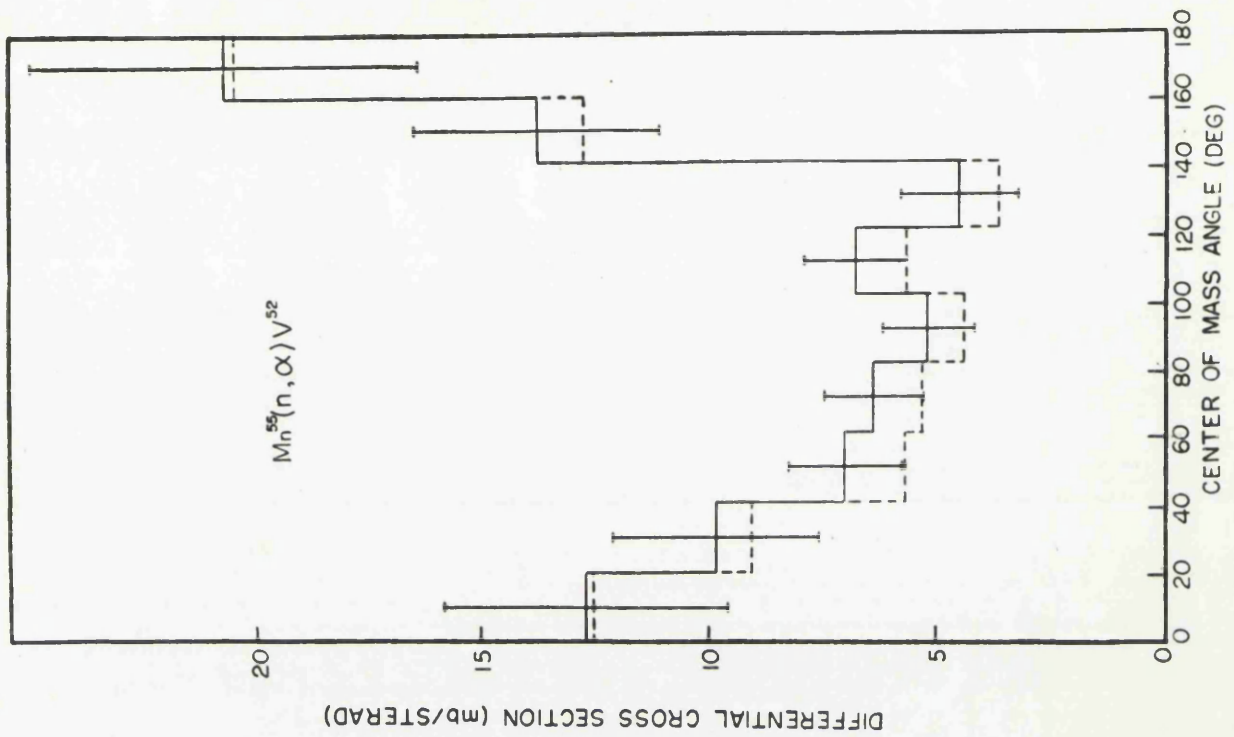


Figure V1.2. Results of Kumabe for the  $(n, \alpha)$  reaction in  $Co^{59}$  and  $Mn^{55}$ .

distributions having a large degree of anisotropy for the  $(n, \alpha)$  reactions in  $\text{As}^{75}$ ,  $\text{Na}^{23}$ ,  $\text{Mn}^{55}$  and  $\text{Ca}^{40}$ , using a loaded emulsion technique. Also, using the emulsion technique, the angular distribution of the reaction  $\text{Al}^{27}(n, \alpha)\text{Na}^{24}$  has been obtained by Cevolani et al, 1960. Although measurements were carried out only in the backward hemisphere, anisotropy again seems to be present (Cevolani et al could not distinguish between alpha particles and protons below 6 Mev in their emulsions.). The energy spectra obtained by all the above workers agree with that expected on the basis of the statistical theory. There is fairly good agreement among the various determinations of the  $(n, \alpha)$  cross sections in the region of light and intermediate weight nuclides, extending to nuclides as heavy as  $\text{As}^{75}$ . However, in the case of the target nucleus  $\text{Al}^{27}$ , the three activations measurements of Forbes, 1952, Yasumi, 1957, and Grundl et al, 1958, are satisfactorily consistent, although they are inconsistent with the determination of Kumabe et al. and Paul and Clarke.

In contrast to the type of angular distributions obtained by Kumabe et al, Sen, Kaul, and Cevolani et al, Patzsch and Vonach, 1962, and Jarvis et al, 1963, have obtained much less anisotropic angular distributions for the  $\text{Al}^{27}(n, \alpha)\text{Na}^{24}$  reaction. (Patzsch and Vonach also studied  $\text{Co}^{59}$ ). Their experimental technique involved the use of an emulsion shielded by a 'shadow-bar', thus enabling an accurate background separation to be made. The results of the two experiments are consistent

within the experimental accuracy. Jarvis et al have suggested that the large degree of anisotropy obtained by Kumabe et al, Kaul, Sen and Cevolani et al, may be due to inaccurate background separation. They suggest that since the  $(n, \alpha)$  reactions in the silver and bromine of the emulsions proceed almost entirely by direct interaction, there will be a marked forward emission of high energy alpha particles; the  $(n, \alpha)$  reactions in oxygen ( $\sigma=300$  mb), carbon and nitrogen give rise to a number of low energy alpha particles. Thus, one would expect a large degree of anisotropy in the background of angular distribution of alpha particles in emulsions, making a background separation very difficult. In contrast with the results of Kumabe et al, the results of Patzsch and Vonach, and Jarvis et al, suggest the presence of a direct interaction mechanism.

Counter techniques have been used to a lesser extent than the emulsion or activation techniques in the study of  $(n, \alpha)$  reactions in the region of 14 Mev neutron energy. The first use of a counter telescope in the study of  $(n, \alpha)$  reactions was made by Ribe and Davis, 1955,. Their apparatus consisted of two proportional counters and a NaI(Tl) crystal. However, the low efficiency of their apparatus did not allow them to use a thin target. Irfan and Jack, 1963, using a telescope consisting of a proportional counter and a CsI(Tl) crystal, determined the energy spectra of emitted alphas with target nuclei  $Al^{27}$ ,  $Fe^{54}$ ,  $Cu^{63}$ ,  $Zn^{64}$  and  $Ag^{107}$ . The energy spectra of emitted alpha particles in each case, with the exception of

the  $\text{Ag}^{107}(n, \alpha)\text{Rh}^{104}$  reaction, are in agreement with the predictions of the statistical theory. In the case of the target nucleus  $\text{Ag}^{107}$ , the relatively high cross section was suggested to be due to a direct surface interaction mechanism. With a telescope of improved geometry, Irfan and Jack determined the angular distribution of the emitted alpha particles from the reaction  $\text{Al}^{27}(n, \alpha)\text{Na}^{24}$ . Their results, Fig. VI.3., show the forward peaking found by other workers in the field. The angular distribution of the  $\text{Al}^{27}(n, \alpha)\text{Na}^{24}$  reaction has also been determined by Seebeck and Bormann, 1964, using pulse shape discrimination in a CsI(Tl) crystal. Their results do not show marked anisotropy found by Kumabe et al. Finally, several studies of  $(n, \alpha)$  reactions in silicon isotopes and in heavy mass targets have been carried out with the aid of silicon semiconductor counters, by various workers (Colli, 1962, Blanc et al, 1962, Aitken and Dixon, 1962, Marcazzan et al, 1963, Cuzzocrea et al, 1964, Kulišić et al, 1964). In general, it was found that direct interaction effects made a considerable contribution to the  $(n, \alpha)$  cross section in the case of the heavy target nuclei.

In view of the large amount of discrepancy in the results of various workers on the angular distributions of alpha particles emitted from  $(n, \alpha)$  reactions, it was considered worthwhile to obtain good angular distributions with several target nuclei, and thus, to determine the relative importance

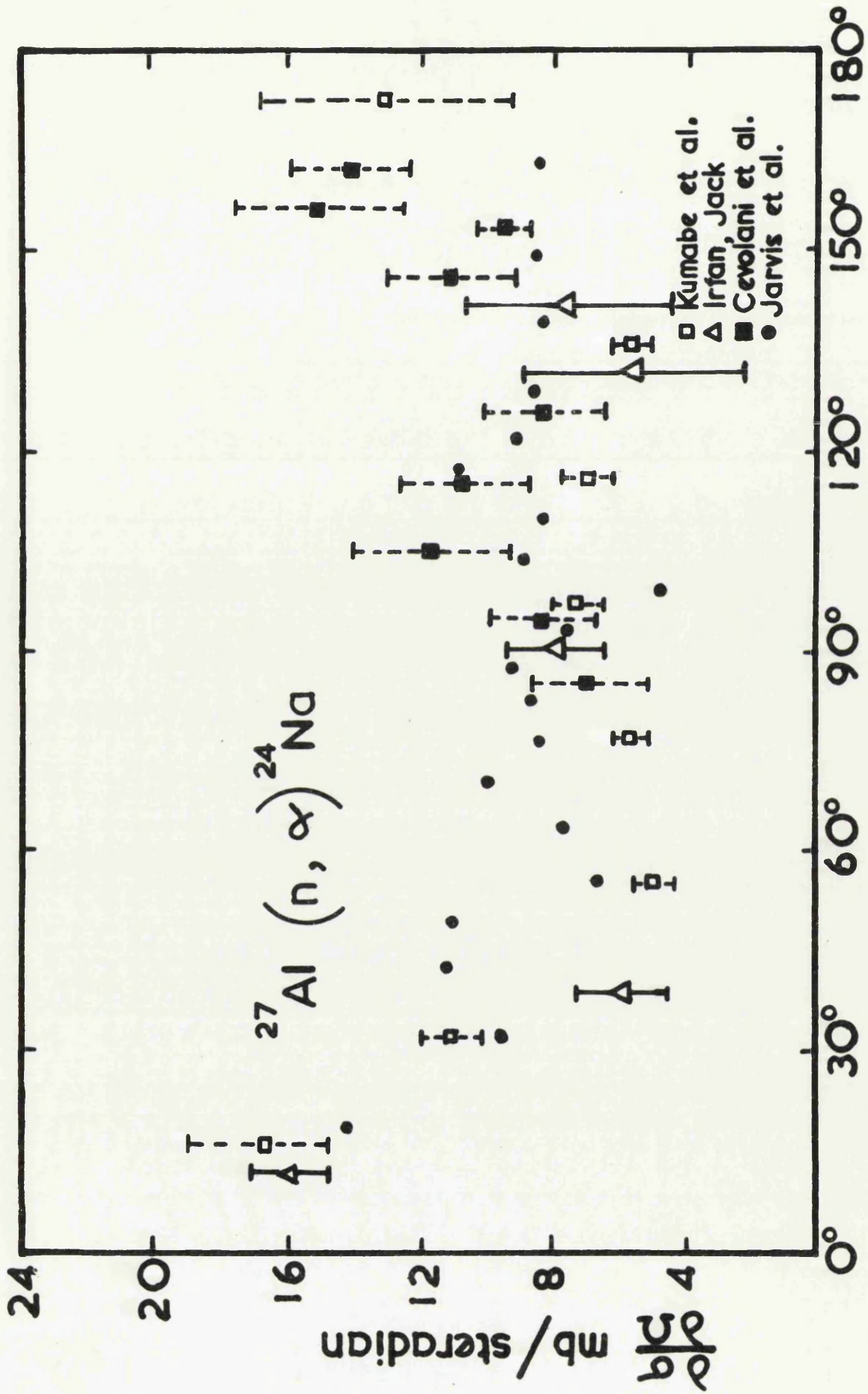


Figure VI.3. Angular distributions for the reaction  $\text{Al}^{27}(n, \alpha)\text{Na}^{24}$ .

of the direct interaction and statistical compound nuclear mechanisms and also aid the estimation of the spin cut-off parameter of level density formulae.

### VI.3/ Experimental Technique.

The main criteria in the design of an experiment to measure the angular distribution of alpha particles may be listed as:-

- a) good geometry necessary, while, at the same time, having adequate efficiency.
- b) the ability to obtain information on all alpha particles emitted between  $0^\circ$  and  $180^\circ$  with respect to the incident neutron beam.
- c) a useful, but not necessary, ability to determine the energy spectra of the emitted particles at the various angles at which measurements are made.

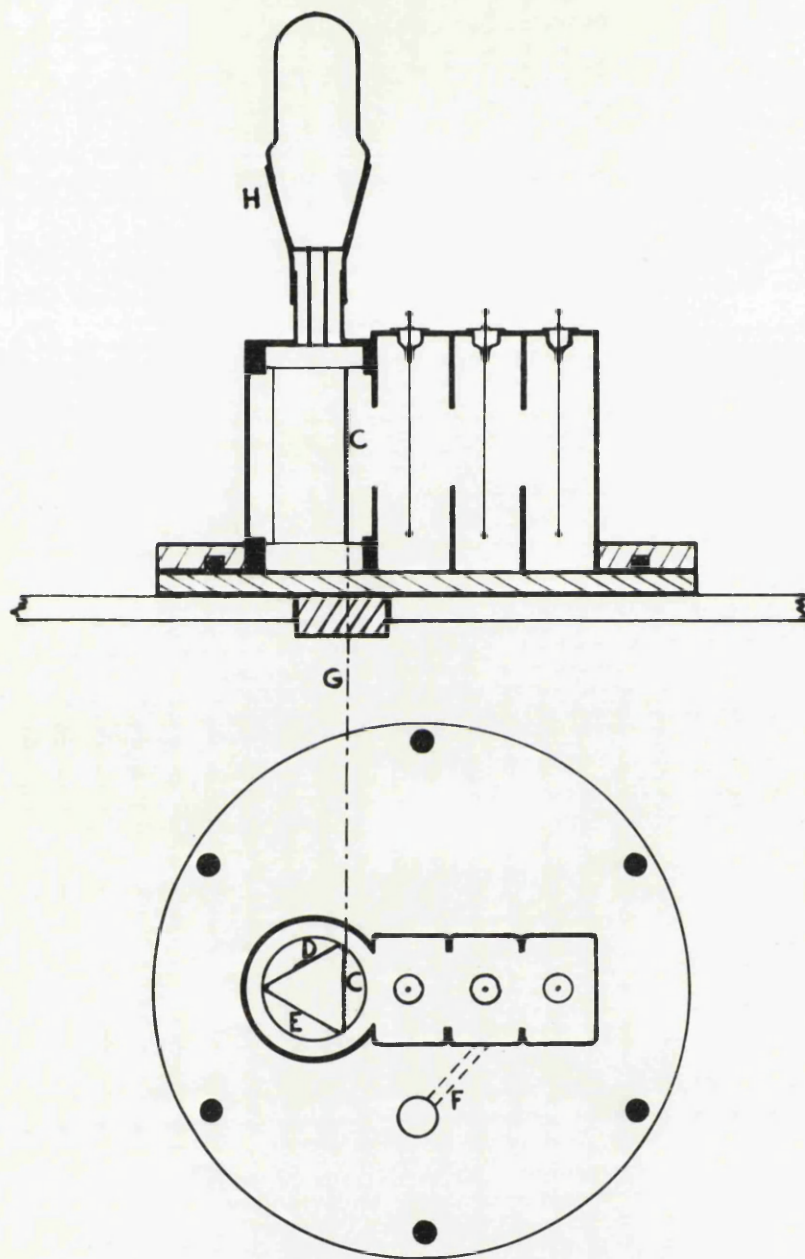
With these points in mind, a counter telescope detection system was devised. The telescope consisted of three proportional counters, operating in coincidence, in close proximity of a thin target foil. An advantage of the use of three proportional counters was that the complete apparatus could be made compact, thus enabling the detection system to be placed between the target and the neutron source while at the same time, the separation between the target and the neutron source is not too large to have a deleterious effect on the efficiency of the system. Hence, measurements could be carried out at all angles between

(and including)  $0^\circ$  and  $180^\circ$ . The use of a CsI(Tl) crystal as an energy counter would not be suitable since it has been found that detection in an angular range greater than  $\sim 140^\circ$  is extremely difficult because of the need for a photomultiplier tube to be attached to the apparatus. A silicon semiconductor counter, although of suitable physical dimensions, could not be used as an energy counter because of the presence of a high background due to  $(n,p)$  and  $(n,\alpha)$  reactions in the silicon isotopes. Since the detection system consisted solely of proportional counters no detailed knowledge of the energy distribution of emitted particles could be obtained; the quantities determined in the experiment were total numbers of alpha particles in a wide energy band emitted into a narrow solid angle at various angles. However, such a procedure is adequate for the determination of angular distributions and, hence, spin cut-off parameters, provided the reaction being studied was known to proceed through a statistical compound nuclear mechanism. A further requirement is that the magnitude of the cross section for the  $(n,n'\alpha)$  reaction should be small, relative to that for the  $(n,\alpha)$  reaction, since the angular distribution for the former reaction is unknown and will probably be different from that of the  $(n,\alpha)$  reaction. The target nuclei chosen were known, from the results of other workers, to give alpha particle energy spectra in agreement with the predictions of the statistical theory.

#### VI.4. Experimental Apparatus.

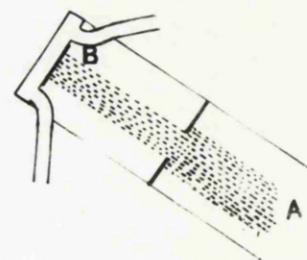
A schematic diagram of the apparatus designed for the study of angular distributions is given in Fig.VI.4. The three proportional counters, which were rectangular in cross section and approximately 1 cm. deep, were mounted on a brass base plate so that the central wires of the counters were parallel to a target tube. The target tube contained a target holder, triangular in cross section, which could be rotated by means of a glass cone-joint without affecting the vacuum of the system. The proportional counters and target chamber could be evacuated through a port F (Fig: VI.4.) in the base plate. Access to the interior of the apparatus was made by removing a flange plate which was attached to the base plate by means of a vacuum seal. The walls of the proportional counters and the target tube were manufactured in thin brass so that the attenuation of the neutron beam was minimised; also, in the interest of low attenuation and scattering, the triangular target holder was formed from three thin brass plates i.e. the target holder was hollow and evacuated. The complete assembly of proportional counter and target chamber was mounted on a smooth horizontal rigid table in such a way that the assembly could be rotated through a vertical axis G (Fig.VI.4.) in the plane of a face of the target holder which was parallel to the apertures of the proportional counters.

The proportional counters had apertures of diameter 1.5 cm.



1 INCH

Figure VI.4 Apparatus designed for the study of angular distributions.



which were covered with  $0.27 \text{ mg/cm}^2$  aluminium foils. The separation between a target foil when in position and the front aperture of the counter which was farthest away from the target foil was 4.4 cm. The diameter of the target foil was 1.2 cm. Hence the solid angle for detection of the emitted particles was .085 steradians. The proportional counters were filled to a pressure of 8 cmHg with a mixture of 10% methane and 90% Argon. Methane was chosen as a quenching agent instead of  $\text{CO}_2$ , to avoid unnecessary background production of alpha particles from the  $(n, \alpha)$  reaction in oxygen; the problem of the  $(n, \alpha)$  reaction in carbon still remained. The central electrode of each proportional counter was a tungsten wire of diameter 0.008". The normal operating voltage with such central electrodes was of the order of 900 volts. The tungsten wires entered the counters from the external electronic system through a 'kovar' seal, while the other end of the wire was sealed in a glass bead to prevent electrical discharge. In an attempt to keep the background production of alpha particles to a minimum, the counters and the target holder were lined with 0.002" gold foil.

#### VI.5. Experimental Method.

A flux of neutrons was obtained from a Glasgow University H.T. set by making use of the reaction  $\text{H}^3(d, n)\text{He}^4$ ,  $Q = 17.6 \text{ Mev}$ . The neutron source target consisted of a thin layer of titanium impregnated with tritium, and mounted on a copper backing; the diameter of the target was approximately 1 cm. With a 100

microamp beam of incident deuterons, of energy 200 Kev, the flux of neutrons emitted into unit solid angle about  $0^\circ$  (with respect to the deuteron beam) was  $4 \times 10^8$  neutrons/sec. The energy of the emitted neutrons at  $0^\circ$ , which are due to the excitation of the 110 Kev resonance in the D-T reaction, is  $14.8 \pm 0.1$  Mev. The quoted energy spread is due to the energy loss ( 70 Kev.) of the deuteron beam in the tritium target. The neutron flux was monitored by means of two proton recoil monitors of the type described in Chapter III. The monitors were rigidly fixed at right angles to each other and in the plane at  $90^\circ$  to the incident deuteron beam. Since the energy of the neutrons that were monitored is 14.1 Mev, the recoil proton peak is well separated from the exponentially rising background. Fig. VI.5. shows typical neutron monitor spectra obtained with and without a polythene foil; the biasing position is shown by means of an arrow. The use of two monitors serves as a check on each monitor during the irradiations and places confidence in the determination of absolute cross sections.

The experimental target was placed at 19 cm. from the centre of the neutron source (B. in Fig. VI.4.). This distance was chosen because a) it gave the necessary narrow geometrical beam spread while at the same time allowing adequate efficiency, and b) the signal to background ratio was not impaired when the detection system was placed between

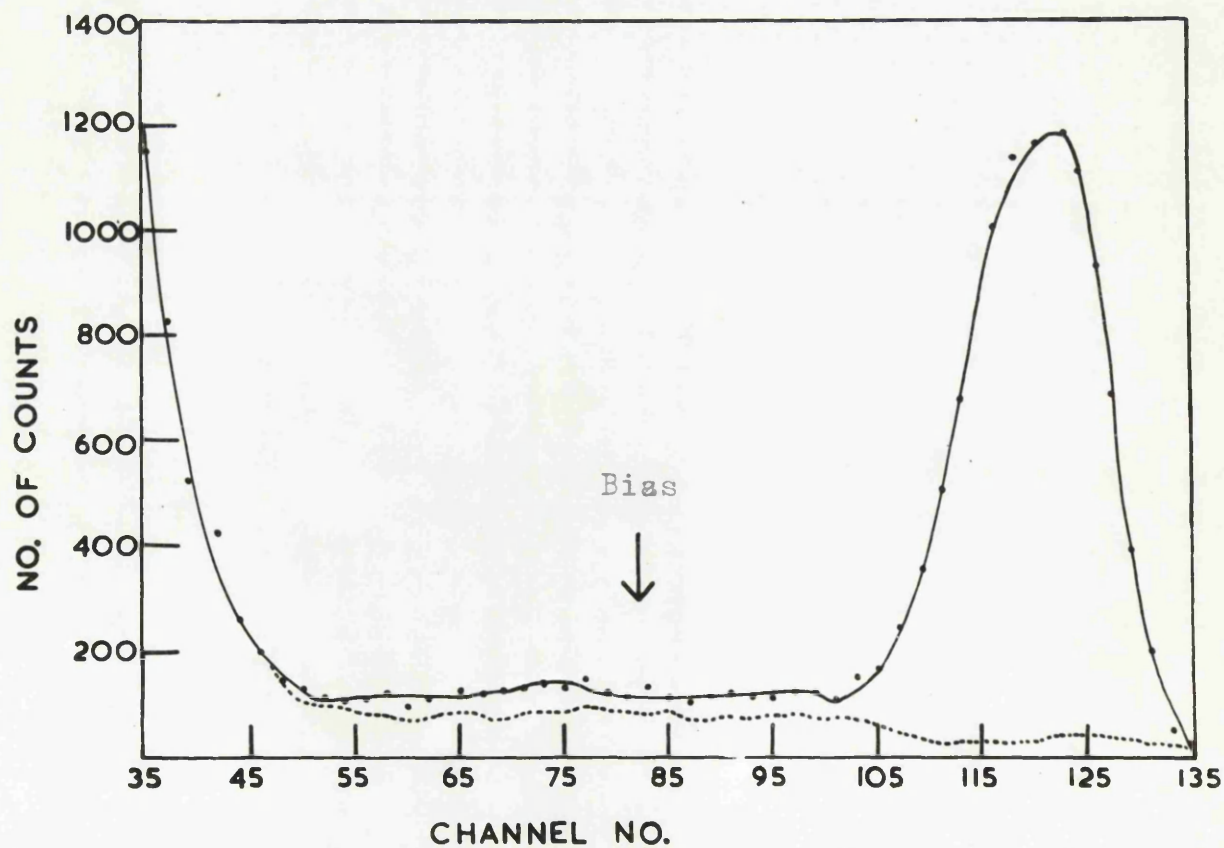
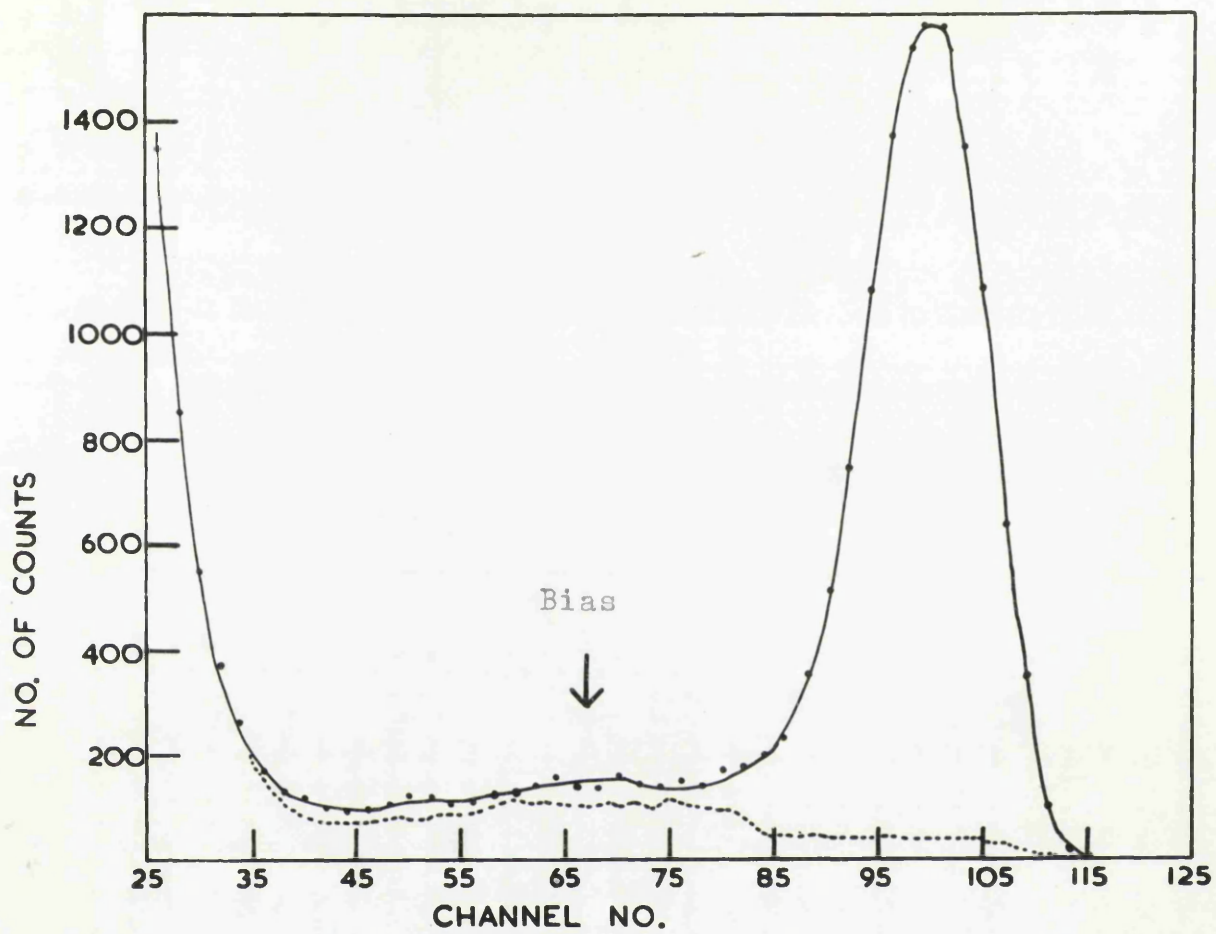


Figure V1.5. Neutron monitor spectra for 14.1 Mev neutrons.

the neutron source and target (i.e. detection of alpha particles emitted at  $180^\circ$ ).

The effective operation of the experiment requires that all alpha particles within a predetermined energy band are detected and that all other particles are rejected. The discrimination of alpha particles against protons was obtained automatically by careful adjustment of the amount of absorbing material in the counters. The stopping power present in the path of a charged particle traversing the three counters (due to counter gas and aluminium windows), was such that the minimum energy of proton which could register a pulse in each counter and, hence, a coincidence pulse, was 0.8 Mev. Protons of energy greater than the minimum value 0.8 Mev gave rise to smaller  $dE/dx$  pulses in each proportional counter and hence could be rejected electronically. The maximum energy of alpha particles which could arise in the reactions studied was 16.5 Mev., and the corresponding  $dE/dx$  pulse was of the order of 1.5 times greater than that due to a 0.8 Mev proton. Hence, allowing for the poor resolution of the proportional counters (30% FWHM) all pulses due to protons were rejected while all alpha particles having energy less than 16.5 Mev were accepted. Alpha particles of energy less than 1 Mev were stopped before reaching the final counter. Deuterons and tritons in the energy range 1.3 Mev to 2.0 Mev and 1.5 Mev to 2.5 Mev, respectively, could be detected. However, since the  $(n, H^2)$  and  $(n, H^3)$  reactions are known to proceed

through a direct mechanism (a 'pick-up' mechanism), the energy spectra of the deuterons or tritons will be peaked towards the energy of the incident neutron and, hence, the cross section for the emission of low energy particles will probably be small in comparison with that for the emission of alpha particles, since the spectra of emitted alpha particles will be of the Maxwellian type predicted by statistical compound nuclear theory. Reactions of the type  $(n, \text{He}^3)$  in medium weight targets are characterised by large negative  $Q$  - values and do not contribute appreciably to the number of particles detected.

The differential energy loss pulses formed at each counter were amplified by a preamplifier - amplifier system; the preamplifiers were ring o'three types with a gain of 100, and the amplifiers were I.D.L., type 652 . Discriminator pulses from the main amplifiers corresponding to pulses greater than a preset level were fed into a coincidence unit (the discriminator levels were set to accept all alpha particles of energy less than 17 Mev). The output from the coincidence unit was used in conjunction with a gate unit to allow the analysis of a pulse from one counter. The energy loss of an alpha particle was calculated to be of a similar magnitude in each counter and, therefore, the pulses to be analysed could be taken from any of the counters. In practice, pulses from the counter adjacent to the target were analysed. Diagrams of the gate and coincidence unit are shown on Fig. VI.6 a,b. The final gated pulses were analysed on a C.D.C. 100 channel



# COINCIDENCE UNIT.

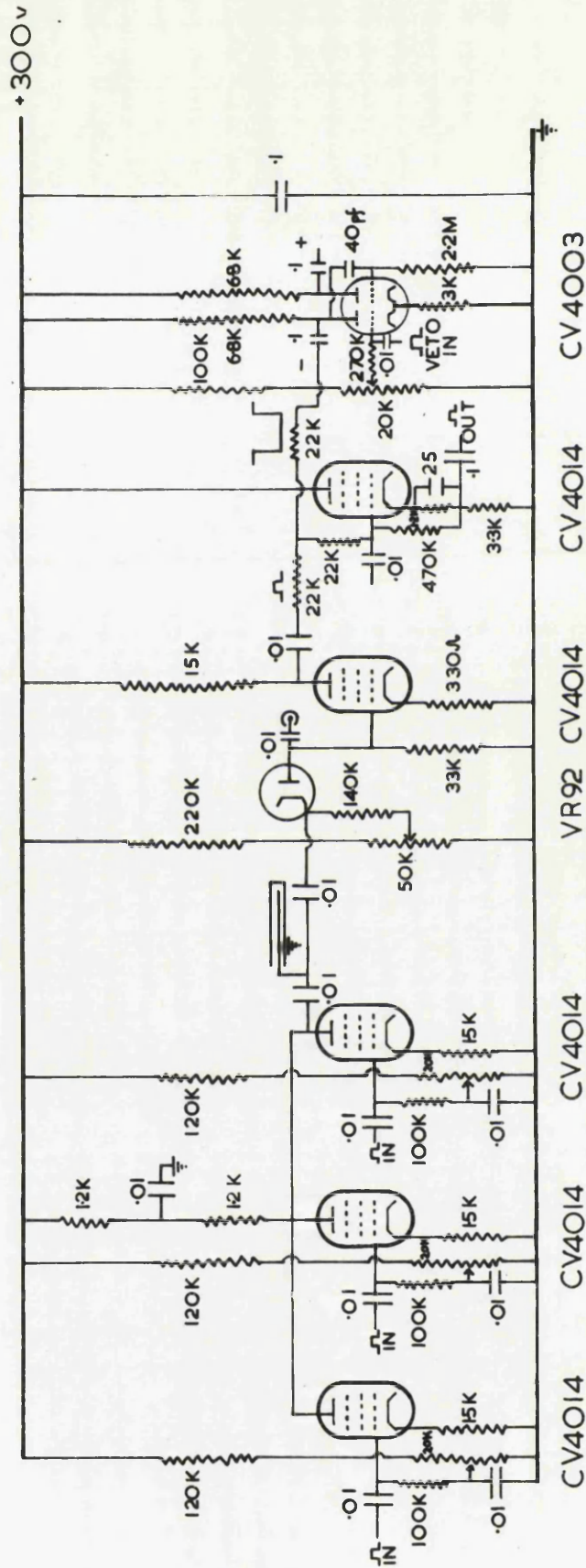


Figure V1.6b.

kicksorter ( or on a Marshall 100 channel kicksorter, at different times). The final pulses were also counted on a scalar unit. To check the reliability of the coincidence unit, a second coincidence unit and scalar were operated in parallel to the main unit during the irradiations. The calculation of the energy loss of the alpha particles in each counter, necessary for the setting of the discriminator levels, was carried out using the tables of Williamson and Boujot, 1962.

Experimental procedure consisted of a series of alternate irradiations on a target and background positions, each of approximately 90 minutes duration. Between irradiations, the stability of the counter and electronic system was checked using a  $\text{Po}^{210}$  alpha source mounted on the third face of the target holder. The reproducibility of the results of each irradiation was checked by comparison of the spectra of  $dE/dx$  pulses obtained. Irradiations were carried out with the system set to detect alpha particles emitted at up to seven angles. To avoid systematic errors, irradiations were performed at each angle at random. Comparison of the spectra obtained at the same angle on either side of  $0^\circ$  checked for the presence of systematic errors in angular positioning of the apparatus. Irradiations were carried out until sufficient counting statistics were obtained ( $\leq 7\%$ ). It was found that the number of background counts were much larger than the number of 'true' counts for a given neutron flux, and, hence, a large amount of irradiation time was required to obtain adequate counting

statistics at each angle.

#### VI.6. Target Materials.

The isotopes chosen for the study of the  $(n, \alpha)$  reaction were  $\text{Al}^{27}$ ,  $\text{Fe}^{54}$ ,  $\text{S}^{32}$ ,  $\text{Br}^{81}$  and  $\text{V}^{51}$ . An attempt was also made to investigate the  $\text{Cu}^{63}(n, \alpha)\text{Co}^{60}$  reaction, but the cross section was found to be very low. The main reasons for the choice of these target materials will be summarized as follows:-

The previous results, especially on the angular distribution, of the  $\text{Al}^{27}(n, \alpha)\text{Na}^{24}$  reaction show much discrepancy. The measured value of the cross section for the  $\text{Fe}^{54}(n, \alpha)\text{Cr}^{51}$  reaction given in the general survey by Chatterjee, 1963, does not agree with the systematics of  $(n, \alpha)$  reactions, (c.f. Fig.VI.1) and may be subject to experimental errors. The suggestion that the large anisotropy in the angular distributions measured by Kumabe and other workers may be due to the presence of the  $(n, n' \alpha)$  reaction can be tested by using a target having a large cross section for the latter reaction. The  $\text{S}^{32}(n, n' \alpha)\text{Si}^{28}$  reaction has been found by Kumabe, 1958, to have a large cross section. Previous results on the target materials  $\text{V}^{51}$  and  $\text{Br}^{81}$  show a certain amount of discrepancy.

The  $\text{Fe}^{54}$  and  $\text{Cu}^{63}$  targets were isotopic targets having a thickness of  $3.4 \text{ mg/cm}^2$  and  $2.9 \text{ mg/cm}^2$  respectively. The  $\text{Br}^{81}$  target was in the form of silver bromide, thickness  $2 \text{ mg/cm}^2$ . The  $\text{Fe}^{54}$ ,  $\text{Cu}^{63}$  and  $\text{Br}^{81}$  targets were supplied by the Atomic Energy Research Establishment, Harwell. The  $\text{V}^{51}$  and  $\text{S}^{32}$  targets were formed as <sup>an</sup> evaporation on a gold foil, in

the Department of Natural Philosophy, Glasgow University, with thicknesses  $3.0 \text{ mg/cm}^2$  and  $3.1 \text{ mg/cm}^2$  respectively. The  $\text{Al}^{27}$  target was a  $1.0 \text{ mg/cm}^2$  natural aluminium foil. All targets were mounted on a  $0.002''$  gold backing foil.

#### VI.7 Experimental Results.

It was found during initial trial irradiations that there existed in each counter a high counting rate (probably due mainly to neutron interactions in the gas.). The high counting rate in each counter (relative to the expected 'true' count rate) necessitated the use of more than one proportional counter operated in coincidence. Fig.VI.7. a is a typical background spectrum obtained from a proportional counter, while Fig.VI.7 b shows the corresponding spectrum obtained when a coincidence-gate system was used in conjunction with the three proportional counters. The requirement of a triple counter-coincidence system can be seen when one considers that the ungated spectrum is a factor of  $\sim 100$  greater than the 'true' spectrum.

The spectra obtained for target-in and target-out irradiations for each target and angle were normalized to the same total neutron flux and subtracted to give the spectrum of alpha particles emitted from the target. The spectra were then corrected for neutron attenuation in the material between the target and neutron source. The cross sections obtained by summing over all alpha particles emitted at a particular angle were converted to the centre of mass

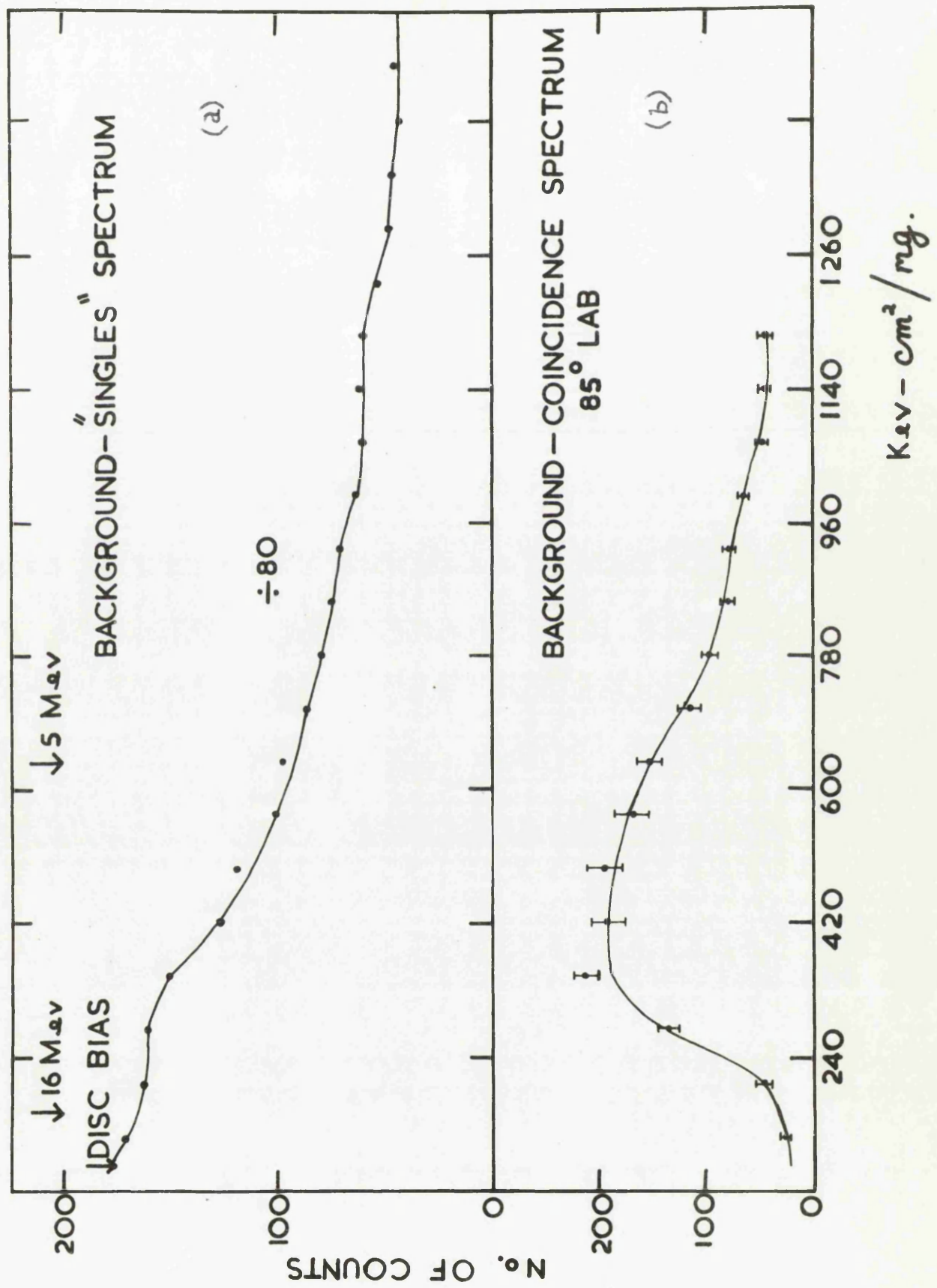


Figure 6.7.a,b.

co-ordinate system. Since a detailed knowledge of the energy spectra of emitted alpha particles was not obtainable from the  $dE/dx$  spectra obtained during irradiations, the conversion to the centre of mass system was carried out by assuming that all the alpha particles were emitted with an energy corresponding to the peak of the energy distributions obtained by other workers. The energy distributions used in the analysis of the  $Fe^{54}(n, \alpha)Cr^{51}$  reaction, was taken from the results of Irfan and Jack, 1963, while that for the  $(n, \alpha)$  reaction in  $Al^{27}$  and  $S^{32}$  was taken from the work of Seebeck and Bormann, 1964 and Kumabe, 1958, respectively. The  $Fe^{54}$ ,  $Al^{27}$  and  $S^{32}$  were the only targets used in a complete angular distribution study. In the case of the remaining targets,  $V^{51}$ ,  $Br^{81}$  and  $Cu^{63}$ , measurements were carried out at one angle only, viz.:  $90^\circ$ , in the interest of economy of machine time. The  $Fe^{54}(n, \alpha)Cr^{51}$  and  $S^{32}(n, \alpha)Si^{29}$  reactions were studied at seven angles while the  $Al^{27}(n, \alpha)Na^{24}$  reaction was studied at four angles. Typical spectra obtained are shown in Figs: VI.8. and VI.9.

## VI. 8. Discussion and Interpretation of Results.

### VI.8 a. $Fe^{54}(n, \alpha)$ .

The peaks of the  $dE/dx$  spectra for the  $(n, \alpha)$  reaction in  $Fe^{54}$  agree well with the value of 8.5 Mev found by Irfan and Jack for alpha particles emitted within a wide angular range with a weighted mean angle of emission of  $55^\circ$ . Since the spectra shown in Fig. VI.8. are  $dE/dx$  spectra, the energy scale is non-linear. The part of the spectra corresponding to

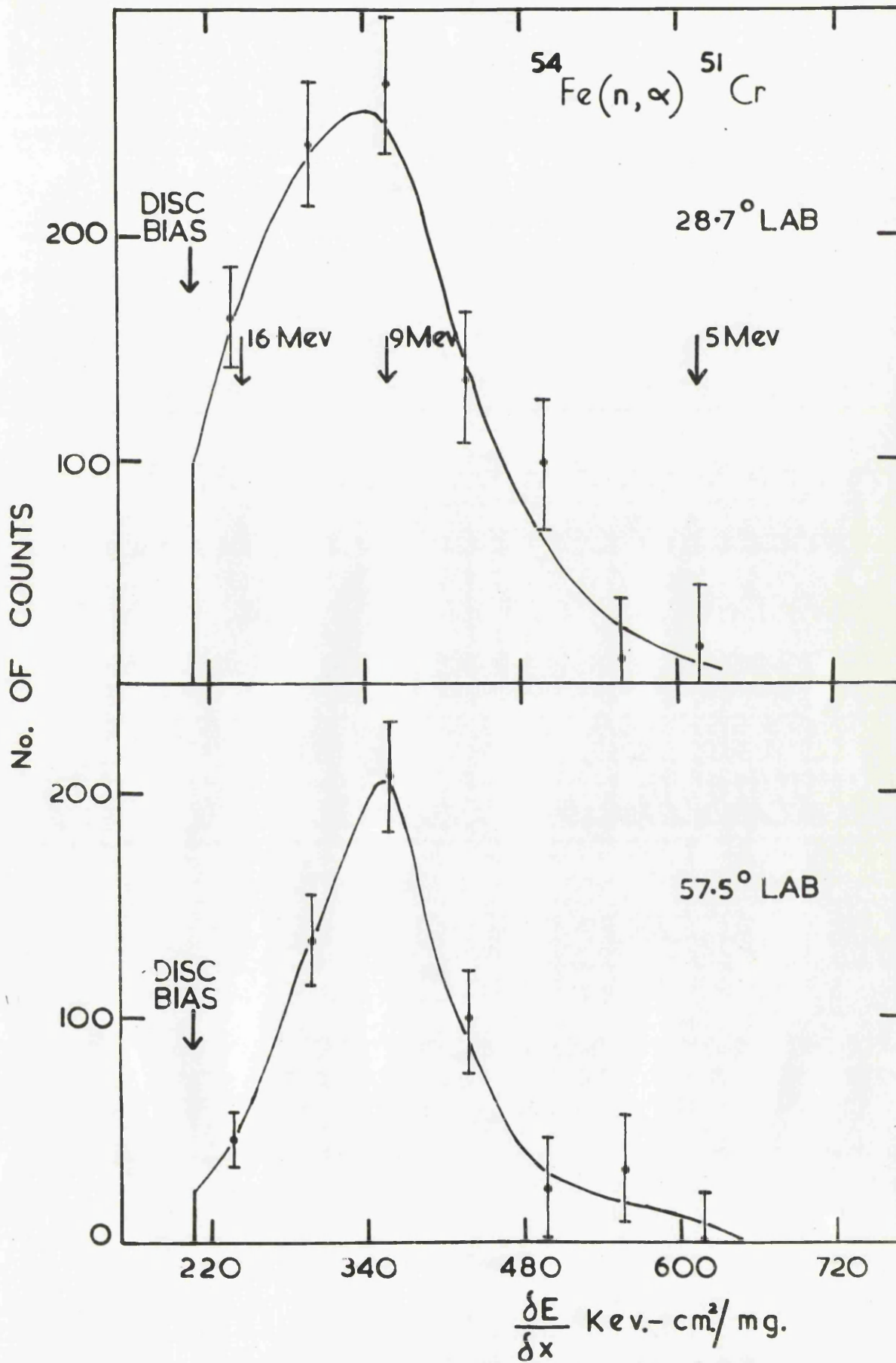


Figure Vl.8. Typical gated  $dE/dx$  spectra.

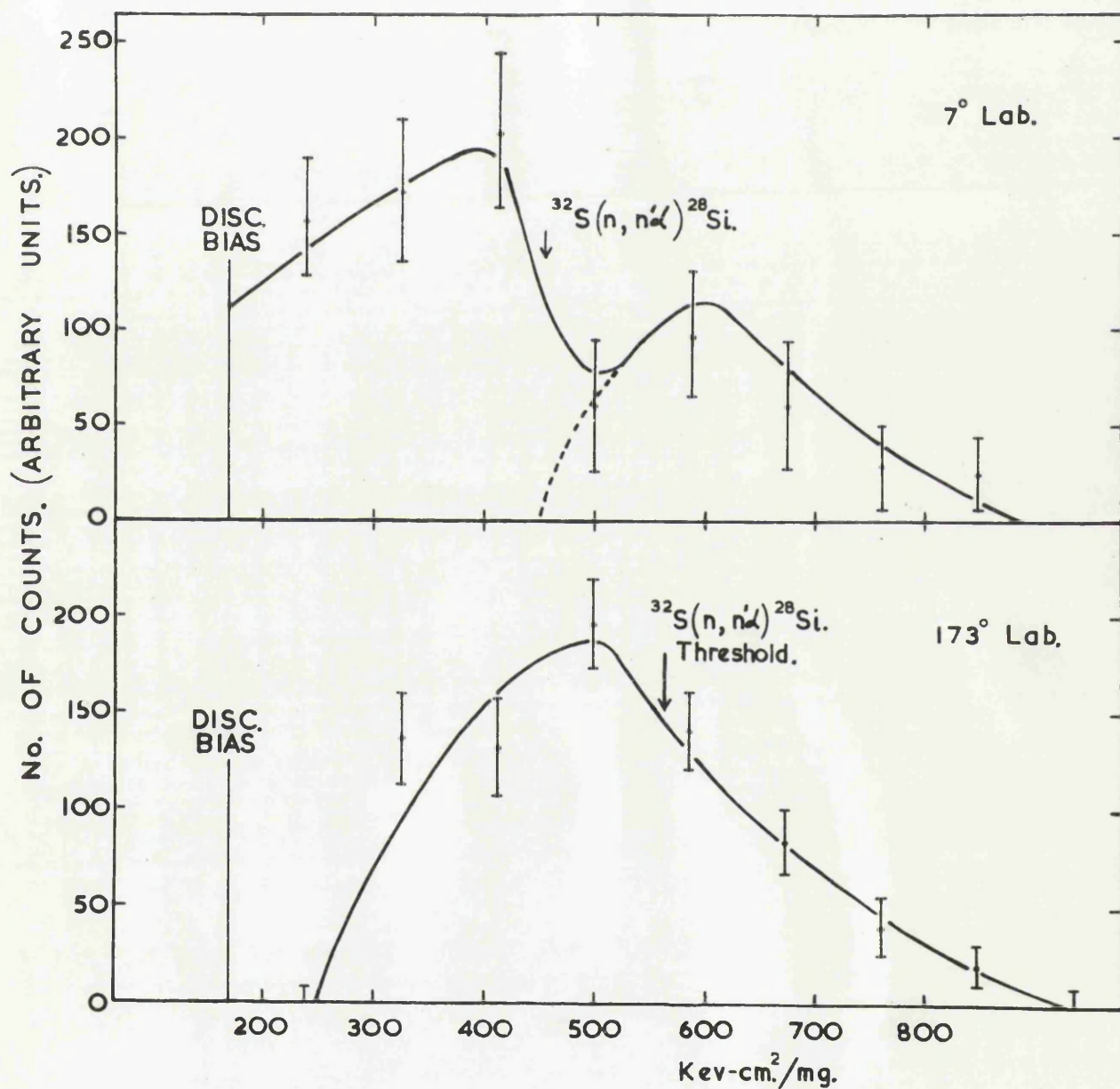


Figure VI.9. Typical gated  $dE/dx$  spectra for the emission of alpha particles from  $\text{S}^{32}$ .

5, 9 and 16 Mev are shown. The spectra show a gradual decrease in the mean energy of emission with increasing angle of emission. The corresponding angular distribution of alpha particles emitted in the energy range 1 Mev to 16 Mev is shown in Fig. VI.10. The solid line is a least squares fit to an angular distribution of the form

$$\sigma(\theta) = a_0 + a_1 P_1(\cos \theta) + a_2 P_2(\cos \theta) \quad (I)$$

where  $\theta$  is the mean angle of emission in the centre of mass system,  $P_1$  and  $P_2$  are Legendre polynomials, and  $a_0$ ,  $a_1$ ,  $a_2$  are constants. The angular distribution is slightly anisotropic with an excess in the forward direction. An estimate of the symmetric and forward peaking contributions was obtained by fitting a curve of the type I above to the backward half of the angular distribution. The expression for the symmetric component in terms of Legendre polynomials may be used to derive a value for the spin cut-off parameter of the residual  $\text{Cr}^{51}$  nucleus. The treatment of Ericson and Strutinski, 1958, leads to an angular distribution of particles emitted by a compound nucleus of the form

$$W(\theta) = 1 + \frac{\langle l^2 \rangle \langle L^2 \rangle}{12 \sigma^4} P_2(\cos \theta) + \frac{3 \langle l^4 \rangle \langle L^4 \rangle}{560 \sigma^4} P_4(\cos \theta).$$

(c.f. Chapter I and VI.1.).

In the present analysis, the mean square angular momentum was estimated by means of the relation

$$\langle L^2 \rangle = \langle L(L+1) \rangle = \frac{\sum_L (2L+1) T_L L(L+1)}{\sum_L (2L+1) T_L}$$

where  $T_L$  are particle penetrabilities.

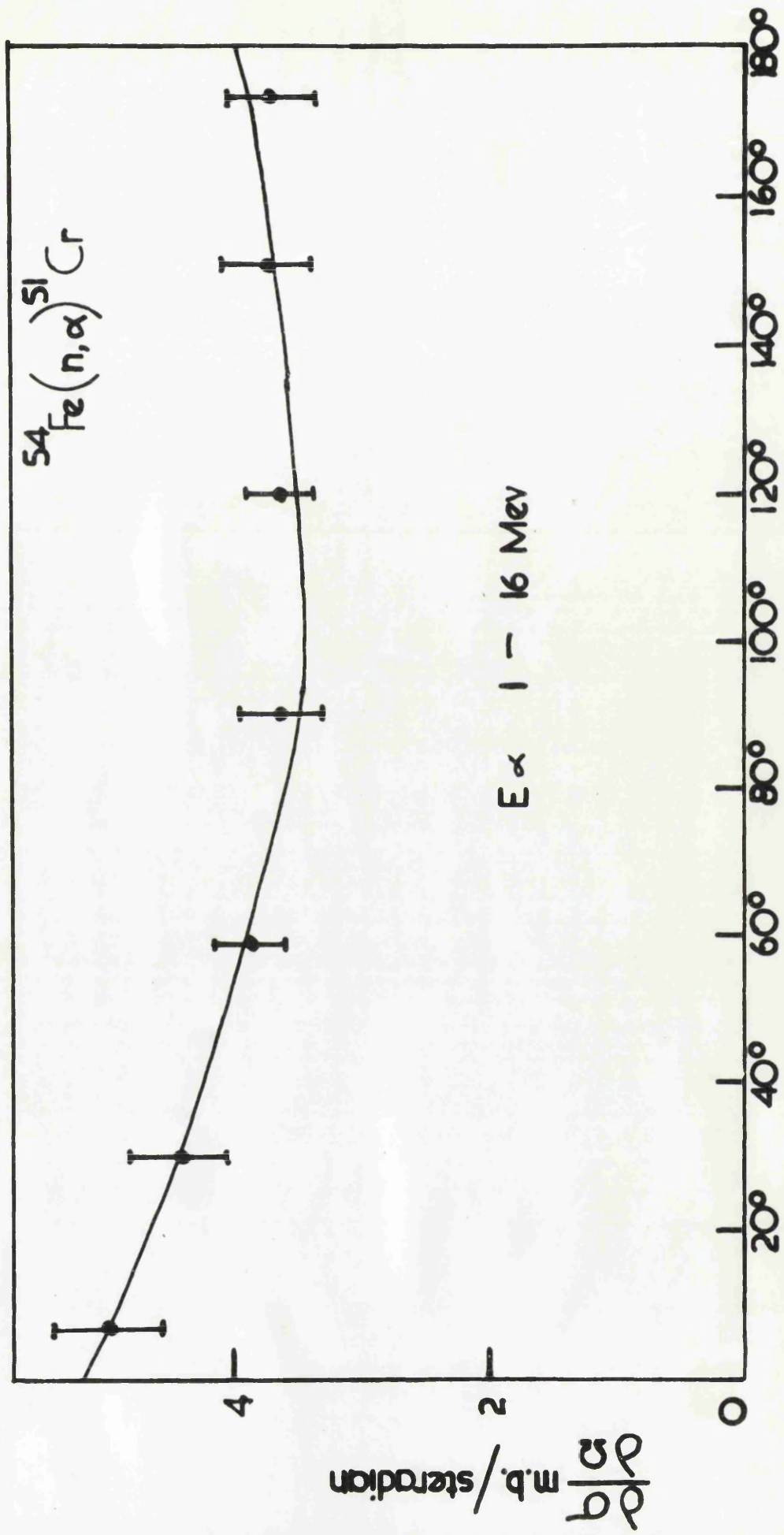


Figure V1.10. Angular distribution for the reaction  $^{54}\text{Fe}(n,\alpha)^{51}\text{Cr}$ .

Assuming all alpha particles were emitted with energy 8 Mev, and using alpha particle penetrabilities from Feshbach et al, 1954, and neutron penetrabilities from Mani et al, 1963, it was found that  $\langle l^2 \rangle \langle L^2 \rangle = 154$ .

The value of  $a^2/a$ , found by fitting a curve of type I to the symmetric component of the angular distribution was 0.057, which may be equated to  $\langle l^2 \rangle \langle L^2 \rangle / 12\sigma^4$ . With an estimate of the errors on the values of  $a_0$  and  $a_2$ , the spin cut-off parameter for the  $\text{Cr}^{51}$  nucleus was found to be

$\sigma = 3.57_{-0.5}^{+0.0}$ . The expression for the angular distribution given by Ericson and Strutinski is subject to the condition

$\frac{\langle l \rangle \langle L \rangle}{\sigma^2} \ll 1$ . In the present case, the value of  $\langle l \rangle \langle L \rangle / \sigma^2$  was found to be  $\sim 0.6$ . There has been no other measured value of the spin cut-off parameter for the  $\text{Cr}^{51}$  nucleus.

Integration over the symmetric component of the angular distribution gives a value for the total cross section of  $46.8 \pm 3.3$  millibarns; this value may be identified with that for that part of the reaction going via a compound nuclear mechanism. The cross section for the emission of alpha particles leading to the forward excess (due probably to direct interaction mechanism) was of the order of 5 millibarns. Using the activation technique, Pollehn and Neuert, 1961, and Gross et al, 1962, have found the  $(n, \alpha)$  cross section in  $\text{Fe}^{54}$  to be  $131 \pm 16$  mb, and  $109 \pm 10$  mb, respectively. However, the present value of the cross section ( $\sim 50$  mb) is in agreement with the general

trend of  $(n, \alpha)$  cross sections ( Chatterjee, 1963, Fig. VI.1.).

VI.8.b.  $Al^{27}(n, \alpha)Na^{24}$

The angular distribution of alpha particles obtained with the  $Al^{27}$  target is shown on Fig. VI.11. The angular distribution is consistent with that found by Jarvis et al, 1963, Patzak and Vonach, 1962, Seebach and Bormann, 1964, but not with that of Kumabe et al, 1957, or Cevoloni et al, 1960, in being peaked in the forward direction but not in the backward direction. In a similar analysis to that carried out on the  $Fe^{54}(n, \alpha)Cr^{51}$  reaction (IV.8.a.), using the ratio of the measured cross sections at  $90^\circ$  and  $180^\circ$ , the spin cut-off parameter for  $Na^{24}$  was found to be  $\sigma \geq 3.6$ . An estimate of the total cross section gave a value of  $119 \pm 7$  millibarns. The value of the spin cut-off parameter is consistent with that found by Patzak and Vonach ( $2\sigma^2 = 13$ ) Seebach and Bormann ( $2\sigma^2 = 13.5_{-2}^{+5}$ ) and Jarvis et al, ( $2\sigma^2 = 16_{-5}^{+\infty}$ ) (The present value is  $2\sigma^2 \geq 26$ ). On the other hand, Douglas and MacDonald, 1959, estimate that the anisotropic distribution found by Kumabe et al, leads to a value of  $2\sigma^2 \leq 5$ . Hibdon, 1961, has obtained a value  $2\sigma^2 = 9.2$  from an analysis of the resonances in the  $Na^{23}(n, \gamma)Na^{24}$  reaction; however, S - wave neutrons were used in his determination of the parameter.

VI. 8. c.  $S^{32}(n, \alpha)Si^{29}$ .

Typical  $\frac{dE}{dx}$  spectra obtained during the bombardment of a  $S^{32}$  target with 14.8 Mev neutrons are shown in Fig. VI.9.

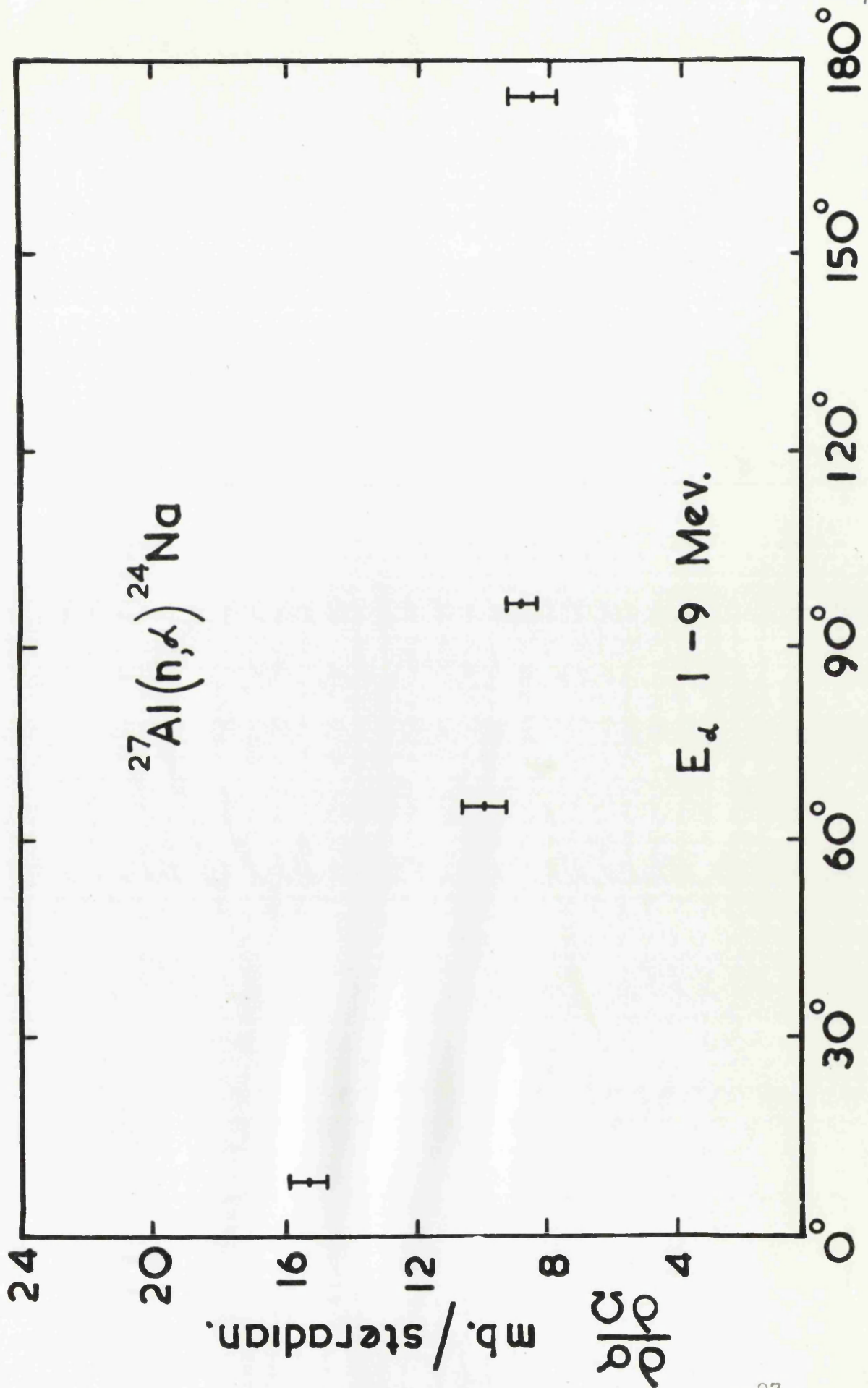


Figure VI.11. Angular distribution for the reaction  $\text{Al}^{27}(n, \alpha)\text{Na}^{24}$ .

The spectra show a discontinuity which was calculated to correspond to the threshold for the  $S^{32}(n, n' \alpha)Si^{28}$  reaction. Bearing in mind the suggestion of Kumabe that the  $(n, n' \alpha)$  reaction may be a cause of the large degree of anisotropy found in some angular distributions of emitted alpha particles, the angular distribution of alpha particles which could correspond to both the  $(n, \alpha)$  and  $(n, n' \alpha)$  reactions, and also that for alpha particles which could only be due to the  $(n, \alpha)$  reaction were calculated. (Figs. VI.12. and 13). The  $(n, \alpha)$  angular distribution was found to be symmetrical about  $90^\circ$  (centre of mass system), while that corresponding to both reactions was very anisotropic. From an analysis of the  $(n, \alpha)$  angular distribution, the spin cut-off parameter was found to be  $\sigma = 2.7^{+0.85}_{-0.6}$ ; the spin cut-off parameter determined from the complete angular distribution was  $3.05^{+\infty}_{-0.75}$ . In the analysis, the results of Kumabe, 1958, on the energy spectra of the emitted alpha particles were used. The angular distributions found in the present experiment were much less anisotropic than that given by Kumabe ( $\sigma < 1.5$ ).

By integration of the angular distributions, the cross section for the  $S^{32}(n, \alpha)Si^{29}$  reaction was found to be  $48 \pm 5$  millibarns, and that for the emission of all alpha particles was found to be  $135 \pm 9$  millibarns. These values agree favourably with those found by Kumabe ( $38.2 \pm 7.6$  mb, and  $109 \pm 16$  mb., respectively).

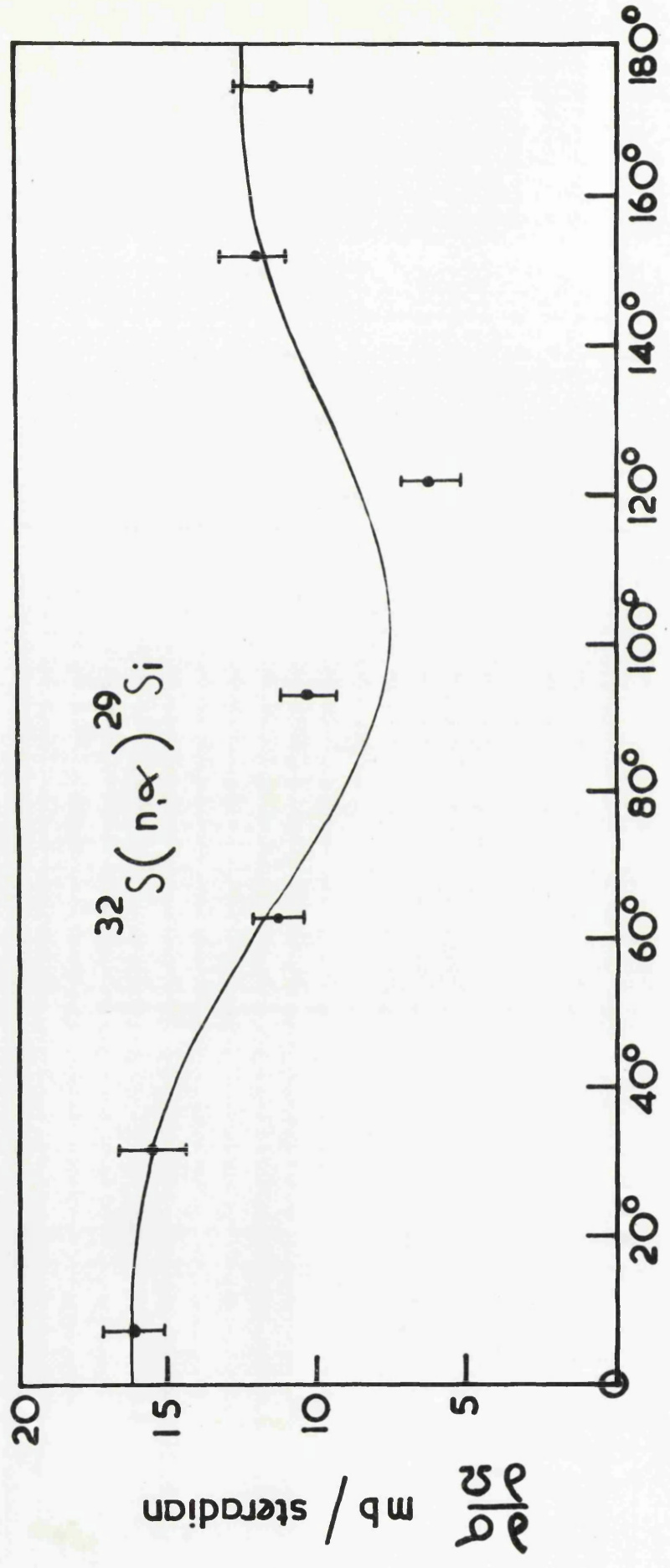


Figure V1.12. Angular distribution of alpha particles from the reactions  $^{32}\text{S}(n,\alpha)^{29}\text{Si}$  and  $^{32}\text{S}(n,n'\alpha)^{28}\text{Si}$ .

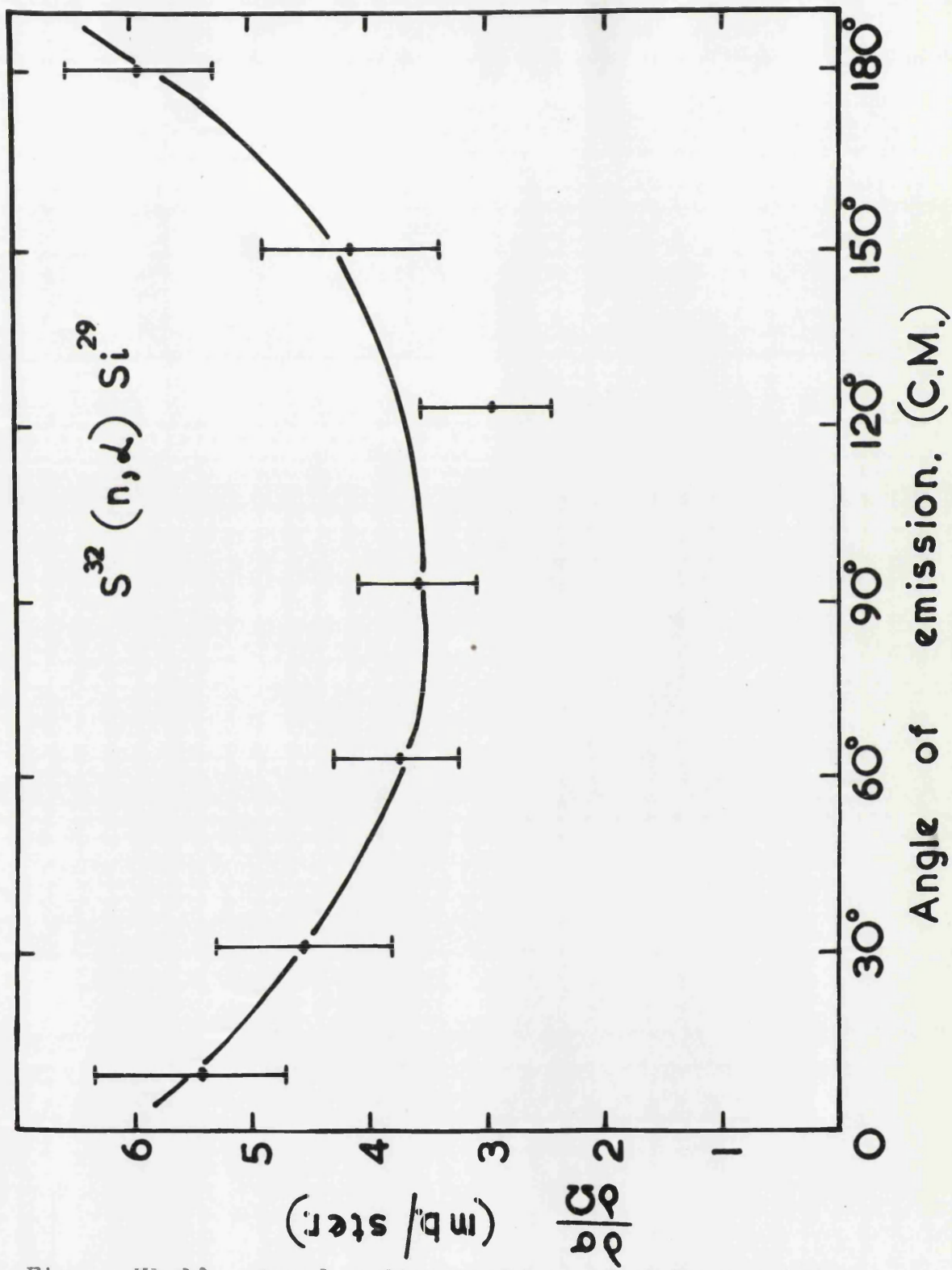


Figure VI.13. Angular distribution of alpha particles from the reaction  $S^{32}(n, \alpha)Si^{29}$ .

VI. 8. d.  $V^{51}(n,\alpha)Sc^{48}$ .

Since the  $V^{51}(n,\alpha)Sc^{48}$  reaction was investigated at only one angle of emission ( $90^\circ$ ), the sole information which could be gained was an estimate of the total cross section for the reaction. Assuming isotropic emission of alpha particles, the total cross section  $\wedge^{was}$  found to be  $67.9 \pm 4.7$  millibarns. The total cross sections found by other workers are lower than that found in the present work. ( $18 \pm 3$  mb., Hillman, 1962;  $28.6 \pm 12$  mb., Paul and Clarke, 1953;  $23 \pm 4$  mb., Bramlett and Fink, 1963;  $43 \pm 7$  mb., Kumabe, 1957;  $43 \pm 4$  mb., Bormann et al., 1961.). However, the values of the cross sections found by the above workers are, to a certain extent, inconsistent within themselves.

VI. 8. e.  $Br^{81}(n,\alpha)As^{78}$ .

A measurement of the cross section for the emission of alpha particles at  $90^\circ$ , gave a value of less than 8 millibarns for the total cross section for the  $Br^{81}(n,\alpha)As^{78}$  reaction (assuming isotropic angular emission),. Since the target material was silver bromide, an allowance for the  $(n,\alpha)$  reaction in silver was made using the result of Irfan and Jack, 1963 ( $\sim 10$  millibarns.). The measured value of the cross section agrees with previous measurements ( $6.6 \pm 1.4$  mb., Bramlitt and Fink, 1963;  $10 \pm 1$  mb., Mukherjee, 1961). The low value found for the cross section is consistent with statistical theory calculations.

VI. 8. f. Cu<sup>63</sup>(n, $\alpha$ )Co<sup>60</sup>.

An estimate of the total cross section for the (n,  $\alpha$ ) reaction in Cu<sup>63</sup> based on a measurement at 90°, gave a value of 20  $\pm$  5 mb., agreeing with the general trend of (n,  $\alpha$ ) cross sections found by Chatterjee (Fig. VI.1.), and with the value of 23  $\pm$  3 mb., found by Kantele and Gardner, 1962. The cross section determined by Irfan and Jack, (~95 mb.) is much higher than the present measurement.

VI.9. Conclusion.

The total cross section and, in some cases, the angular distributions of (n, $\alpha$ ) reactions in several targets have been found, in general, to be in agreement with previous measurements, where such measurements exist. The experimental technique used in the present work has the advantage over the much used emulsion technique in that a good background subtraction is obtainable, and also, detection to lower alpha particle energies is possible. Calculations on the effect of Ericson fluctuations on the measured angular distributions due to neutron beam width show it to be negligible (<0.01 %).

However, a main disadvantage of the work carried out on the present series of (n,  $\alpha$ ) experiments was that the high background made the collection of adequate counting statistics extremely time consuming, thus limiting further studies on other target materials.

APPENDIX A.The Effect of Neutron Energy Spread on Measured Excitation Curves.

An estimate of the error involved in obtaining excitation curves under conditions of a large neutron energy spread may be calculated from the known energy spread. As considered in section V.1., information as to the fluctuation of level densities with excitation energy is lost with the use of a wide neutron energy spread. Thus, any estimate of the excitation curves which exist in the limit of narrow neutron energy spread, derived from the measured excitation curves, must necessarily vary smoothly with excitation energy since the experimental measurements show a smooth variation (Figs. V.1; V.3.).

If the "true" excitation curve in the limit of narrow neutron energy spread (bearing in mind the above remarks) is described as a function of excitation energy  $E$  by  $f(E)$ , then the measured excitation curve may be described in terms of the mean energy,  $\langle E \rangle$ , of the incident neutron "packet" by the function  $g(\langle E \rangle)$ ,

$$g(\langle E \rangle) = \frac{\int f(E) \phi(E) dE}{\int \phi(E) dE} \quad (1)$$

where  $\phi(E)$  is the incident neutron flux per unit energy. Since the measured excitation curves are smoothly varying with energy,  $f(E)$  and  $g(\langle E \rangle)$  may be expressed as polynomials in increasing powers of  $E$ . If one makes the assumption that the "true" excitation curve may be expressed as a polynomial of degree 3:-

$$f(E) = a_0 + a_1 E + a_2 E^2 + a_3 E^3 \quad (11)$$

then by equation (1) above,

$$g(\langle E \rangle) = \left[ \int a_0 \phi(E) dE + \int a_1 E \phi(E) dE + \int a_2 E^2 \phi(E) dE + \int a_3 E^3 \phi(E) dE \right] / \int \phi(E) dE$$

$$= a_0 + a_1 \langle E \rangle + a_2 \langle E^2 \rangle + a_3 \langle E^3 \rangle \quad (111)$$

However, the corresponding values of the "true" excitation curve at the values of the mean energy  $\langle E \rangle$  are given by

$$f(\langle E \rangle) = a_0 + a_1 \langle E \rangle + a_2 \langle E \rangle^2 + a_3 \langle E \rangle^3$$

$$\therefore f(\langle E \rangle) - g(\langle E \rangle) = a_2 (\langle E \rangle^2 - \langle E^2 \rangle) + a_3 (\langle E \rangle^3 - \langle E^3 \rangle) \quad (1V)$$

Calculations of the mean values of  $E$ ,  $E^2$  and  $E^3$  from the calculated neutron energy spread (Fig. III.2 and calculated geometrical neutron energy spread) together with a determination of the constants  $a_0$ ,  $a_1$ ,  $a_2$  and  $a_3$  by fitting equations (111) to the measured excitation curves, enabled an estimate of the deviation of the measured values of the cross-sections from the expected values in the limit of narrow neutron energy spread to be made through equation (1V). The results of such a calculation show that the greatest deviation is 8%, occurring for a neutron emission angle  $\psi_n = 27^\circ$  i.e. occurring at the largest neutron energy spread; the measured cross-sections are less than the "true" cross-sections. For smaller neutron energy spreads the percentage deviation is less than 8%; for neutron emission angles  $\psi_n \geq 60^\circ$  the deviation is negligible. The estimated error in the values of the experimental cross-sections arising from effects other than neutron beam spread was calculated to be  $\pm 10\%$ .

- Agodi, A., Pappalardo, G., Ricamo, R., Vinciguerra, D., 1962, Nuovo Cim. 23, 1136.
- Agodi, A., Pappalardo, G., 1963, Nuc. Phys., 47, 129.
- Ahn, S.H., Roberts, J.H., 1957, Phys. Rev., 108, 110.
- Aitken, J.H., Dixon, W.R., 1962, Physics Letters, 2, 152.
- Allan, D.L., 1957, Proc. Phys. Soc., A70, 195; 1958, Nuc. Phys. 6, 464; 1959, Ibid, 10, 348; 1961, Ibid, 24, 274.
- Amaldi, E., Fermi, E., 1936, Ricerca Sci. 1, 310.
- Armstrong, A.H., Rosen, L., 1960, Nuc. Phys., 19, 40.
- Austern, N., Butler, S., McManus, H., 1953, Phys. Rev., 92, 350.
- Bame, S.J., Jr., Haddad, E., Perry, J.E., Jr., Smith, R.K., 1957, Rev. Sci. Instr., 28, 997.
- Barry, J.F., 1962, Journal Nuc. Energy, Reactor Sci. and Tech., 16, 467.
- Barschall, H.H., 1952, Phys. Rev., 86, 431.
- Bethe, H.A., 1936, Phys. Rev., 50, 332; 1937, Rev. Mod. Phys., 9, 69.
- Bethe, H.A., Placzek, G., 1937, Phys. Rev., 51, 450.
- Bjorklund, F., Fernbach, S., Proceedings of the International Conference on the nuclear optical model. The Florida State University Studies, No. 32, Tallahassee, 1959.
- Blanc, D., Cambou, F., Devillers, D., Reme, H., Vedrenne, G., Ambrosino, G., 1962, Nuovo Cim, 23, 1140.
- Bloch, C., 1954, Phys. Rev., 93, 1094.
- Blosser, H.G., Goodmann, C.D., Handley, T.H., Randolph, M.L., 1955, Phys. Rev., 100, 429; 1958, Ibid, 110, 531.
- Bohr, N., 1936, Nature, 137, 344.
- Bjerger, T., Westcott, C. H., 1935, Proc. Roy. Soc. (London) A150, 709

- Bormann, M., Langkau, R., 1961, Z. Naturforsch., 16a, 444.
- Bramlitt, E.T., Fink, R.W., 1963, Phys. Rev., 131, 2649.
- Breit, G., Wigner, E.P., 1936, Phys. Rev., 49, 519 and 642.
- Brown, G., Morrison, G.C., Muirhead, H., Morton, W.T., 1957, Phil. Mag., 2, 785.
- Brown, G., Muirhead, H., 1957, Phil. Mag., 2, 479.
- Buechner et al., 1954, Phys. Rev., 95, 609.
- Bulloch, R.E., Moore, R.G., 1960, Phys. Rev., 119, 721.
- Cagnon, P.R., Owen, G.E., 1956, Phys. Rev., 101, 1798.
- Cameron, A.G.W., 1958, Canad. J. Phys., 36, 1040.
- Cevelani, M., Petralia, S., Righini, B., Valdre, U., Venturini, G., 1960, Nuovo Cim., 16, 950.
- Chatterjee, A., 1963, Nuc. Phys., 47, 511; 1963, Ibid, Nuc. Phys., 49, 686.
- Coleman, R.F., Hawker, B.E., O'Conner, L.P., Perkin, J.L., 1959, Proc. Phys. Soc., 73, 215.
- Colli, L., Facchini, U., 1956, Nuovo Cim., 4, 671.
- Colli, L., Iori, I., Marcazzan, M.G., Millazzo, M., 1962, Physics Letters, 2, 12.
- Coon, J.H., Davis, R.W., Felthouser, H.E., Nicodemus, D.B., 1958, Phys. Rev., 111, 250.
- Cuzzocrea, P., Nottarrigo, S., Ricamo, R., Vinci, F., 1960, Nuov<sup>e</sup> Cim., 18, 671.
- Cuzzocrea, P., Nottarrigo, S., Rubbino, A., 1964, Nuc. Phys., 55, 364.
- Dearnley, G., Whitehead, A.B., 1961, AERE-R3662.
- Dostrovski, I., Fraenkel, Z., Friedlander, G., 1959, Phys. Rev., 116, 683.

- Douglas, A.C., MacDonald, N., 1959, Nuc. Phys., 13, 382.
- Ericson, T., 1960, Phil. Mag. (Suppl.) 9, 425.
- Ericson, T., Strutinski, V., 1958, Nuc. Phys., 8, 284;  
Addendum, 1958/59, 9, 689.
- Facchini, U., Saetta-Menichella, E., Tonolini-Severgnini, F.,  
1964, Nuc. Phys., 51, 460.
- Feshbach, H., Porter, C.E., Weisskopf, V.F., 1953, Phys. Rev.,  
90, 166; 1954, *ibid*, 96, 448.
- Feshbach, H., Peaslee, D.C., Weisskopf, V., 1947, Phys. Rev.,  
71, 145.
- Feshbach, H., Weisskopf, V.F., 1949, Phys. Rev., 76, 1550.
- Forbes, S.G., 1952, Phys. Rev., 88, 1309.
- Friedman, F.L., Weisskopf, V.F., 'Niels Bohr and the Development  
of Physics', Pergamon Press, London, 1955, Pg.134.
- Fuller, J.C., Danco, W.E., Ralf, D.C., 1957, Phys. Rev., 108, 91.
- Gardner, D.G., 1962, Nuc. Phys., 29, 373; 1962, *ibid*, 35, 303.
- Gonzalez, L., Rapaport, J., Van Loef, J.J., 1960, Phys. Rev.,  
120, 1319.
- Gonzalez, L., Trier, A., Van Loef, J.J., 1962, Phys. Rev., 126, 271.
- Gross, W.G., Clarke, R.L., Morin, K., Slim, G., Ahmed, N.M.,  
Beg, K., 1962, Bull. Am. Phys. Soc., 7, 335.
- Grundl, J.A., Henkel, R.L., Perkins, B.L., 1958, Phys. Rev., 109,  
425.
- Haling, R.K., Peck, R.A., Eubank, H.P., 1957, Phys. Rev., 106, 971.
- Hauser, W., Feshbach, H., 1952, Phys. Rev., 87, 366.
- Hausman, H.J., Dell, G.F., Bowsher, H.F., 1960, Phys. Rev., 118,  
1237.
- Hayakawa, S., Kawai, M., Kikuchi, K., 1955, Prog. Theor. Phys.  
Japan, 13, 415.
- Hibdon, C.T., 1961, Phys. Rev., 122, 1235.

- Hillman, M., 1962, Nuc. Phys., 37, 78.
- Hughes, D.J., Swartz, R.B., Neutron Cross-sections, BNL-325.
- Hunter, G.T., Richards, H.T., 1949, Phys. Rev., 76, 1445.
- Irfan, M., Jack, W., 1963, Proc. Phys. Soc., 81, 800; 1963, Ibid, 81, 808.
- Jarvis, C.J.D., Dixon, W.R., Storey, R.S., 1963, Nuc. Phys., 44, 680.
- Kantele, J., Gardner, D.G., 1962, Nuc. Phys., 35, 353.
- Kapur, P.L., Peierls, R.E., 1938, Proc. Roy. Soc. (London), A166, 277.
- Kaufman, S., 1960, Phys. Rev., 117, 1532.
- Kaul, O.N., 1962, Nuc. Phys., 29, 522; 1962, Ibid., 33, 177; 1962, Ibid., 39, 325; 1964, Ibid., 55, 127.
- Konijn, J., Lauber, A., 1963, Nuc. Phys., 48, 191.
- Kulišić, P., Ajdačić, V., Cindro, N., Lalović, B., Strohal, P., 1964, Nuc. Phys., 54, 17.
- Kumabe, I., 1958, J. Phys. Soc. Japan, 13, 325.
- Kumabe, I., Takekoshi, E., Ogata, H., Tsuneoke, Y., Ōki, S., 1957, Phys. Rev., 106, 155; 1958, J. Phys. Soc. Japan, 13, 129.
- Kumabe, I., Fink, R.W., 1960, Nuc. Phys., 15, 316.
- Lamarsh, J.R., Feshbach, H., 1956, Phys. Rev., 104, 1633.
- Lane, A.M., Thomas, R.G., 1958, Rev. Mod. Phys., 30, 257.
- Lane, A.M., Thomas, R.G., Wigner, E.P., 1955, Phys. Rev., 98, 693.
- Lang, J.M.B., LeCouteur, K.J., 1954, Proc. Phys. Soc., A67, 585.
- Mani, G.S., Melkanoff, M.A., Iori, I., 1963, Report C.E.A., 2379; 1963, Report C.E.A., 2380.
- Marcazzan, G.M., Tonolini, F., Zetta, L., 1963, Nuc. Phys., 46, 51.
- Marsh, P.V., Morton, W.T., 1958, Phil. Mag., 3, 143; 1958, Ibid, 3, 577; 1958, Ibid, 3, 1256.

- Meadows, J.W., Whalen, J.F., 1963, Phys. Rev., 130, 2022.
- Moon, P.B., Tillman, J.R., 1935, Nature, 135, 904.
- Mukherjee, S.K., Ganuly, A.K., Majumdar, N.K., 1961, Proc. Phys. Soc., 77, 508.
- McManus, H., Sharpe, W.T., 1952, Phys. Rev., 87, 188.
- Nakai, K., Gotoh, H., Ameno, H., 1962, J. Phys. Soc. Japan, 17, 1215.
- Newton, T.D., 1956, Canad. J. Phys., 34, 804.
- Patzak, W., Vonach, H., 1962, Nuc. Phys., 39, 263.
- Paul, E.B., Clarke, R.L., 1953, Canad. J. Phys., 31, 267.
- Peck, R.A., Jr., 1957, Phys. Rev., 106, 965; 1961, Ibid, 123, 1738; 1961, Nuc. Phys., 27, 596.
- Pollehn, H., Neuert, H., 1961, Z. Nat., 16A, 227.
- Preston, P.S., Shaw, P.F., Young, S.A., 1954, Proc. Roy. Soc., A226, 206.
- Rapaport, J., Van Loef, J.J., 1959, Phys. Rev., 114, 565.
- Ribe, F.L., Davis, W., 1955, Phys. Rev., 99, 331.
- Rosen, L., Stewart, L., 1955, Phys. Rev., 99, 1052.
- Seebeck, U., Bormann, 1964, Private Communication.
- Sen, B., 1962, Nuc. Phys., 38, 601.
- Sen Gupta, A.K., Van Patter, D.M., 1964, Nuc. Phys., 50, 17.
- Seward, F.D., 1959, Phys. Rev., 114, 514.
- Szilard, L., 1935, Nature, 136, 150.
- Taketani, H., Alford, W.P., 1962, Nuc. Phys., 32, 430.
- Trier, A., 1962, Z. Naturf., 17A, 275.
- Urech, S., Jeannet, E., Rossel, J., 1961, Hel. Phys. Acta, 34, 954.

- Van Loef, J.J., 1961, Nuc. Phys., 24, 340.
- Wenzel, W.A., Whaling, W., 1952, Phys. Rev., 87, 499.
- Weigold, E., 1960, Aust. J. Phys., 13, 186.
- Weinberg, L.G., Blatt, J.M., 1953, Am. J. Phys., 21, 124.
- Weisskopf, V.E., 1937, Phys. Rev., 52, 295.
- Wigner, E.P., Eisenbud, L., 1947, Phys. Rev., 72, 29.
- Williamson, C., Boujot, J.P., 1962, C.E.A. 2189.
- Wolfenstein, L., 1951, Phys. Rev., 82, 690.
- Yasumi, S., 1957, J. Phys. Soc. Japan, 12, 443.
- Weisskopf, V. E., Ewing, D. H., 1940, Phys. Rev., 57, 472.
-

SOME STUDIES OF FAST NEUTRON REACTIONS

IN MEDIUM WEIGHT ELEMENTS

by

P.J. STONES

A summary of a thesis presented for the degree of Ph.D

in the University of Glasgow.

## Some Studies of Fast Neutron Reactions in Medium Weight Elements

### Summary

The theory, experimental method, and results of studies of  $(n, p)$  and  $(n, \alpha)$  reactions induced in medium weight nuclei in the neutron energy regions 3 Mev and 15 Mev, respectively, are presented.

The main part of the thesis is concerned with the determination of the absolute cross sections for the  $(n, p)$  reaction in the target nuclei  $\text{Ni}^{58}$ ,  $\text{Fe}^{54}$ , and  $\text{Cu}^{63}$  at several neutron energies between 2.4 Mev and 3.4 Mev. Protons emitted into a large solid angle in the backward direction (with respect to the incident neutron beam) were detected. The experimental apparatus consisted of a) a Cockcroft-Walton set for the production of a neutron flux by means of the reaction  $\text{H}^2 (\text{H}^2, n) \text{He}^3$ , b) a target material in the form of a thin foil and c) a detection system consisting of a silicon semiconductor counter; the neutron flux was monitored absolutely by the detection of recoil protons from a hydrogenous foil. With the same detection system, a measurement of the cross section for the emission of protons into a large solid angle in the forward direction was also carried out, at one neutron energy. The energy spectra of the emitted protons from the target nuclei  $\text{Fe}^{54}$  and  $\text{Ni}^{58}$  were determined with a detection system of improved resolution, incorporating a proportional counter and semiconductor counter.

The variation of the cross sections with energy of incident neutrons is monotonically increasing in the case of the target nuclei  $\text{Fe}^{54}$  and  $\text{Ni}^{58}$ , while the cross section for the case of the target nucleus  $\text{Cu}^{63}$  is relatively independent of neutron energy in the energy range considered. The results are in fair agreement with the results of

activation experiments carried out by other workers in the field. The ratio of the cross sections for the emission of protons in the forward and backward directions show the reaction mechanism to be compound nuclear, with no contribution from the direct interaction mechanism. The energy spectra of the emitted protons suggest the presence of previously unknown levels in the residual nuclei  $Mn^{54}$  and  $Co^{58}$ . Also presented are the results of theoretical Hauser-Feshbach calculations on the cross section for the  $Ni^{58} (n, p) Co^{58}$  reaction, with different assumptions for the possible modes of neutron and proton decay channels.

The account of the experimental method and results of a study of the angular distribution of alpha particles produced by the  $(n, \alpha)$  reaction in various target materials for an incident neutron energy of 14.8 Mev is presented in less detail.

The detection system used in this series of experiments consisted of three  $dE/dx$  proportional counters. Total numbers of alpha particles emitted into a narrow solid angle, at several mean angles of emission, were obtained. Absolute total cross sections for the  $(n, \alpha)$  reactions were determined by integration over the angular distributions. From the resultant angular distributions an estimate was obtained of a) the relative importance of direct interaction and compound nuclear mechanism, and b) the magnitude of the 'spin out-off' parameter present in the expression for the density of levels in the residual nuclei.

A comparison of the experimental results with those of other workers is given, and the position of the results in the general scheme of nuclear reactions<sup>vs</sup> considered.  
h

---